Spin current & spin pumping effect

Yu-Ting Fanchiang, M. Hong
Department of Physics, National Taiwan University

J. Kwo
Department of Physics, National Tsing Hua University

Outline

- **Introduction to spin current and spin transfer torques**

- **Measuring spin Hall angle and IEE length**
  - **Spin pumping**
  - **Spin-torque ferromagnetic resonance (ST-FMR)**
  - **Modulation of magnetization damping (MOD)**

Y. T. Fanchiang
Advanced Nano Thin Film Epitaxy Lab

Spin transfer torques

Nature Materials **11**, 372–381 (2012)

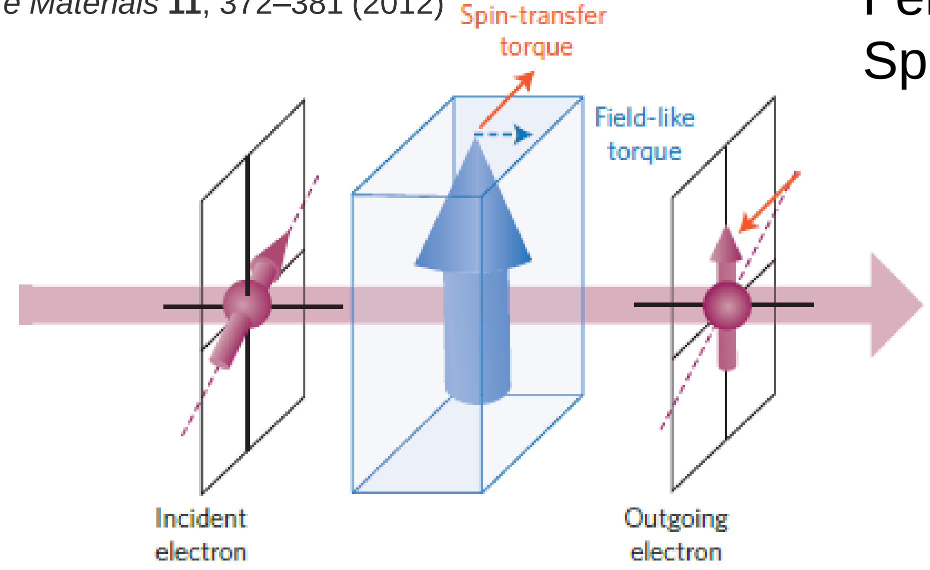

Ferromagnetic resonance (FMR)
Spin pumping

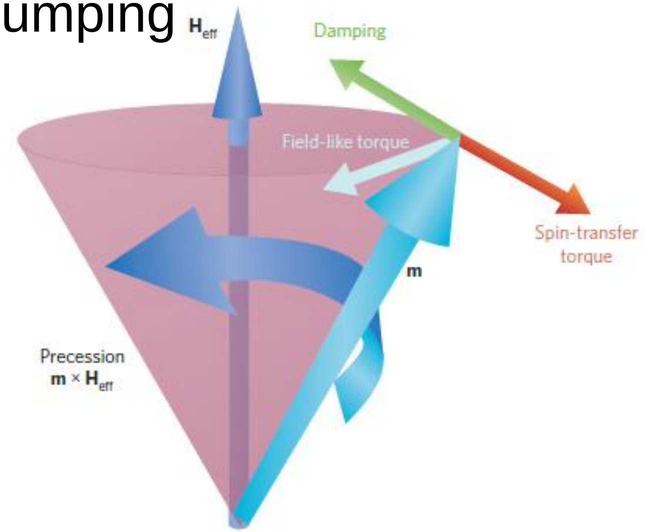

A. Brataas, et al., Nat. Mater. **11**, 372 (2012)

LLG equation with torque terms:

$$\frac{\partial \mathbf{m}}{\partial t} = -y\mathbf{m} \times H_{eff} + \alpha \mathbf{m} \times \frac{\partial \mathbf{m}}{\partial t} + \boldsymbol{\tau}$$

Damp-like torque:

$$-\frac{\gamma\hbar}{2eM_sV}\mathbf{m}\times(\mathbf{m}\times I_s)$$

Field-like torque:

$$-\frac{\gamma\hbar}{2eM_sV}\mathbf{m}\times I_s$$

Spin current

$$\mathbf{Q} = \mathbf{v} \otimes \mathbf{s}$$

$$= \frac{\hbar^2}{2m} \mathrm{Im}\left(\psi^* \boldsymbol{\sigma} \otimes \nabla \psi\right)$$

For a spinor plane-wave wavefunction in x direction:

$$\psi = \frac{e^{ikx}}{\sqrt{\Omega}} \mathrm{Im}\left(a\left|\uparrow\right\rangle + b\left|\downarrow\right\rangle\right)$$

$$Q_{xx} = \frac{\hbar^2 k}{2m\Omega} 2\,\mathrm{Re}\left(ab^*\right)$$

$$Q_{xy} = \frac{\hbar^2 k}{2m\Omega} 2\,\mathrm{Im}\left(ab^*\right)$$

$$Q_{xz} = \frac{\hbar^2 k}{2m\Omega} 2\,\mathrm{Re}\left(|a|^2 - |b|^2\right)$$

Conservation of angular momentum
Spin transfer torque:

$$\mathbf{N}_{st} = -\int_{pillbox} d^2 R \hat{\mathbf{n}} \cdot \mathbf{Q}$$

$$= -\int_{pillbox} d^3 r \nabla \cdot \mathbf{Q}$$

Y. T. Fanchiang
Advanced Nano Thin Film Epitaxy Lab

D. C. Ralph, J. Magn. Magn. Mat. **320**, 1190 (2012)

$$\psi_{in} = \frac{e^{ikx}}{\sqrt{\Omega}}\left(\cos(\theta/2)\left|\uparrow\right\rangle + \sin(\theta/2)\left|\downarrow\right\rangle\right)$$

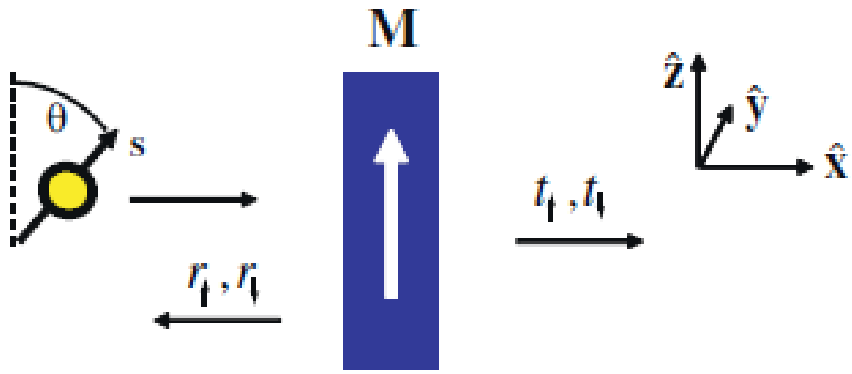

$$\psi_{trans} = \frac{e^{ikx}}{\sqrt{\Omega}}\left(t_\uparrow\cos(\theta/2)\left|\uparrow\right\rangle + t_\downarrow\sin(\theta/2)\left|\downarrow\right\rangle\right)$$

$$\psi_{refl} = \frac{e^{-ikx}}{\sqrt{\Omega}}\left(r_\uparrow\cos(\theta/2)\left|\uparrow\right\rangle + r_\downarrow\sin(\theta/2)\left|\downarrow\right\rangle\right)$$

$$\mathbf{Q}_{in} = \frac{\hbar^2 k}{2m\Omega}\left[\sin(\theta)\hat{\mathbf{x}} + \cos(\theta)\hat{\mathbf{z}}\right]$$

$$\mathbf{Q}_{trans} = \frac{\hbar^2 k}{2m\Omega}\sin(\theta)\,\mathrm{Re}\left(t_\uparrow t_\downarrow^*\right)\hat{\mathbf{x}} + \frac{\hbar^2 k}{2m\Omega}\sin(\theta)\,\mathrm{Im}\left(t_\uparrow t_\downarrow^*\right)\hat{\mathbf{y}}$$
$$+\frac{\hbar^2 k}{2m\Omega}\left(\left|t_\uparrow\right|^2\cos^2(\theta/2) - \left|t_\downarrow\right|^2\sin^2(\theta/2)\right)\hat{\mathbf{z}}$$

$$\mathbf{Q}_{refl} = -\frac{\hbar^2 k}{2m\Omega}\sin(\theta)\,\mathrm{Re}\left(r_\uparrow r_\downarrow^*\right)\hat{\mathbf{x}} - \frac{\hbar^2 k}{2m\Omega}\sin(\theta)\,\mathrm{Im}\left(r_\uparrow r_\downarrow^*\right)\hat{\mathbf{y}}$$
$$-\frac{\hbar^2 k}{2m\Omega}\left(\left|r_\uparrow\right|^2\cos^2(\theta/2) - \left|r_\downarrow\right|^2\sin^2(\theta/2)\right)\hat{\mathbf{z}}$$

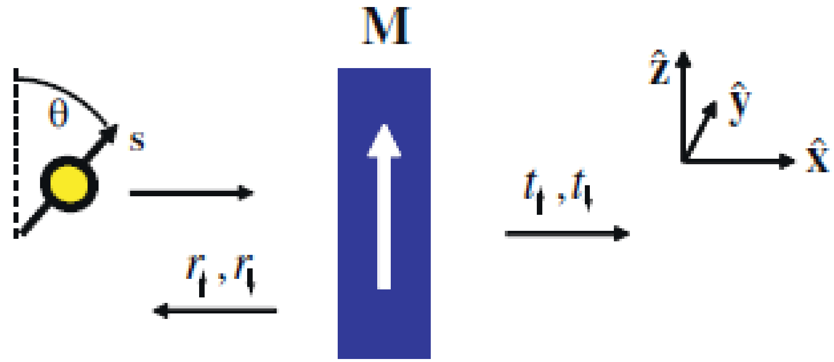

$$\mathbf{N}_{st} = A\hat{\mathbf{x}}\cdot\left(\mathbf{Q}_{in} + \mathbf{Q}_{refl} - \mathbf{Q}_{trans}\right)$$

$$= \frac{A\hbar^2 k}{2m\Omega}\sin(\theta)\left[1-\mathrm{Re}\left(t_\uparrow t_\downarrow^* + r_\uparrow r_\downarrow^*\right)\right]\hat{\mathbf{x}}$$

Damp-like torque

$$- \frac{A\hbar^2 k}{2m\Omega}\sin(\theta)\,\mathrm{Im}\left(t_\uparrow t_\downarrow^* + r_\uparrow r_\downarrow^*\right)\hat{\mathbf{y}}$$

Field-like torque

$$\left(\left|t_\uparrow\right|^2 + \left|r_\uparrow\right|^2 = 1\right.$$

$$\left.\left|t_\downarrow\right|^2 + \left|r_\downarrow\right|^2 = 1\right)$$

Spin mixing conductance

$$\begin{pmatrix} a' \\ b' \end{pmatrix} = \begin{pmatrix} G_{\uparrow\uparrow} & G_{\uparrow\downarrow} \\ G^*_{\downarrow\uparrow} & G_{\downarrow\downarrow} \end{pmatrix}\begin{pmatrix} a \\ b \end{pmatrix}$$

$\mathrm{Re}\left(G_{\uparrow\downarrow}\right) >> \mathrm{Im}\left(G_{\uparrow\downarrow}\right)$ for metals

Ferromagnetic resonance (FMR)

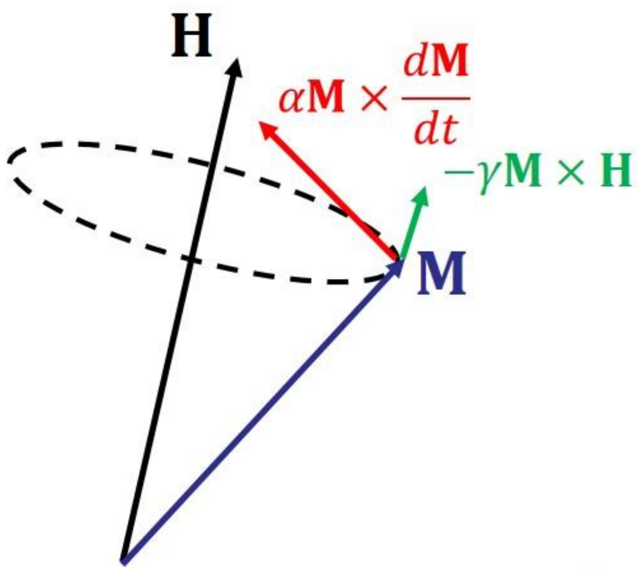

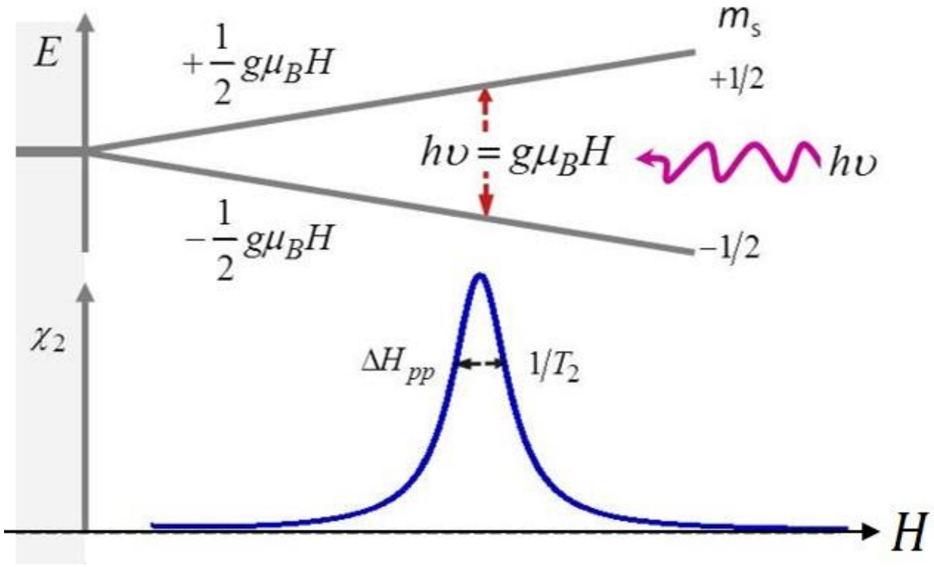

Landau–Lifshitz–Gilbert equation

$$\frac{d\mathbf{M}}{dt} = -\gamma\mathbf{M}\times\mathbf{H} + \alpha\mathbf{M}\times\frac{d\mathbf{M}}{dt}$$

Cavity

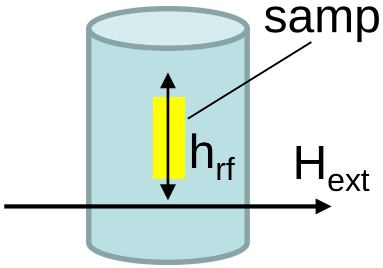

Coplanar waveguide

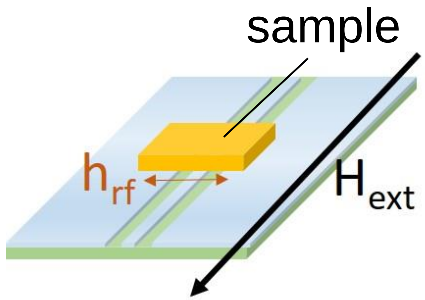

Application:
Measurement of magnetic anisotropy
Measurement of damping constant α
Spin pumping

Spin pumping

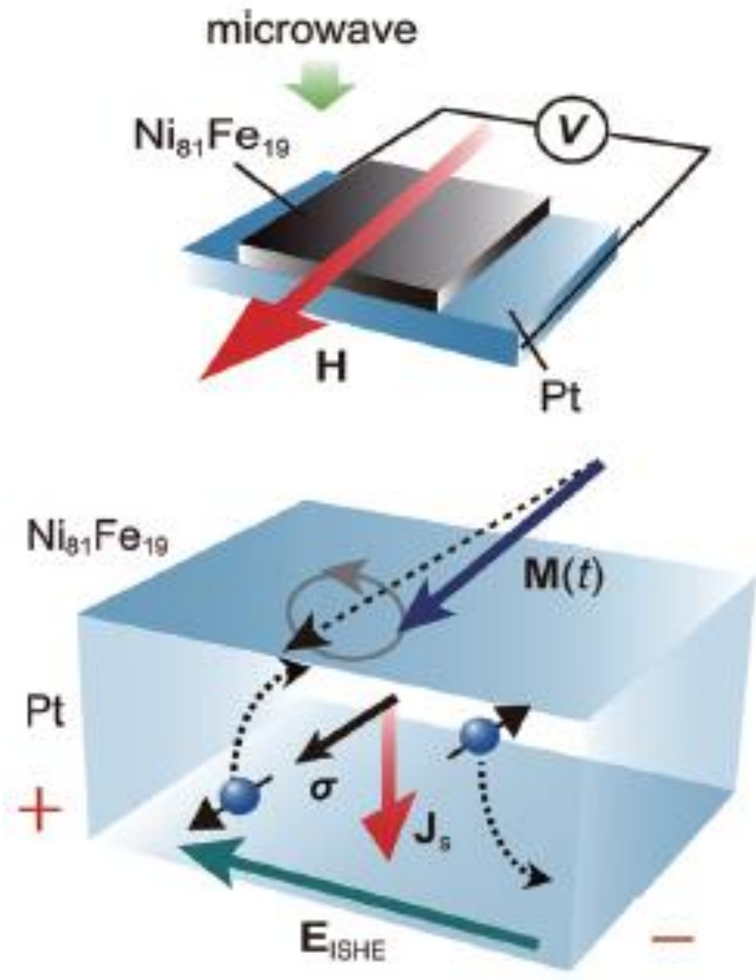

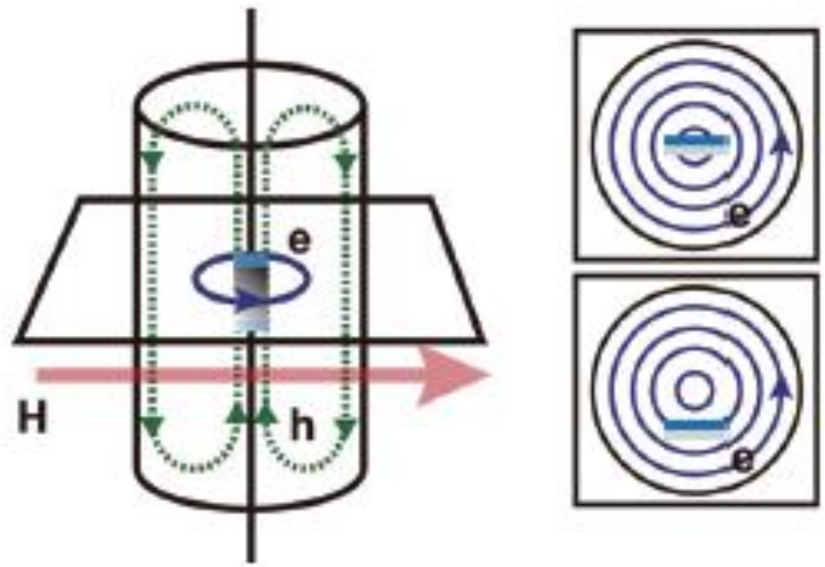

Spin current projected along H_{ext}:

$$j_s = \frac{\omega}{2\pi}\int_0^{2\pi/\omega} \frac{\hbar}{4\pi} g_r^{\uparrow\downarrow} \frac{1}{M_s^2}\left[\mathbf{M}(t) \times \frac{d\mathbf{M}(t)}{dt}\right]_z dt.$$

$$V_{\mathrm{ISHE}} \propto \boldsymbol{J}_{\mathbf{c}} \propto \theta_{\mathrm{SH}} \boldsymbol{J}_{\mathbf{s}} \times \boldsymbol{\sigma} \propto \theta_{\mathrm{SH}} \boldsymbol{J}_{\mathbf{s}} \times \boldsymbol{M}$$

$$\propto \theta_{\mathrm{SH}} \boldsymbol{J}_{\mathbf{s}} \times \boldsymbol{H} \propto \theta_{\mathrm{SH}} \sin\theta_{\mathrm{H}},$$

E. Saitoh et al., Appl. Phys. Lett. **88**, 182509 (2016)
K. Ando, et al., J. Appl. Phys. **109**, 103913 (2011)
H. Nakayama, et al., Phys. Rev. B **85**, 144408 (2012)

A phenomenological model

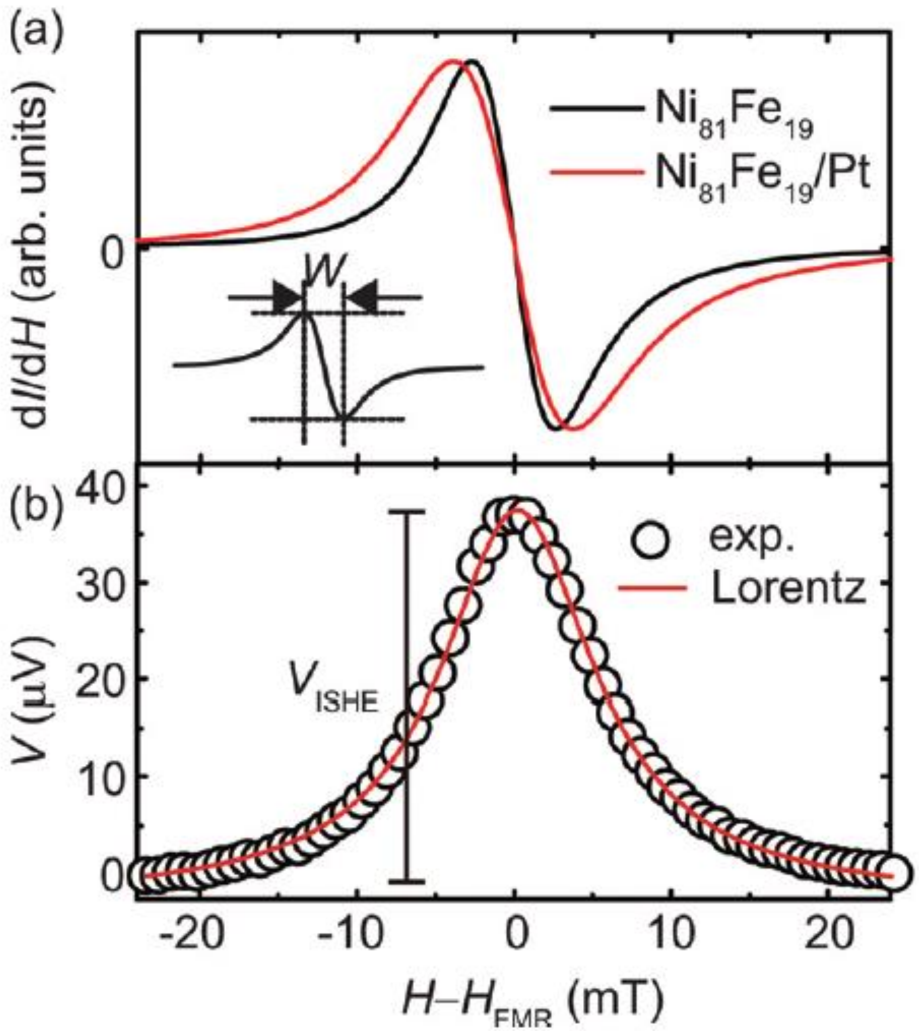

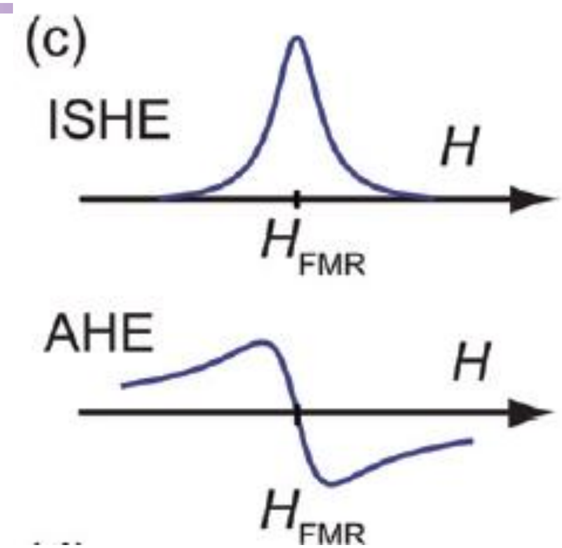

$$V = V_{ISHE}\frac{\Gamma^2}{(H-H_0)^2+\Gamma^2} + V_{AHE}\frac{-2\Gamma(H-H_0)}{(H-H_0)^2+\Gamma^2}$$

$$g_r^{\uparrow\downarrow} = \frac{2\sqrt{3}\pi M_s \gamma d_F}{g\mu_B\omega}\left(W_{F/N} - W_F\right)$$

or $$g_r^{\uparrow\downarrow} = \frac{4\pi M_s d_F}{g\mu_B}\left(\alpha_{F/N} - \alpha_F\right)$$

E. Saitoh et al., Appl. Phys. Lett. **88**, 182509 (2016)
K. Ando, et al., J. Appl. Phys. **109**, 103913 (2011)
H. Nakayama, et al., Phys. Rev. B **85**, 144408 (2012)

Antisymmetric lineshape from AHE or AMR

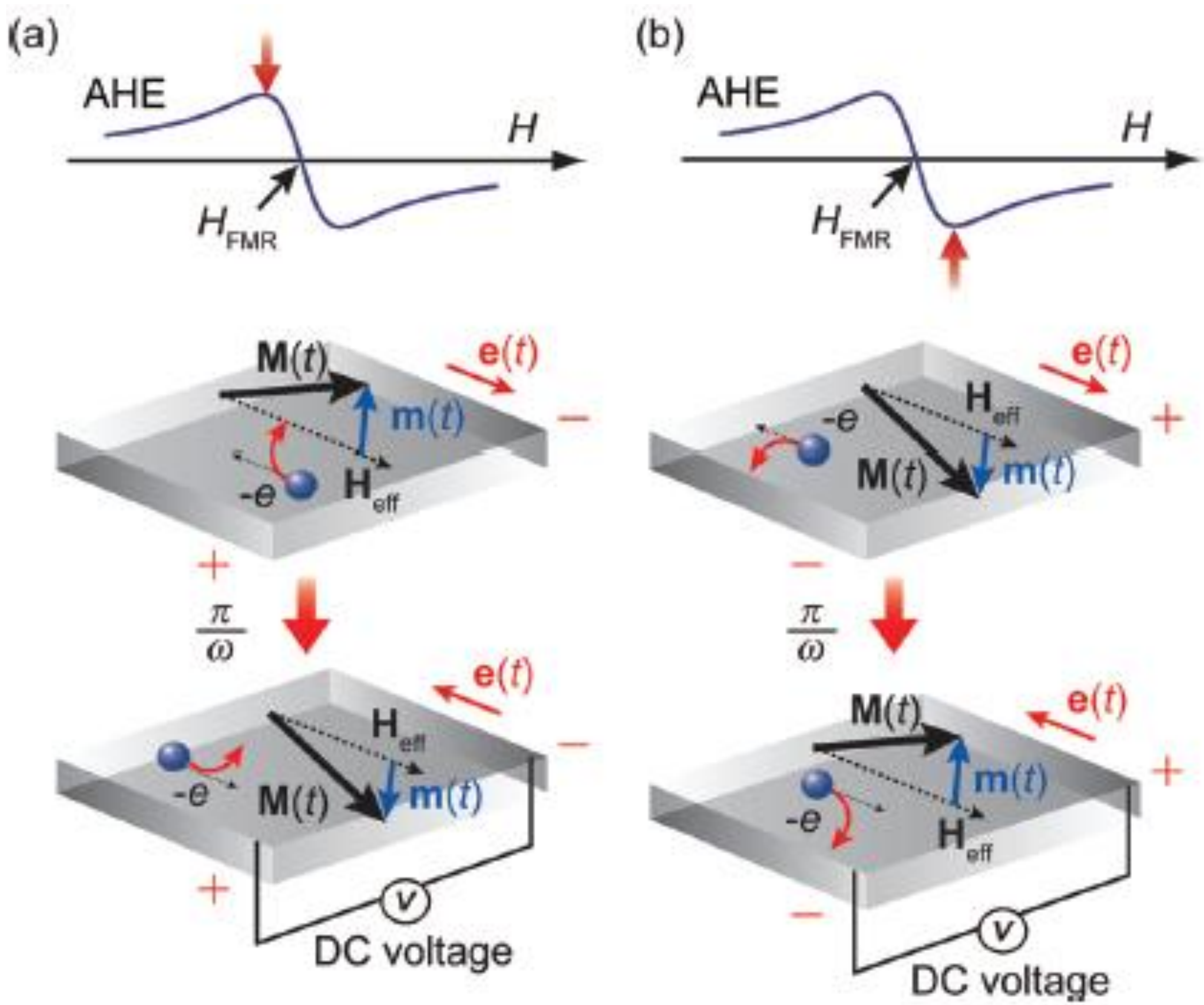

Phase shift between the microwave and magnetization determine the polarity.

Small cone angle (linear) regime

Linear power dependence

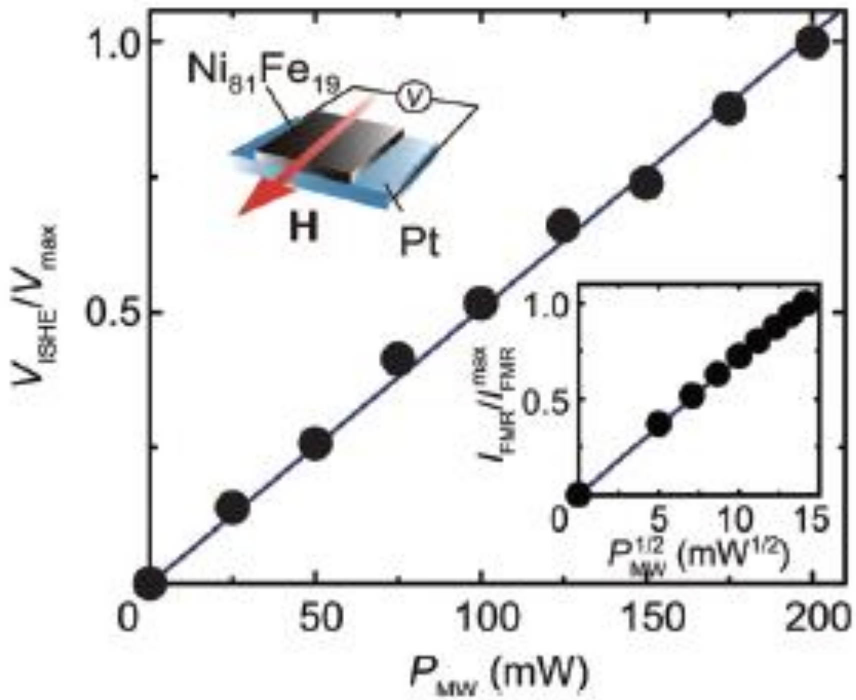

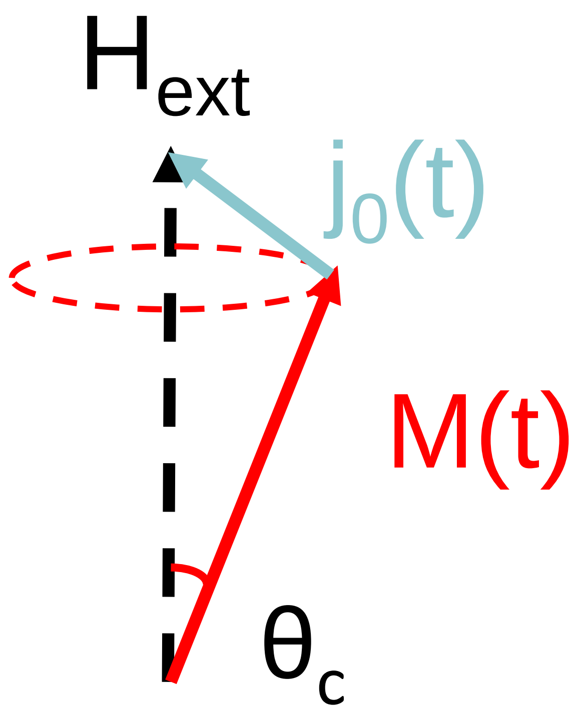

$$j_0 = \frac{g_r^{\uparrow\downarrow}\gamma^2 h_{rf}^2 \hbar\left[4\pi M_s\gamma + \sqrt{(4\pi M_s)^2\gamma^2 + 4\omega^2}\right]}{8\pi\alpha^2\left[(4\pi M_s)^2\gamma^2 + 4\omega^2\right]}$$

$$= g_r^{\uparrow\downarrow} fP\left(\frac{\gamma h_{rf}}{2\alpha\omega}\right)^2 = g_r^{\uparrow\downarrow} fP\theta_c^2$$, where $h_{rf}^2 \propto$ power

The P factor

$$P = \frac{2\omega\left[4\pi M_s\gamma + \sqrt{(4\pi M_s)^2\gamma^2 + 4\omega^2}\right]}{(4\pi M_s)^2\gamma^2 + 4\omega^2}$$

can be viewed as a correction factor.

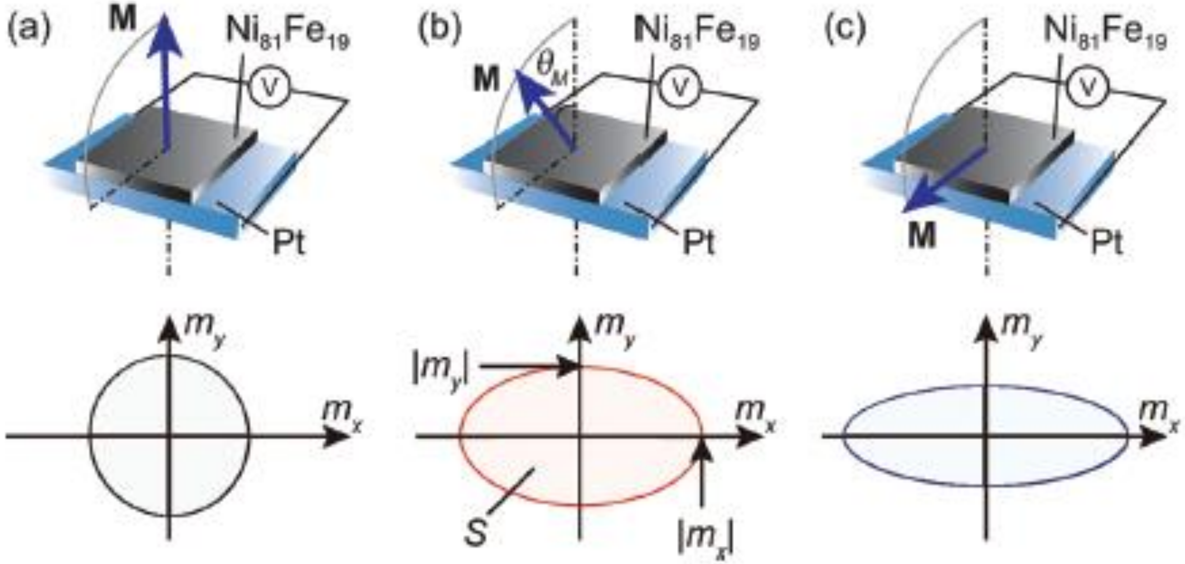

The pumped spin current is proportional to the trajectory area.

Spin pumping is an adiabatic process. (think about the Carnot engine.)

Spin distribution in normal metals

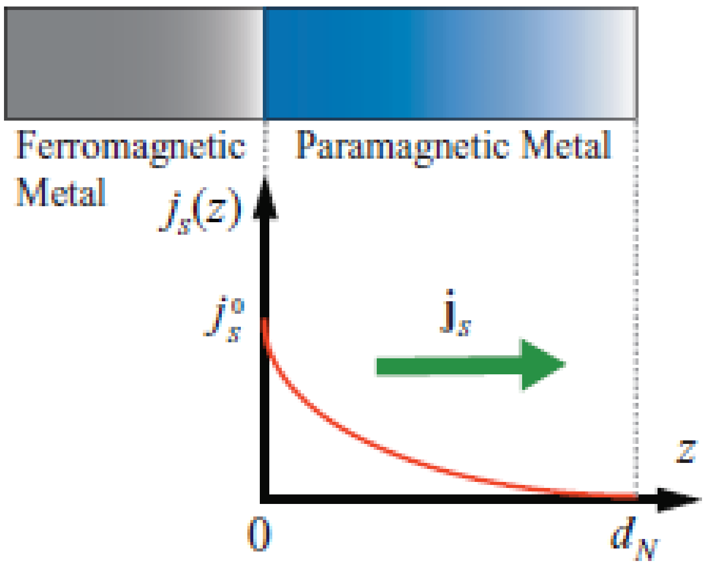

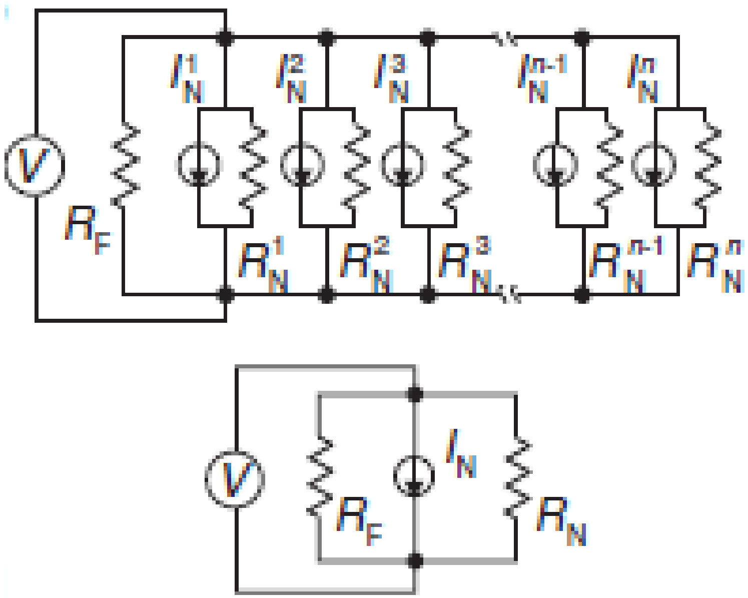

Spin Hall effect acts as a charge current source.

Solving the spin diffusion equation…

$$j_s(z) = \frac{\sinh\left[(d_N - z)/\lambda_N\right]}{\sinh(d_N/\lambda_N)} j_s^0$$

Thickness dependence

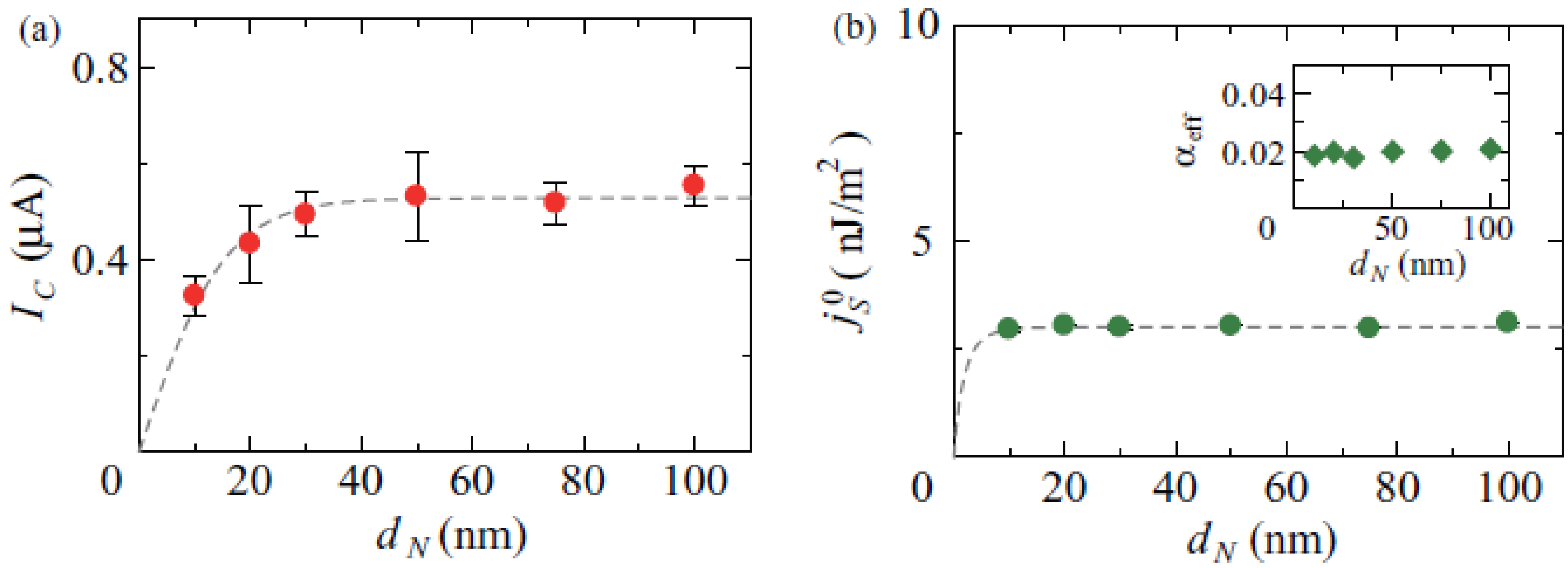

$$\langle j_c \rangle = \frac{1}{d_N}\int_0^{d_N} j_c(y)\,dy$$

$$= \theta_{SH}\left(\frac{2e}{\hbar}\right)\frac{\lambda_N}{d_N}\tanh\left(\frac{d_N}{2\lambda_N}\right) j_s^0$$

Spin backflow depends on the spin diffusion length.

Need to get the thickness dependence data to calculate the spin Hall angle

PRL 112, 197201 (2014) PHYSICAL REVIEW LETTERS week ending 16 MAY 2014

Scaling of Spin Hall Angle in 3d, 4d, and 5d Metals from $Y_3Fe_5O_{12}$/Metal Spin Pumping

H. L. Wang,[1] C. H. Du,[1] Y. Pu,[1] R. Adur,[1] P. C. Hammel,[1,*] and F. Y. Yang[1,†]
[1]*Department of Physics, The Ohio State University, Columbus, Ohio 43210, USA*
(Received 23 September 2013; revised manuscript received 24 December 2013; published 15 May 2014)

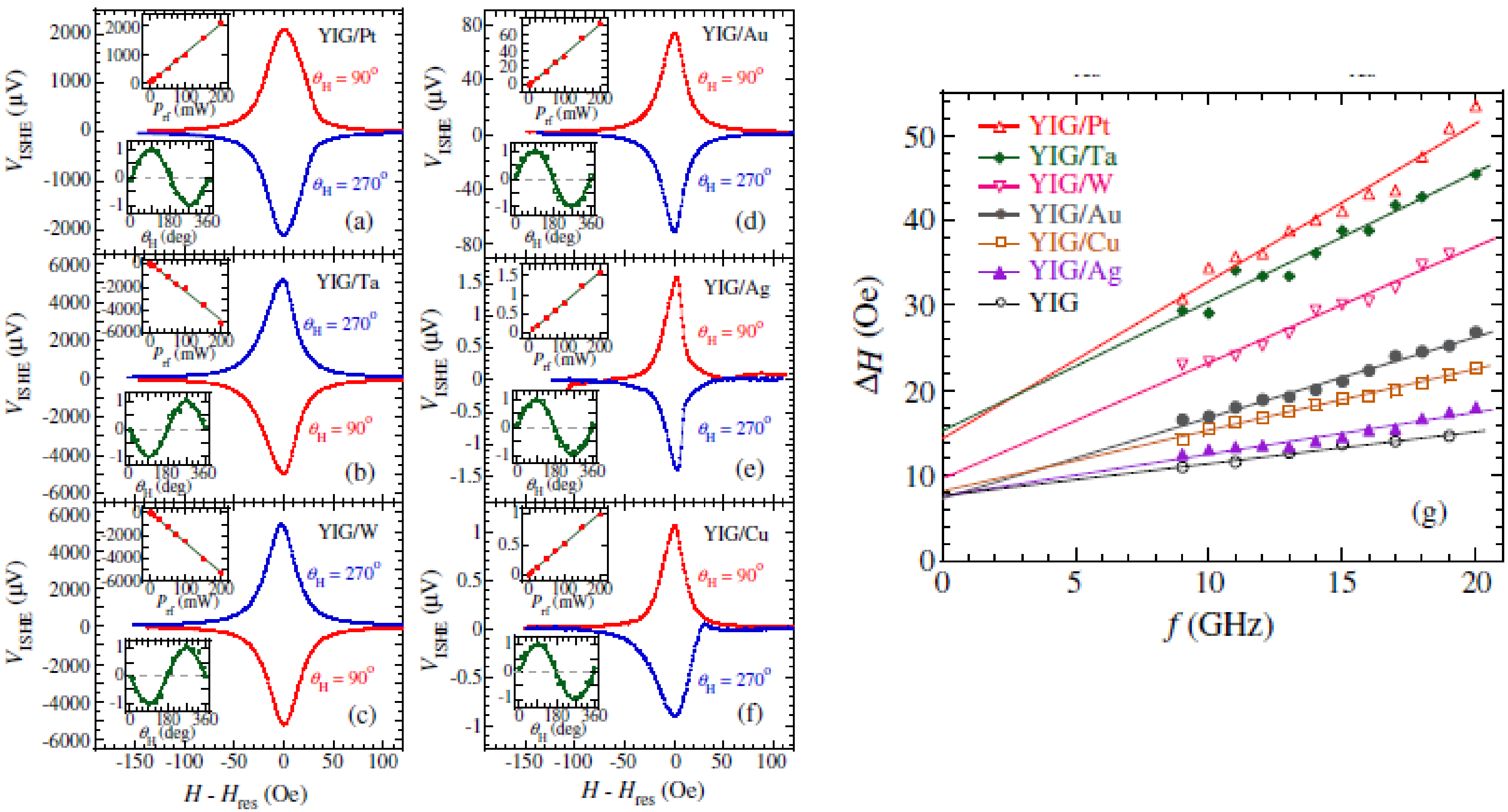

Bilayer	V_{ISHE}	ΔH change	α_{sp}	$\rho(\Omega m)$	$g_{\uparrow\downarrow}(m^{-2})$	λ_{SD}(nm)	θ_{SH}	$J_s(A/m^2)$
YIG/Pt	2.10 mV	24.3 Oe	$(3.6 \pm 0.3) \times 10^{-3}$	4.8×10^{-7}	$(6.9 \pm 0.6) \times 10^{18}$	7.3	0.10 ± 0.01	$(2.0 \pm 0.2) \times 10^{7}$
YIG/Ta	−5.10 mV	16.5 Oe	$(2.8 \pm 0.2) \times 10^{-3}$	2.9×10^{-6}	$(5.4 \pm 0.5) \times 10^{18}$	1.9	-0.071 ± 0.006	$(1.6 \pm 0.2) \times 10^{7}$
YIG/W	−5.26 mV	12.3 Oe	$(2.4 \pm 0.2) \times 10^{-3}$	1.8×10^{-6}	$(4.5 \pm 0.4) \times 10^{18}$	2.1	-0.14 ± 0.01	$(1.4 \pm 0.1) \times 10^{7}$
YIG/Au	72.6 μV	5.50 Oe	$(1.4 \pm 0.1) \times 10^{-3}$	4.9×10^{-8}	$(2.7 \pm 0.2) \times 10^{18}$	60	0.084 ± 0.007	$(7.6 \pm 0.7) \times 10^{6}$
YIG/Ag	1.49 μV	1.30 Oe	$(2.7 \pm 0.2) \times 10^{-4}$	6.6×10^{-8}	$(5.2 \pm 0.5) \times 10^{17}$	700	0.0068 ± 0.0007	$(1.5 \pm 0.1) \times 10^{6}$
YIG/Cu	0.99 μV	3.70 Oe	$(8.1 \pm 0.6) \times 10^{-4}$	6.3×10^{-8}	$(1.6 \pm 0.1) \times 10^{18}$	500	0.0032 ± 0.0003	$(4.6 \pm 0.4) \times 10^{6}$

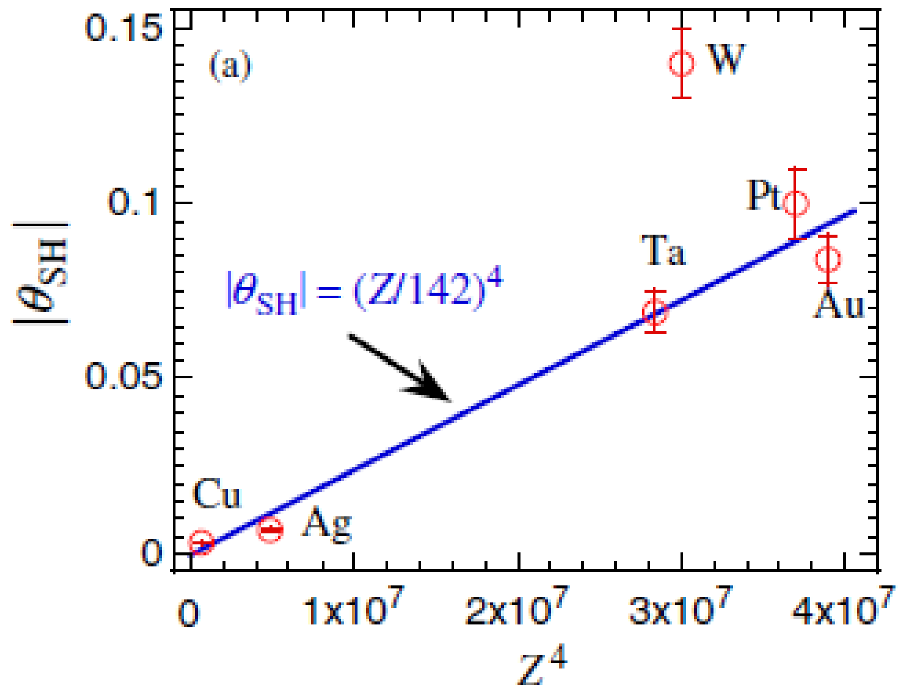

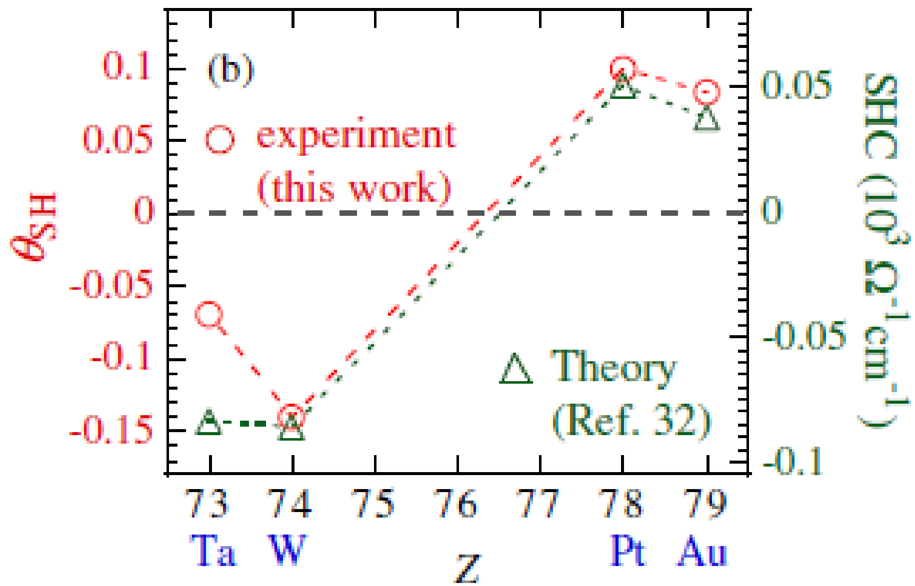

Spin Hall angles strongly depend on the d-electron count.

	T (K)	λ_{sd} (nm)	σ_{NM} (10^6 S/m)	α_{SH} (%)
Al	4.2	455 ± 15	10.5	0.032 ± 0.006
	4.2	705 ± 30	17	0.016 ± 0.004
Au	295	86 ± 10	37	11.3
	295	83	37	3
	4.5	65*	48.3	<2.3
	295	36*	25.7	<2.7
	295	35 ± 4	28	7.0 ± 0.1
	295	27 ± 3	14	7.0 ± 0.3
	295	25 ± 3	14.5	12 ± 4
	295	50 ± 8	16.7	0.8 ± 0.2
	<10	40 ± 16	25	1.4 ± 0.4
	295	35 ± 3*	25.2	0.35 ± 0.03
	295	35	20	0.25 ± 0.1
	295	35 ± 3*	5.25	1.6 ± 0.1
	295	35 ± 3*	7	0.335 ± 0.006
	295	35*		1.1 ± 0.3
	295	60	20.4	8.4 ± 0.7
AuW	295	1.9	1.75	>10
Ag	295	700	15	0.7 ± 0.1
Bi	3	0.3 ± 0.1	-	>0.3
	295	-	2.4 ± 0.3(I)	−(7.1 ± 0.8)(I)
			50 ± 12(V)	1.9 ± 0.2(V)
Cu	295	500	16	0.32 ± 0.03
CuIr	10	5–30		2.1 ± 0.6
CuMn$_x$T$_y$				0.7(Ta); 2.6(Ir)
IrO$_2$	300	3.8(P)	0.5(P); 0.18(A)	4(P); 6.5(A)

	T (K)	λ_{sd} (nm)	σ_{NM} (10^6 S/m)	α_{SH} (%)
Mo	10	10	3.03	−0.20
	10	10	0.667	−0.075
	10	8.6 ± 1.3	2.8	−(0.8 ± 0.18)
	295	35 ± 3*	4.66	−(0.05 ± 0.01)
Nb	10	5.9 ± 0.3	1.1	−(0.87 ± 0.20)
Pd	10	13 ± 2	2.2	1.2 ± 0.4
	295	9*	1.97	1.0
	295	15 ± 4*	4.0	0.64 ± 0.10
	295	5.5 ± 0.5	5	1.2 ± 0.3
	295	2.0 ± 0.1	3.7	0.8 ± 0.20
Pt	295		6.41	0.37
	5	8	8.0	0.44
	295	7	5.56	0.9
	10	11 ± 2	8.1	2.1 ± 0.5
	10	~10	8.1	2.4
	295	7*	6.4	8.0
	295	10 ± 2*	2.4	1.3 ± 0.2
	295	10*	2	4.0
	295	3.7 ± 0.2	2.42	8 ± 1
	295	8.3 ± 0.9	4.3 ± 0.2	1.2 ± 0.2
	295	7.7 ± 0.7	1.3 ± 0.1	1.3 ± 0.1
	295	1.5 – 10*	2.45 ± 0.1	$3^{+4}_{-1.5}$
	295	4	4	2.7 ± 0.5
	295	8 ± 1*	1.02	2.012 ± 0.003
	295	1.3*	2.4	2.1 ± 1.5
	295	1.2		8.6 ± 0.5
	295	1.4*		12 ± 4
W	295	2.1	0.55	−14 ± 1
	295		0.38 ± 0.06	−(33 ± 6)

1. The larger spin Hall angles, the shorter spin diffusion lengths.
2. Depending on techniques, materials preparation and geometry, the calculated spin Hall angle can vary by 1 order of magnitude.
3. Rashba effect (broken inversion symmetry) at the interface adds complexity to analyses.

Spurious effects

- Microwave induced Seebeck effect in semiconductor.

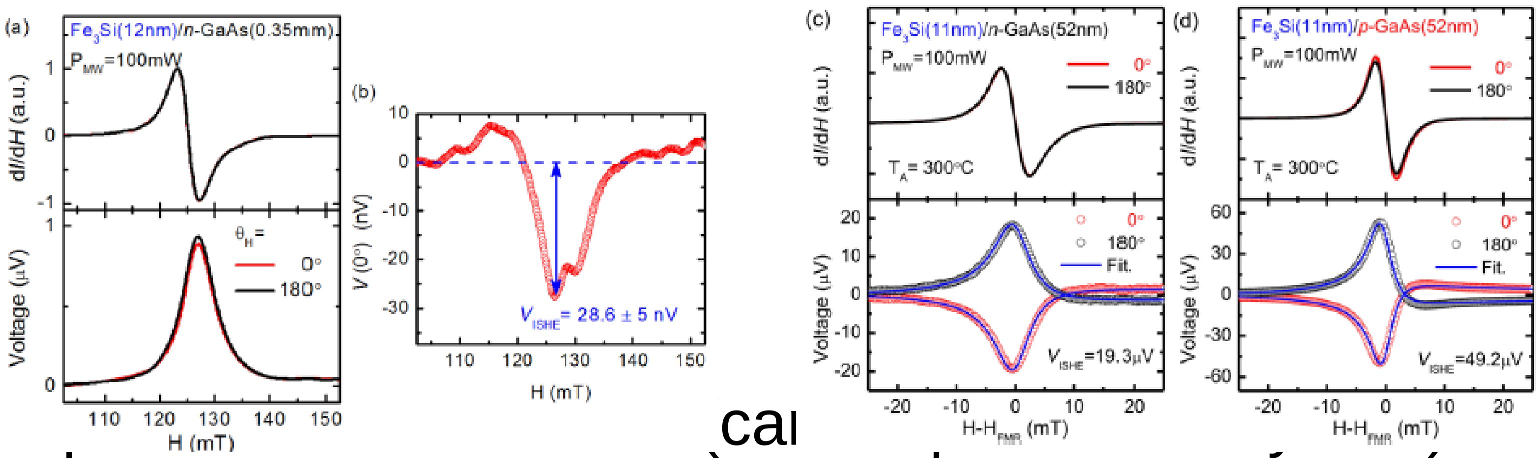

- cal

  - the boundary conditions, phase shift between E and B field can strongly affect voltage signals.

- Self-induced ISHE and spin backflow. (can be prevented by YIG)

Universal Method for Separating Spin Pumping from Spin Rectification Voltage of Ferromagnetic Resonance

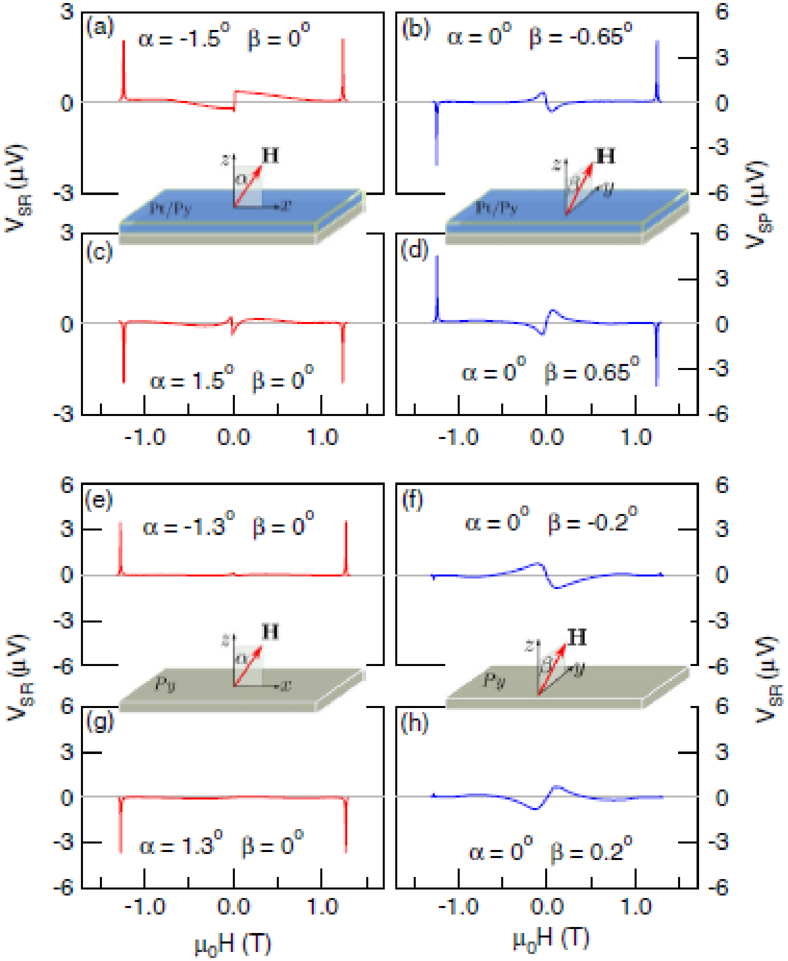

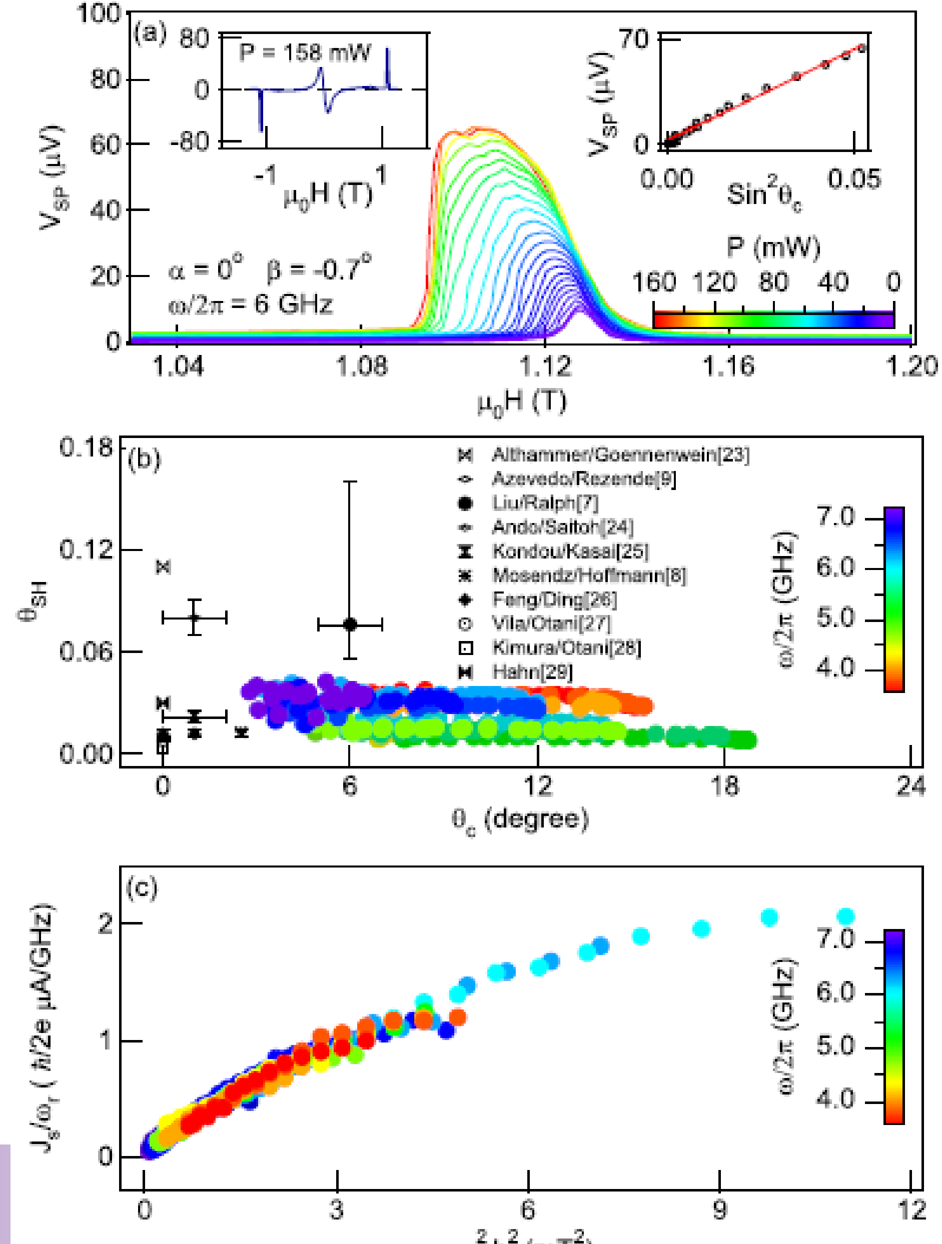

NTU/NTHU

Spin-torque ferromagnetic resonance (ST-FMR)

PRL 106, 036601 (2011) PHYSICAL REVIEW LETTERS week ending 21 JANUARY 2011

Spin-Torque Ferromagnetic Resonance Induced by the Spin Hall Effect

Luqiao Liu, Takahiro Moriyama, D. C. Ralph, and R. A. Buhrman
Cornell University, Ithaca, New York, 14853
(Received 12 October 2010; published 20 January 2011)

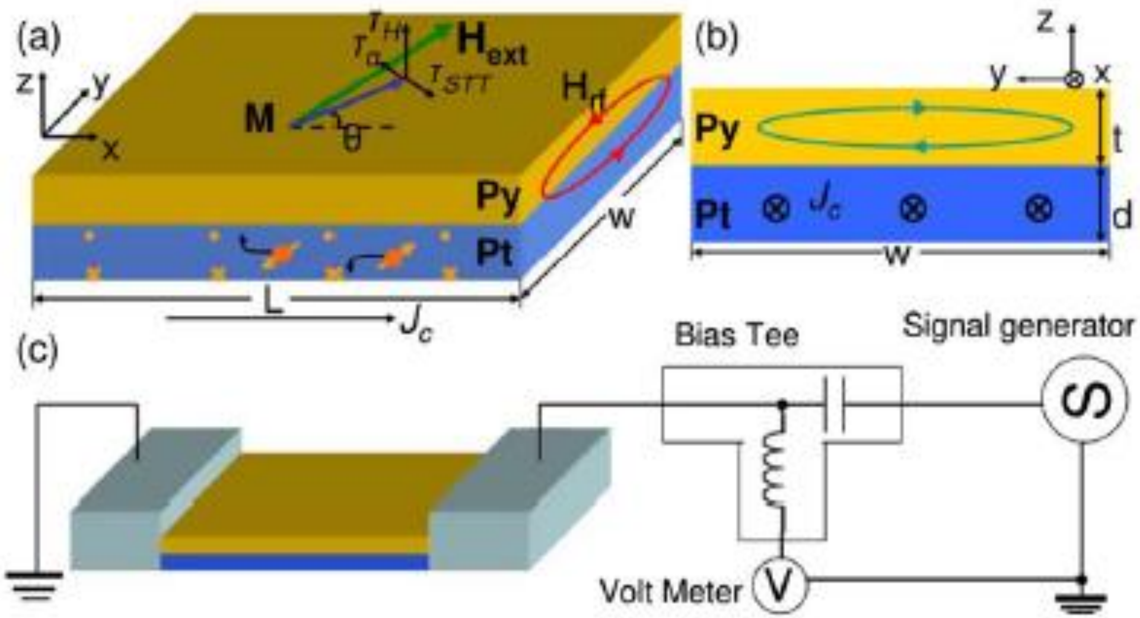

$$\frac{d\hat{m}}{dt} - \gamma\hat{m}\times\vec{H}_{eff} + \alpha\hat{m}\times\frac{d\hat{m}}{dt} + \gamma\frac{\hbar}{2e\mu_0 M_S t}J_{S,rf}\left(\hat{m}\times\hat{\sigma}\times\hat{m}\right) - \gamma\hat{m}\times\vec{H}_{rf}$$

Anti-damp torques

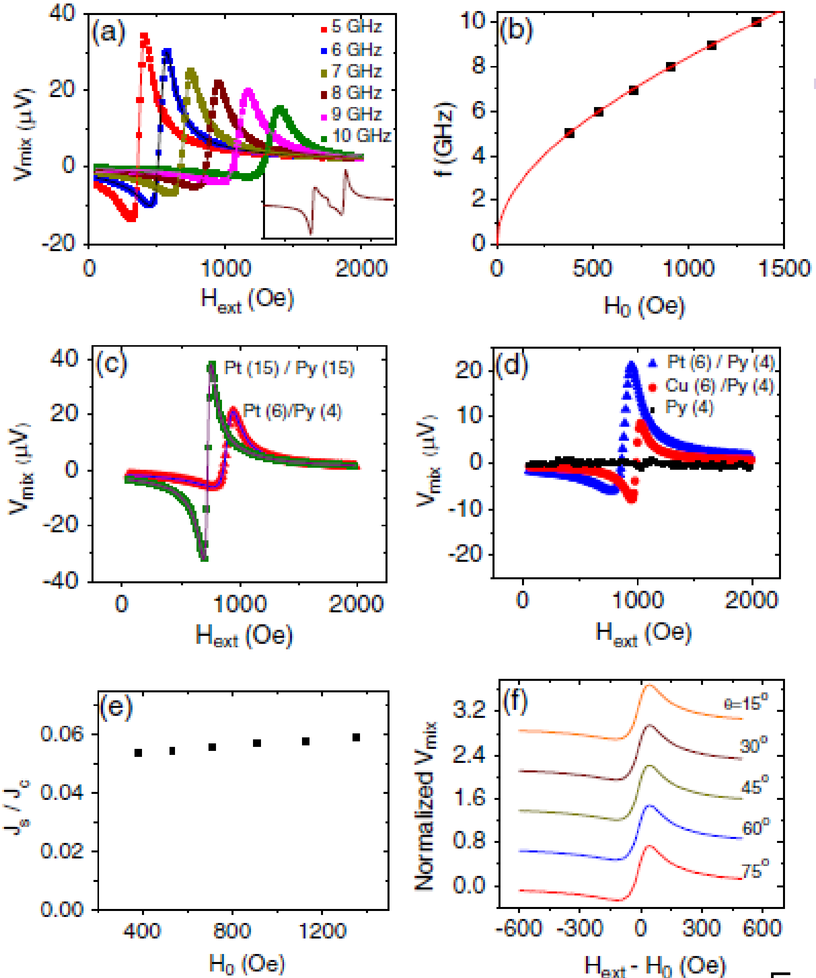

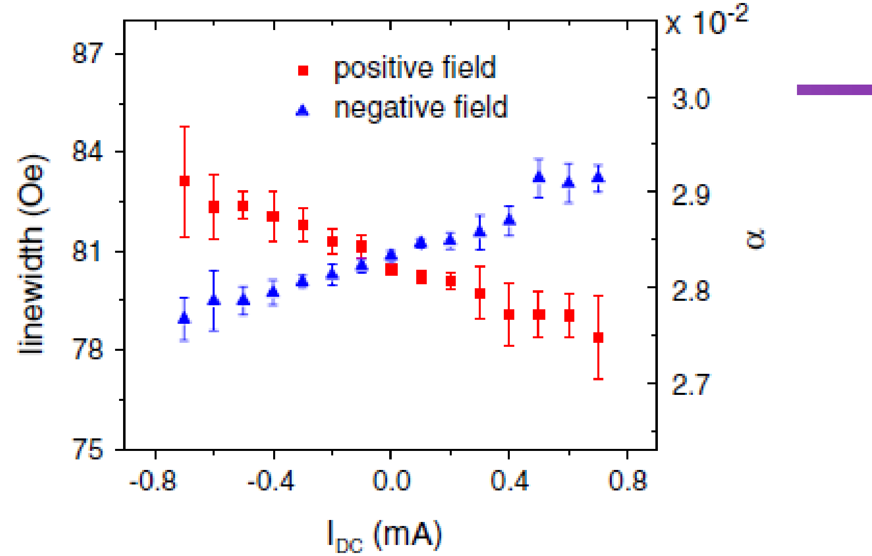

Rely on AMR to generate voltage signals. Not suitable for magnetic insulator.

Special case: Pt/YIG, Ta/YIG…

$$V_{mix} = -\frac{1}{4}\frac{dR}{d\theta}\frac{\gamma I_{rf}\cos\theta}{\Delta 2\pi\left(df/dH\right)|_{H_{ext}=H_0}}\left[S\frac{\Delta^2}{\Delta^2+\left(H_{ext}-H_0\right)^2}+A\frac{\left(H_{ext}-H_0\right)\Delta}{\Delta^2+\left(H_{ext}-H_0\right)^2}\right]$$

$$\frac{J_{S,rf}}{J_{C,rf}} = \frac{S}{A}\frac{e\mu_0 M_S td}{\hbar}\left[1+\left(4\pi M_{eff}/H_{ext}\right)\right]^{1/2}$$

The spin Hall angle can be determined from the relative magnitude of the two components.

Modulation of magnetization damping (MOD)

PRL **101,** 036601 (2008)

PHYSICAL REVIEW LETTERS

week ending
18 JULY 2008

Electric Manipulation of Spin Relaxation Using the Spin Hall Effect

K. Ando,[1,*] S. Takahashi,[2,3] K. Harii,[1] K. Sasage,[1] J. Ieda,[2,3] S. Maekawa,[2,3] and E. Saitoh[1,4]

[1]*Department of Applied Physics and Physico-Informatics, Keio University, Yokohama 223-8522, Japan*
[2]*Institute for Materials Research, Tohoku University, Sendai 980-8577, Japan*
[3]*CREST, Japan Science and Technology Agency, Kawaguchi, Saitama 332-0012, Japan*
[4]*PRESTO, Japan Science and Technology Agency, Kawaguchi, Saitama 332-0012, Japan*

(Received 17 March 2008; published 18 July 2008)

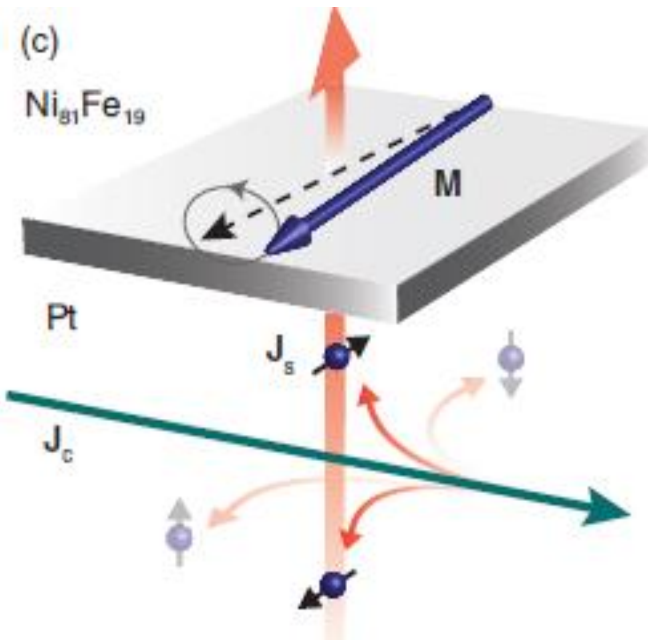

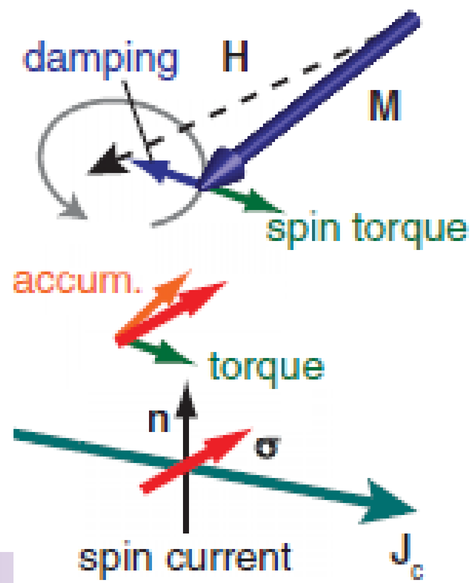

Modulation of magnetization damping (MOD)

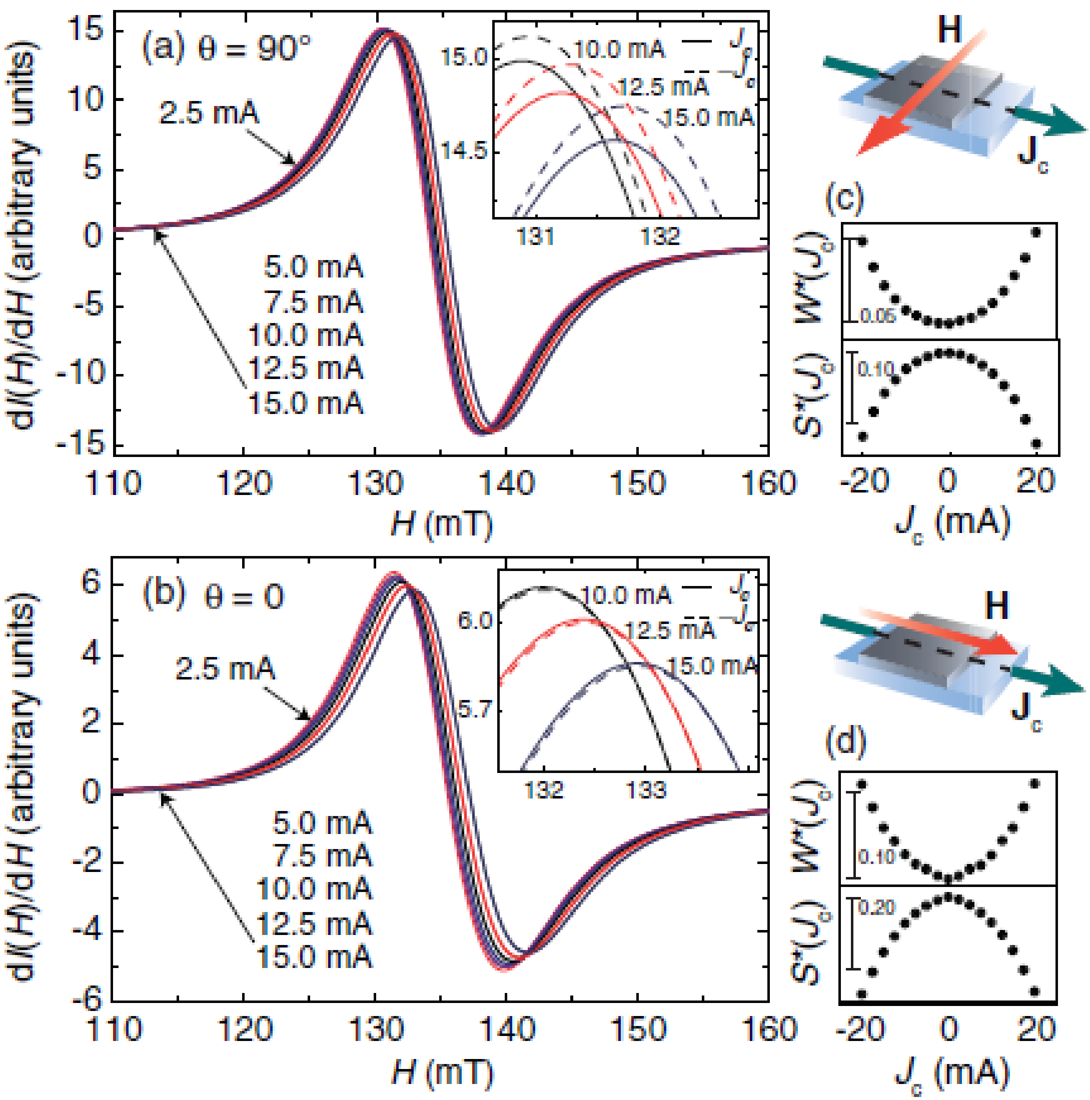

Thermal effects on FMR spectra can be serious.

Need to change the in-plane field angle to separate the spin-transfer effect from the thermal effect.

Modulation of magnetization damping (MOD)

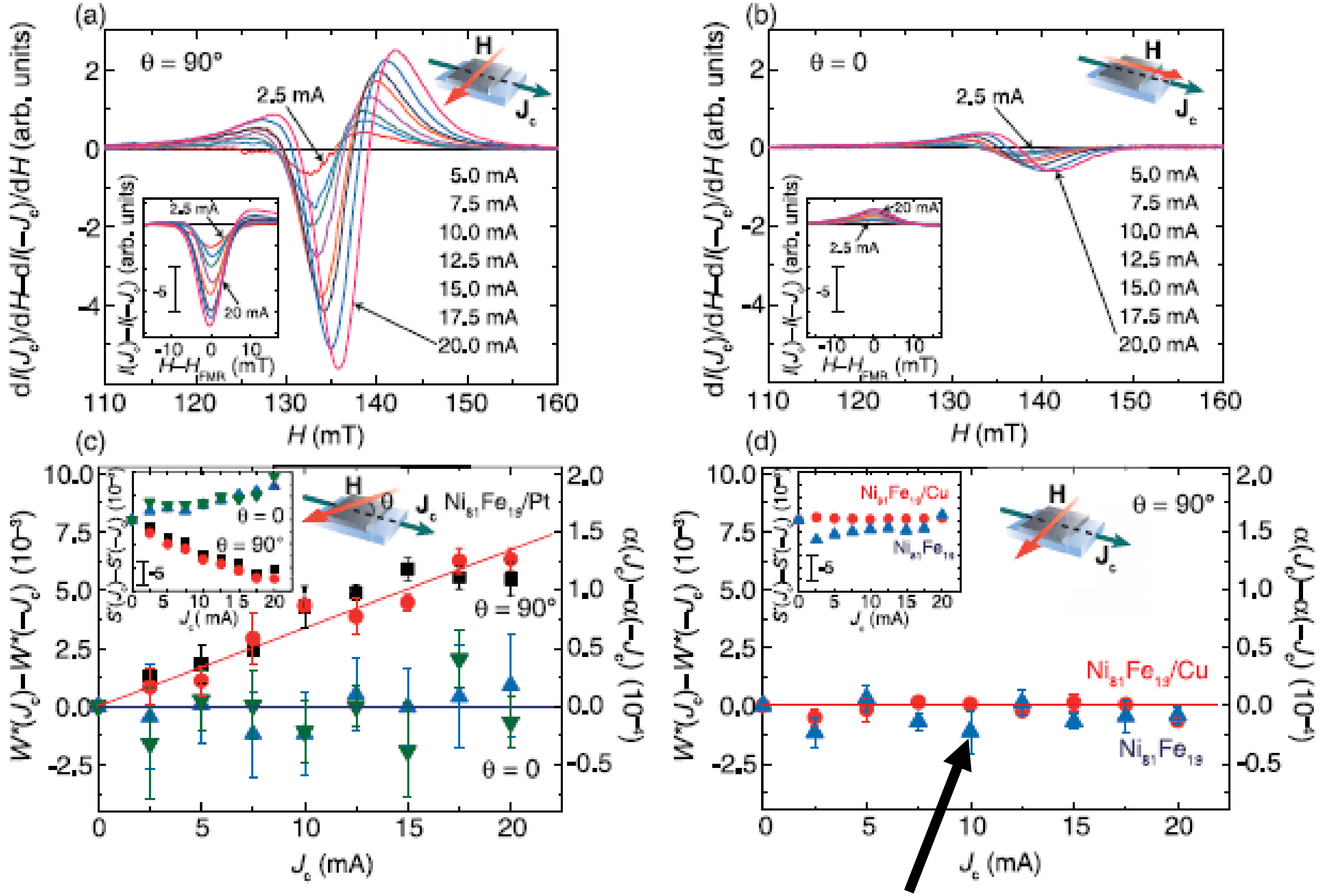

Controlled sample Py/Cu: Cu has small spin Hall angle.

Investigation of interfacial and spin transport properties of topological insulator/magnetic insulator heterostructures by spin pumping

Yu-Ting Fanchiang, Y. H. Lin, K. Y. Lin, C. K. Cheng, M. Hong

Department of Physics, National Taiwan University

H. Y. Hung, C. N. Wu, Y. C. Liu, H. Y. Lin, K. H. Chen, C. C. Tseng, C. C. Chen, S. R. Yang, S. W. Huang, M. X. Guo, J. Kwo

Department of Physics, National Tsing-Hua University

S. F. Lee

Institute of Physics, Academia Sinica

J. G. Lin

Center for Condensed Matter Sciences, National Taiwan University

Outline

Introduction

- Spin pumping in topological insulators (TIs)
- Magnetic proximity effect (MPE) in TI/magnetic insulator heterostructures

Experimental results

- Spin pumping and spin-to-charge conversion (SCC) in TI/ferromagnetic metals and Py/Al_2O_3/Bi_2Se_3
- Surface-state-modulated magnetization dynamics in Bi_2Se_3/YIG
- Signatures of MPE in Bi_2Se_3/YIG and zero-field FMR
- Negative magnetoresistance (MR) and exchange gap opening in Bi_2Se_3/ReIG
- Spin pumping and SCC in transferred Bi_2Se_3/Au/YIG

Conclusions

Topological insulators (TI)

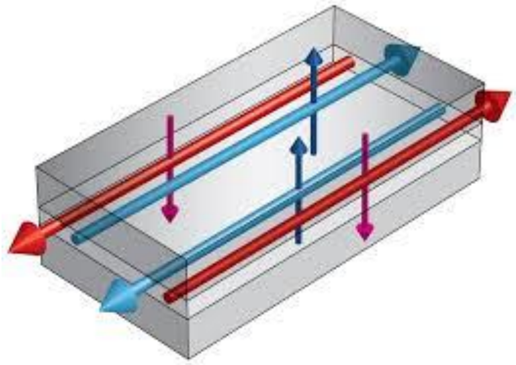

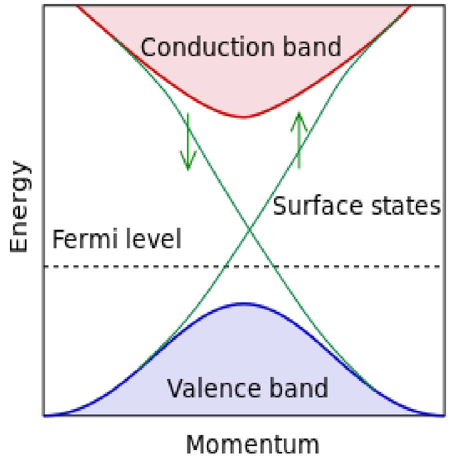

band inversion

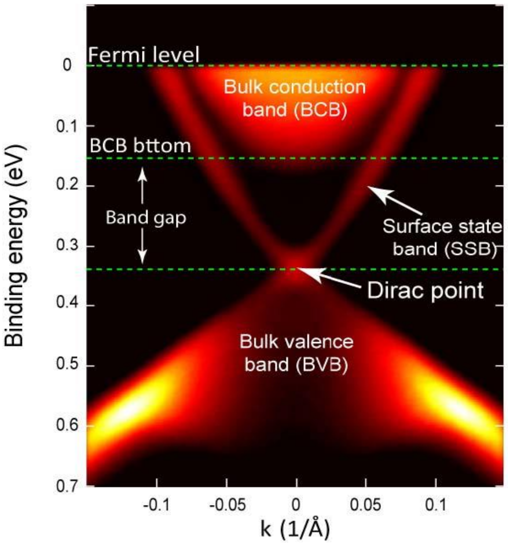

Electronic band structure along K-Γ-K of undoped Bi_2Se_3 by ARPES, Y. L. Chen et al, Science, (2010).

- **Extraordinary physical properties**
  - Quantum spin Hall state
  - Strong spin orbit coupling + time-reversal symmetry
  - ⇒ Spin-momentum locking

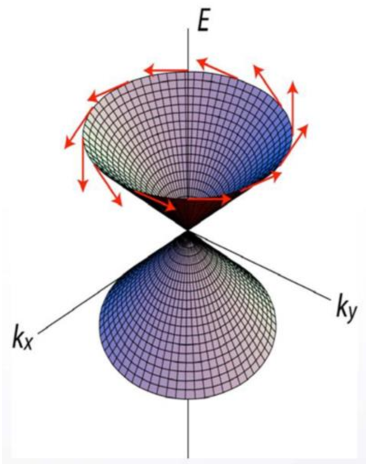

- **Applications**
  - Low dissipation spintronics and spin-caloritronics
  - High spin–charge conversion device, such as a “spin battery”.
  - Interface of TI and superconductor - Majorana fermion, quantum computation

Ferromagnetic resonance (FMR)

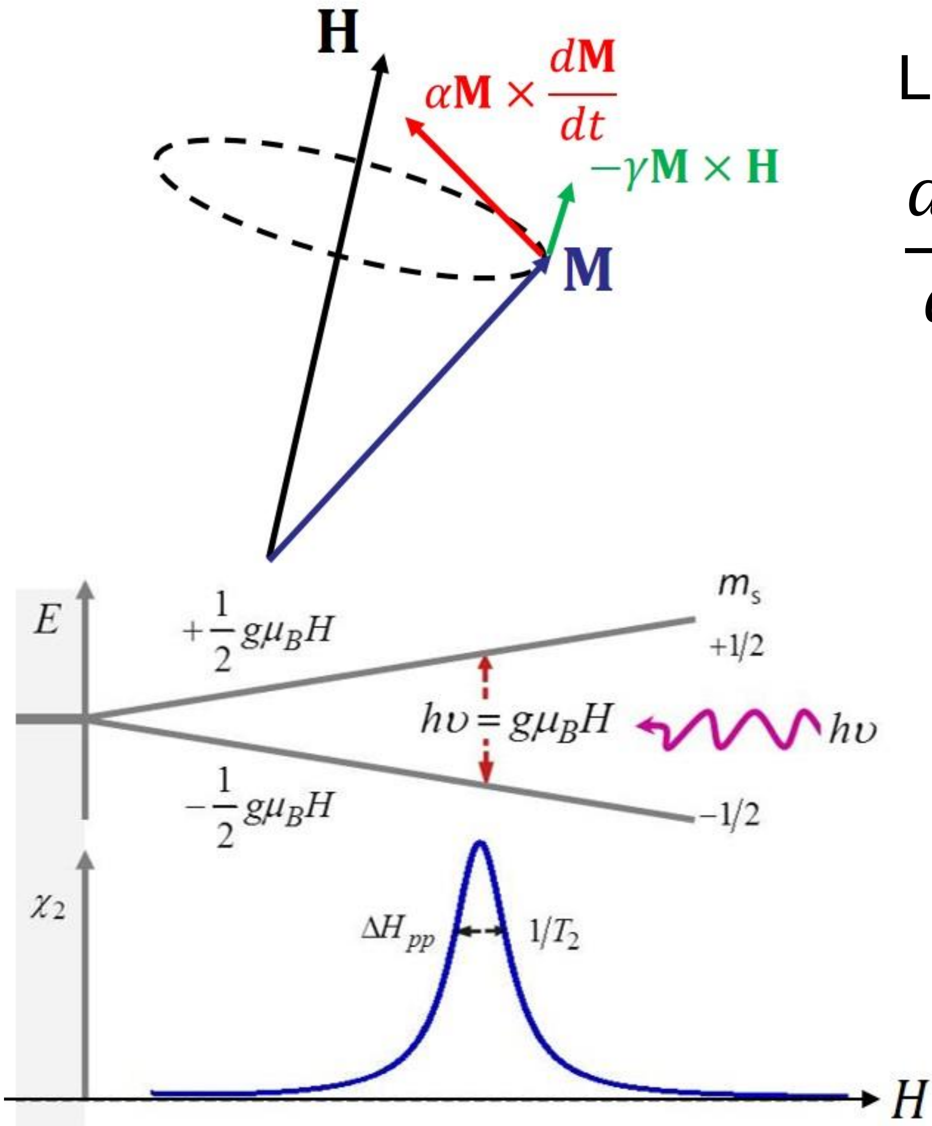

Landau–Lifshitz–Gilbert equation

$$\frac{d\mathbf{M}}{dt} = -\gamma \mathbf{M} \times \mathbf{H} + \alpha \mathbf{M} \times \frac{d\mathbf{M}}{dt}$$

Cavity

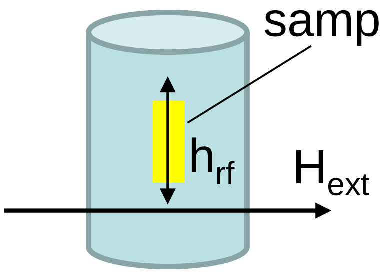

Coplanar waveguide

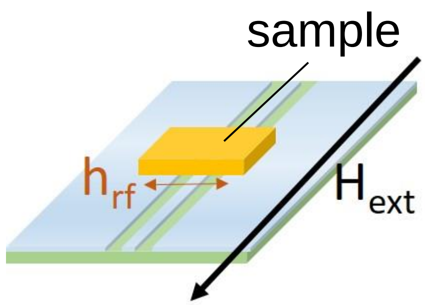

Application:
Measurement of magnetic anisotropy
Measurement of damping constant α
Spin pumping

Spin pumping: a solution to impedance mismatch problem

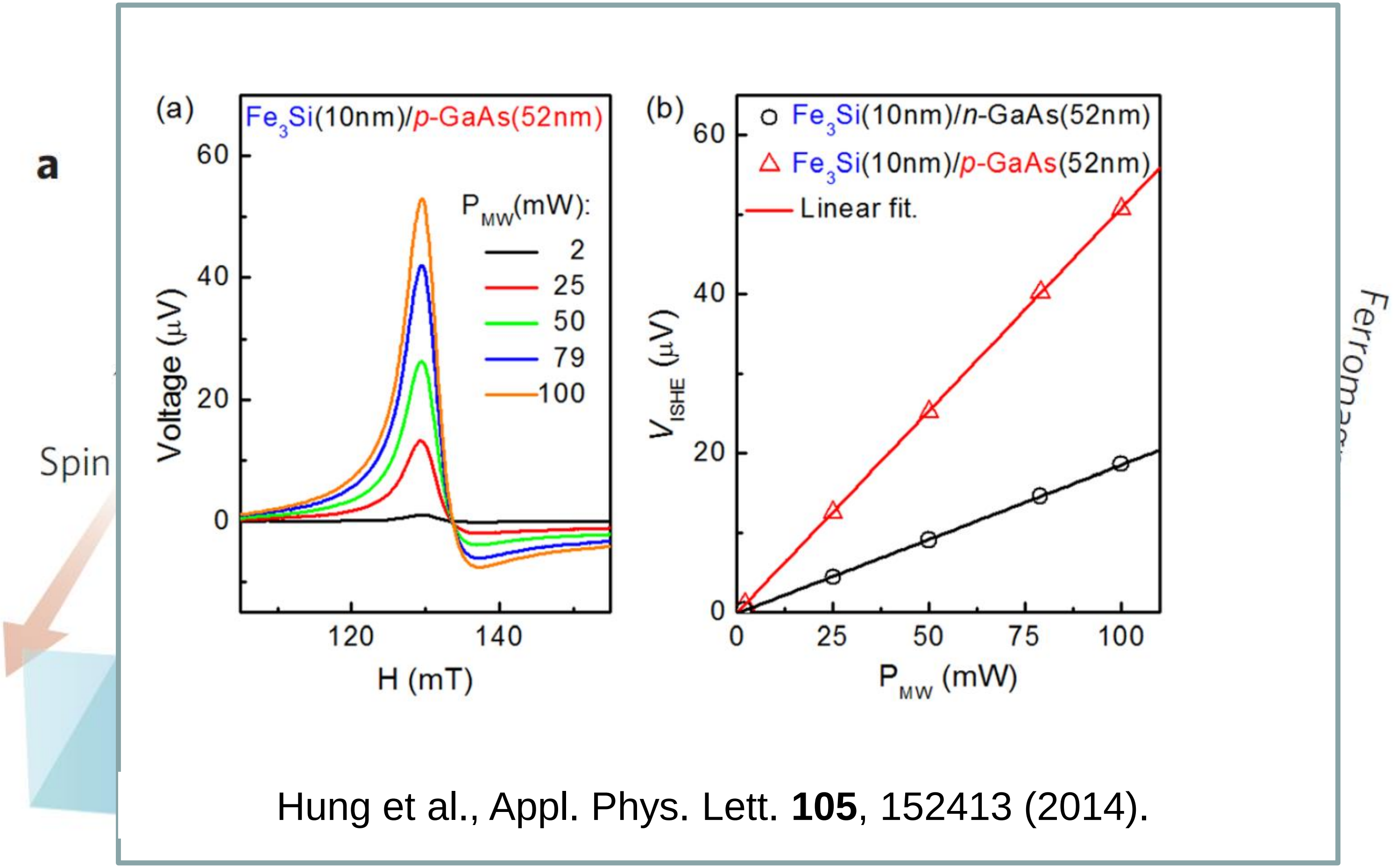

Hung et al., Appl. Phys. Lett. **105**, 152413 (2014).

Ando et al., Nat. Mater. **10**, 655 (2013).

Concept of "Spin pumping to TI" experiment

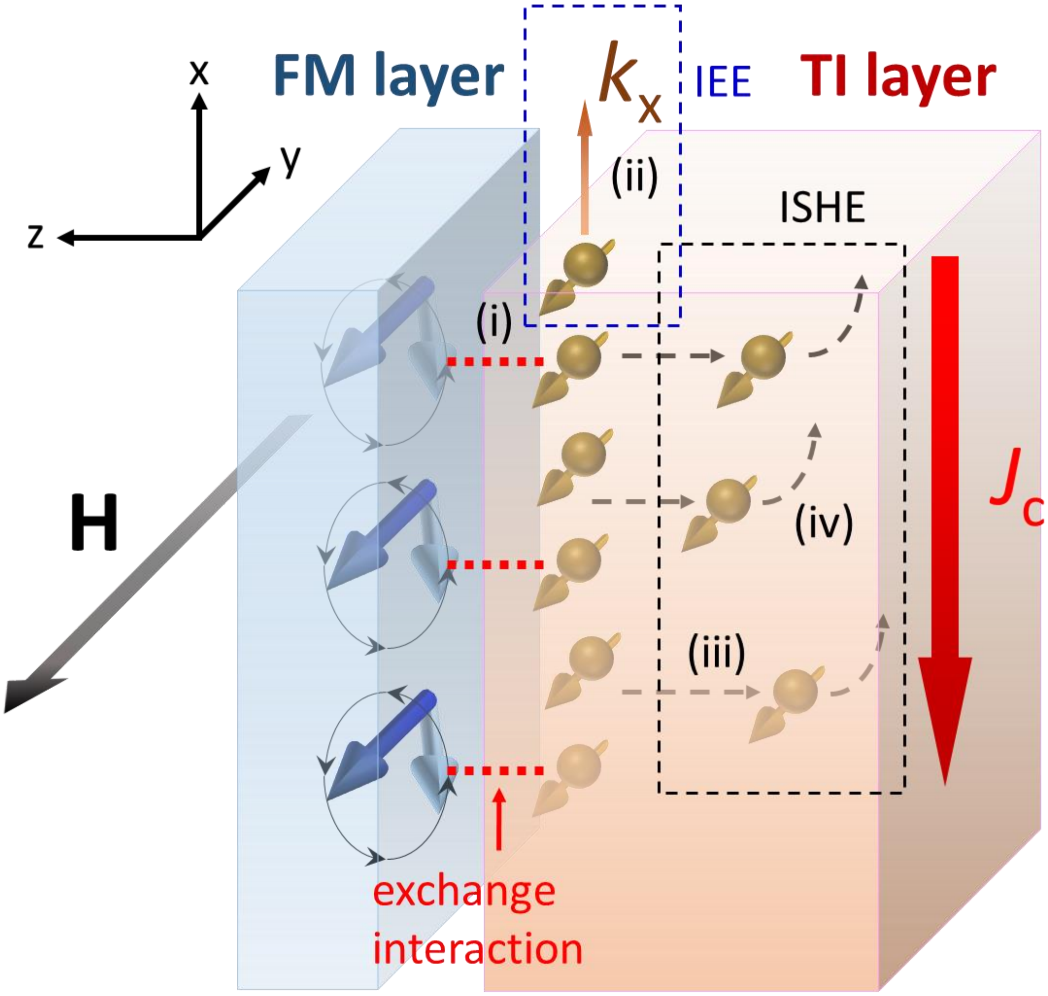

(i) Spin injection to the TI layer by exchange interaction

(ii) SCC by spin-momentum locking of TSS

(iii) Spin diffusion to the TI bulk

(iv) SCC by SHE of the TI bulk

Spin-charge conversion in 2D systems

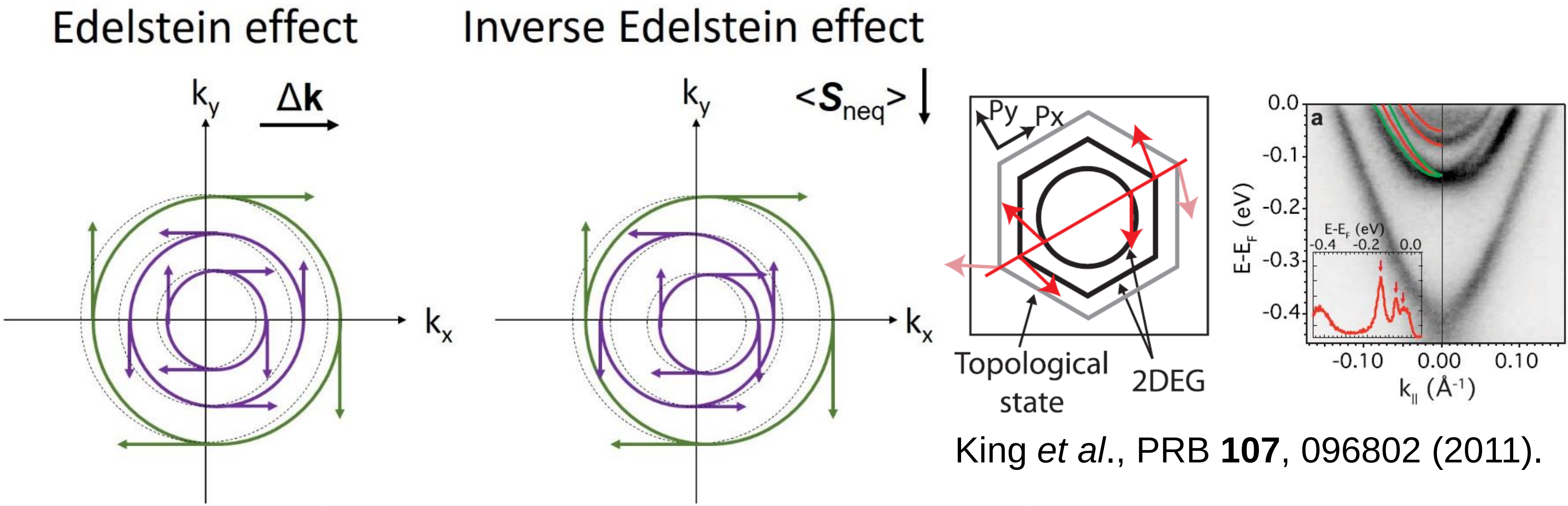

King *et al*., PRB **107**, 096802 (2011).

	Inverse spin Hall effect (ISHE)	Inverse Edelstein effect (IEE)
location	bulk	surface
condition	Spin current normal to the interface	"non-equilibrium" spin density at interface
material	Normal metals and semiconductors including 3D TIs	TIs and Rasba materials possessing k-dependent spin-polarized states

Spin pumping as an effective way to probe the spin-momentum locking

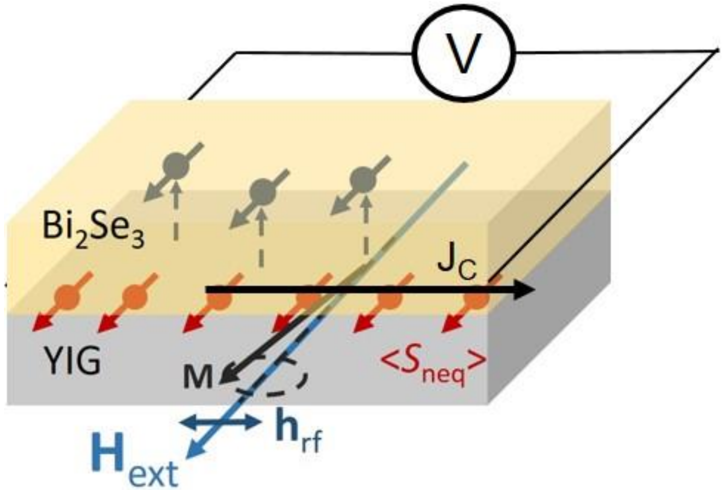

Spin pumping: a widely used spin injection method

FMR in the magnetic layer

→Exchange interaction at the interface: transfer of spin angular momentum

→Spin accumulation at the interface

→Charge current generated via spin-momentum locking

Various material systems and experimental configurations have been reported.

E. Saitoh group

Py/Cu/Sn-BiTeSe

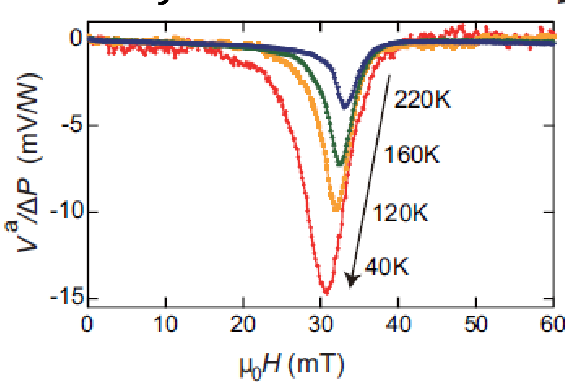

PRB **94**, 204404 (2016).

A. Fert group

Fe/Ag/α-Sn

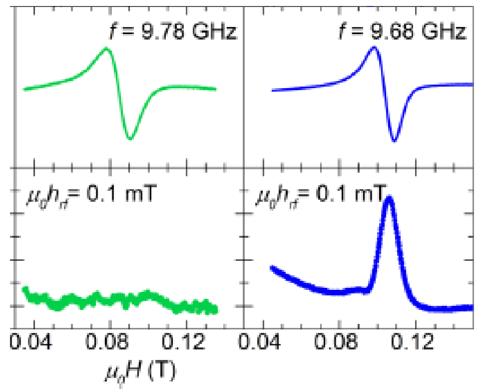

PRL **116**, 096602 (2016).

N. Samarth group

Bi_2Se_3/YIG

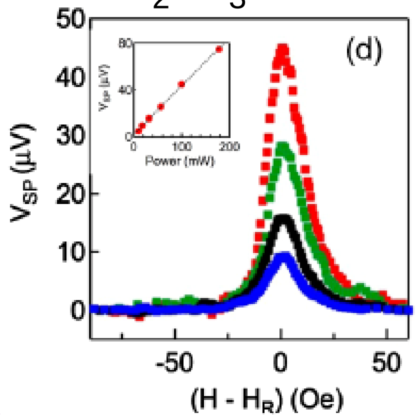

PRL **117,** 076601 (2016).

Challenges of spin pumping into TIs

- Bulk conduction of TIs obscures the effect of topological surface states
- Large variation in reported effective spin Hall angle θ_{SH}
  - **0.022** in Bi_2Se_3/Py at 15 K (Deorani et al. (2014))
  - **~10^{-4}** in bulk insulating $Bi_{1.5}Sb_{0.5}Te_{1.7}Se_{1.3}$ at 15 K (Shiomi et al. (2014))
  - **0.021-0.43** in Bi_2Se_3/CoFeB at RT (Jamali et al. (2015))
  - **0.27-0.62** in Fe/Ag/α-Sn at RT (Rojas-Sánchez et al. (2016))
  - **~0.02** in Bi_2Se_3/YIG at RT (Wang et al. (2016))
- Current shunting effect by ferromagnetic metals in ST-FMR measurement

Ferrimagnetic insulator YIG with high thermal stability is an ideal spin source.

Breaking the time-reversal-symmetry of TI surface state

Experimental observations

1. Gap opening of TI surface states
2. Quantum anomalous Hall effect (QAHE)
3. Topological magnetoelectric effe

$(Bi_{0.58}Fe_{0.12})_2Se_{3.7}$

Fe 16%

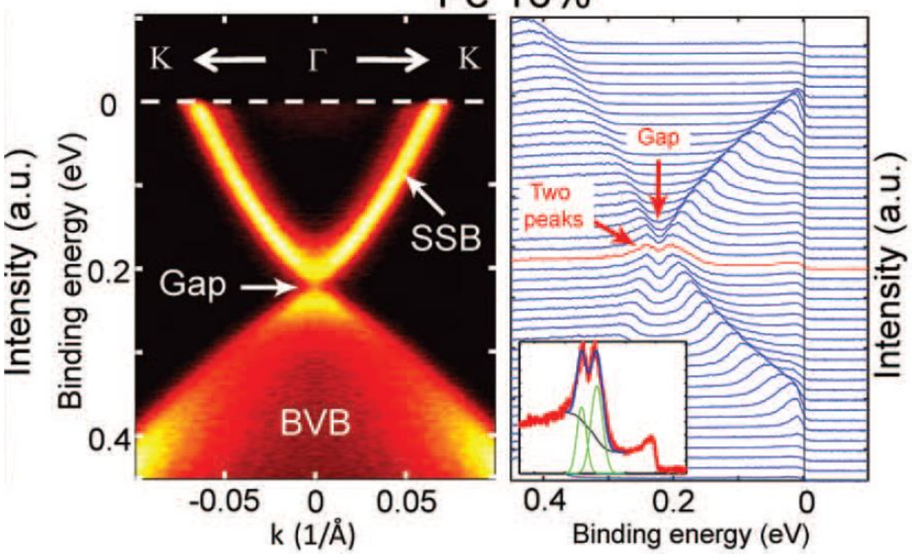

$Cr_{0.15}(Bi_{0.58}Sb_{0.12})_{1.85}Te_{3.7}$
at 30 mK

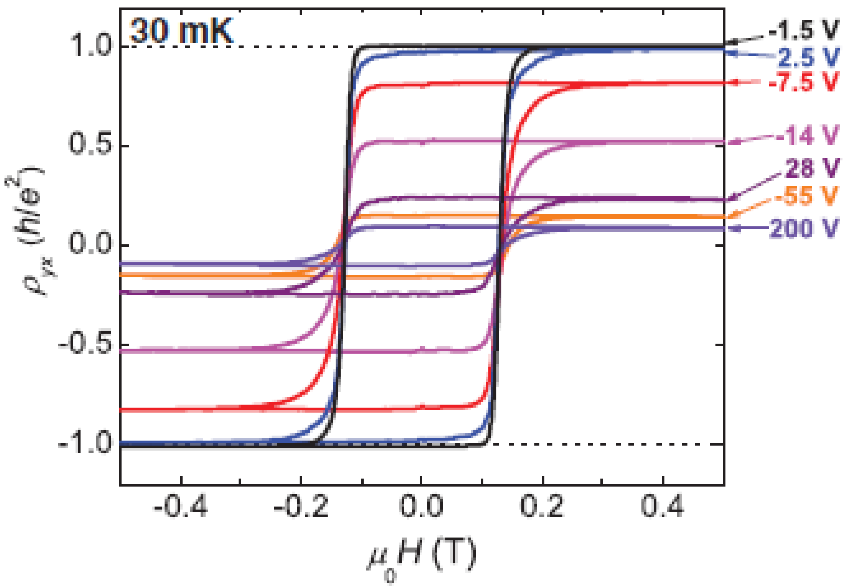

Chen et al., Science **329**, 659 (2010).
Chang et al., Science **340**, 167 (2013).

Magnetic proximity effect (MPE) in TI/magnetic layer heterostructures

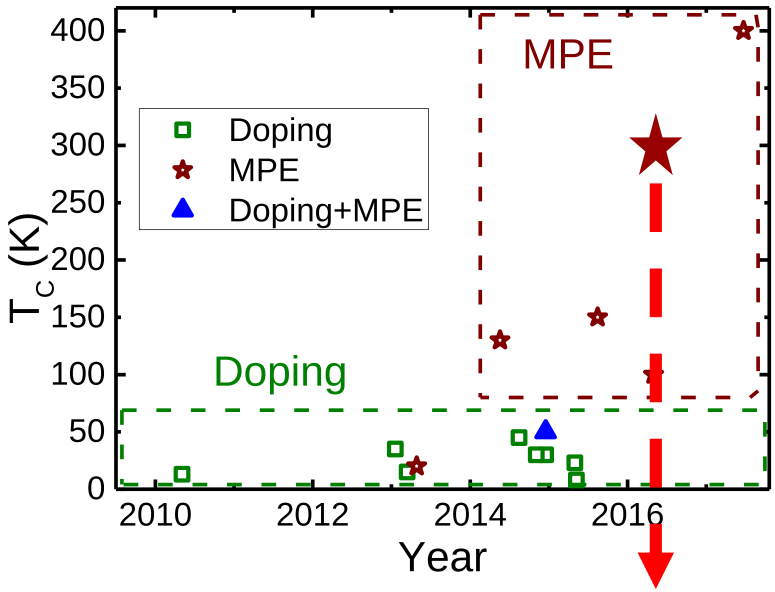

Advantages of using the MPE to break time reversal symmetry:

- Higher T_C than that of magnetic doping
- No crystal defects
- Uniform magnetization

Discovery of RT MPE in EuS/Bi_2Se_3, exhibiting an interfacial PMA.

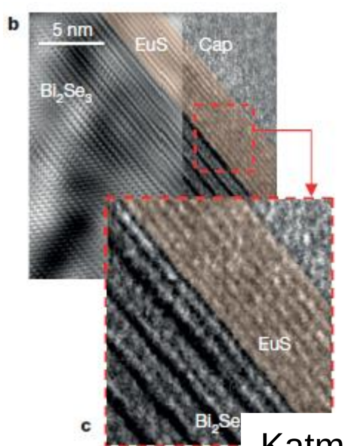

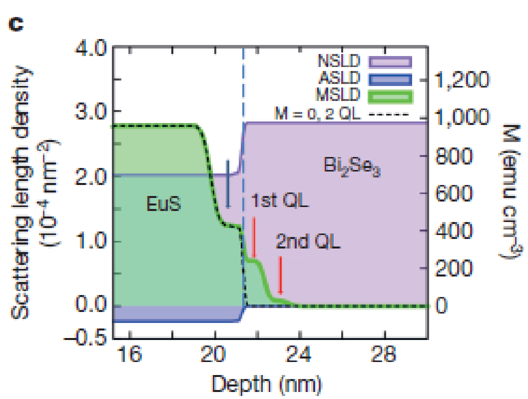

Katmis *et al*., Nature **533**, 513 (2016).

How about MPE and the interfacial magnetic anisotropy in Bi_2Se_3/YIG?

High T IMA and low T PMA!

Y. T. Fanchiang
Advanced Nano Thin Film Epitaxy Lab

Spin Pumping in Bi_2Se_3/Fe_3Si and Fe/Bi_2Te_3 Structures

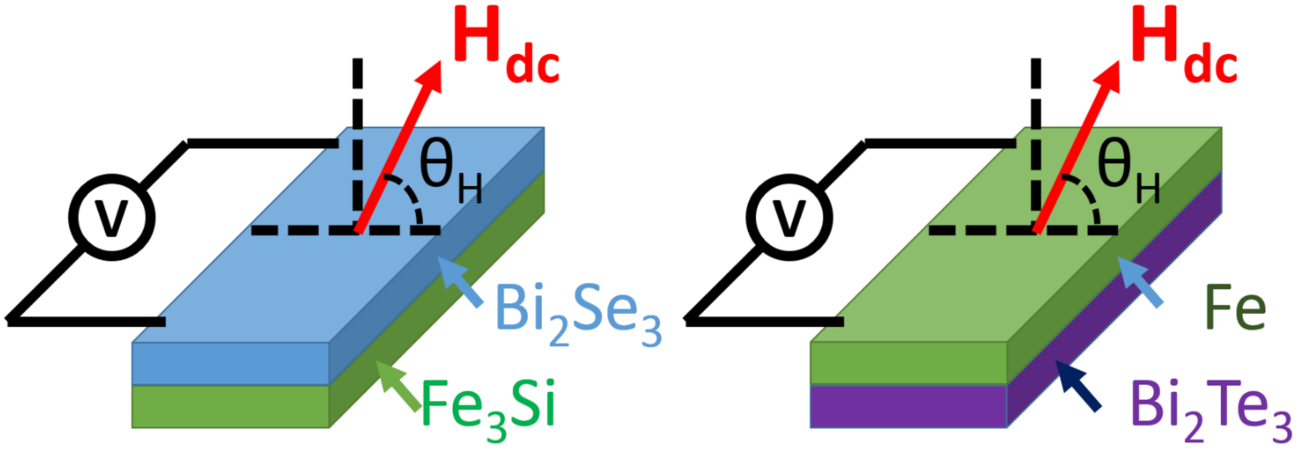

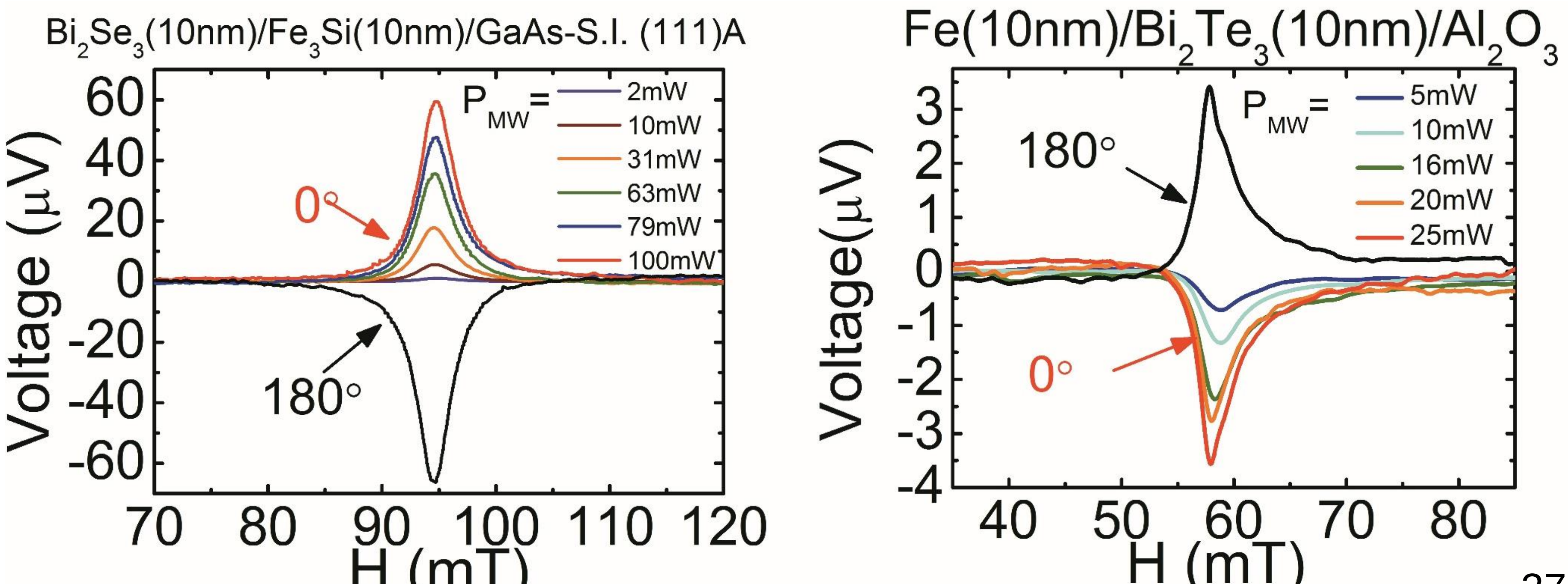

C. N. Wu *et al.*, J. Appl. Phys. **117**, 17D148 (2015)

Converted Charge Current Density Comparison

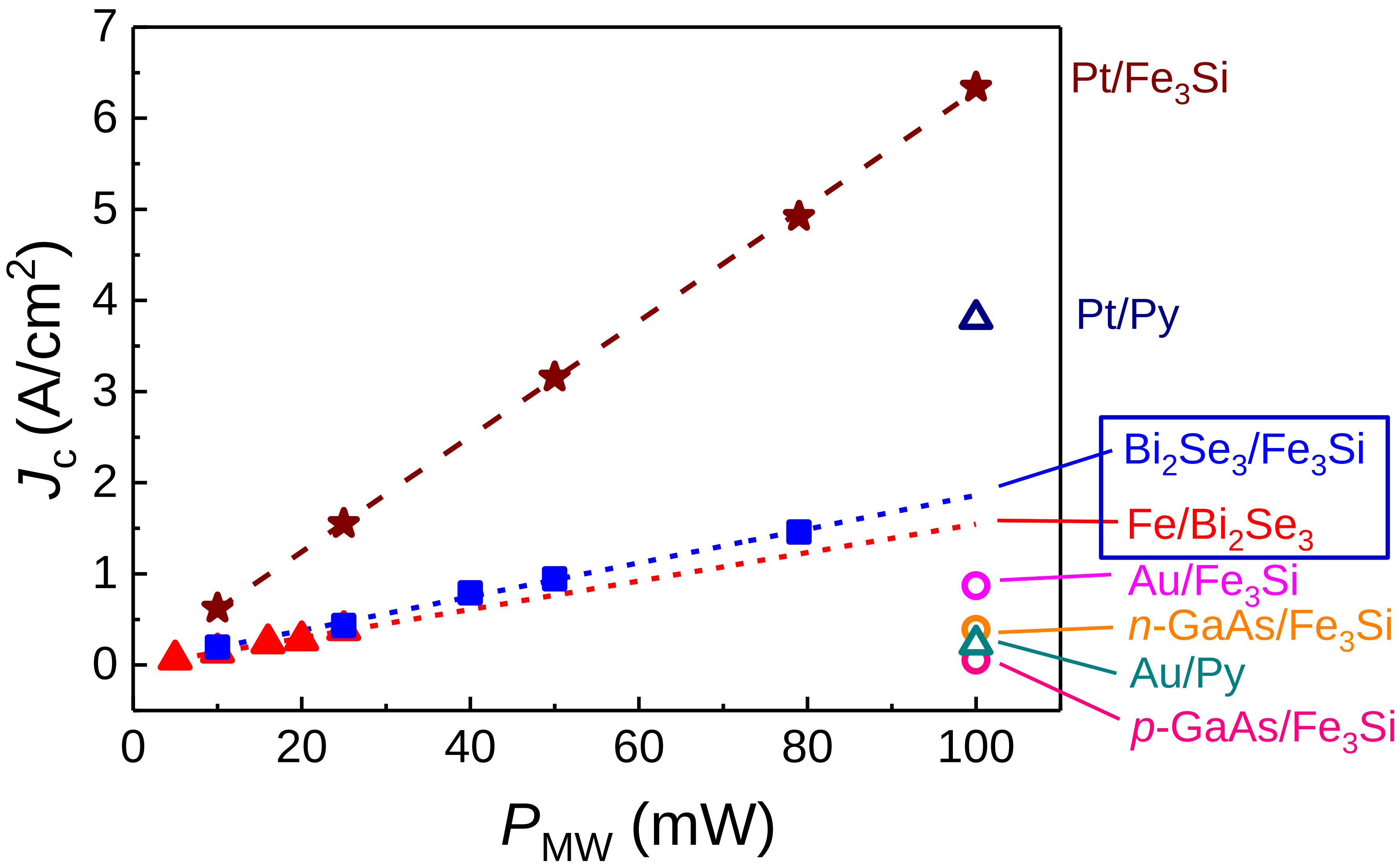

Comparison of θ_{ISHE}

NM (FM)	Spin mixing conductance (m^{-2})	Spin current density (Jm^{-2})	Spin Hall Angle θ_{ISHE}	J_c (A/cm^2)
Bi_2Se_3 (Fe_3Si)	6.66×10^{18}	1.98×10^{-9}	0.0053 ± 0.002	1.32
Bi_2Te_3 (Fe)	2.36×10^{18}	1.15×10^{-9}	0.0068 ± 0.003	1.00
p-GaAs(Fe_3Si)	5.89×10^{18}	8.91×10^{-10}	0.00019	0.0087
n-GaAs(Fe_3Si)	1.46×10^{19}	1.53×10^{-9}	0.000028	0.061
Au (Fe_3Si)	4.24×10^{18}	6.48×10^{-10}	0.00505	0.49
Pt (Fe_3Si)	1.29×10^{19}	1.96×10^{-9}	0.023	6.34

- Much larger spin current density and θ_{ISHE} than conventional semiconductor GaAs.
- Comparable to θ_{ISHE} ~0.009 from S. Oh et al
- Comparable ISHE to Au, but smaller than Pt

H. Y. Hung *et al.*, J. Appl. Phys. **113**, 17C507 (2013)
H. Y. Hung *et al.*, Appl. Phys. Lett. **105**, 152413 (2014)
P. Deorani *et al.*, Phys. Rev. B **90**, 094403 (2014)

Using Al_2O_3 as a barrier layer to prevent interdiffusion

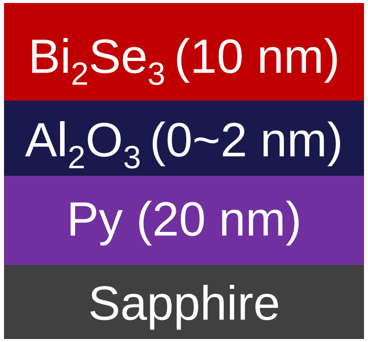

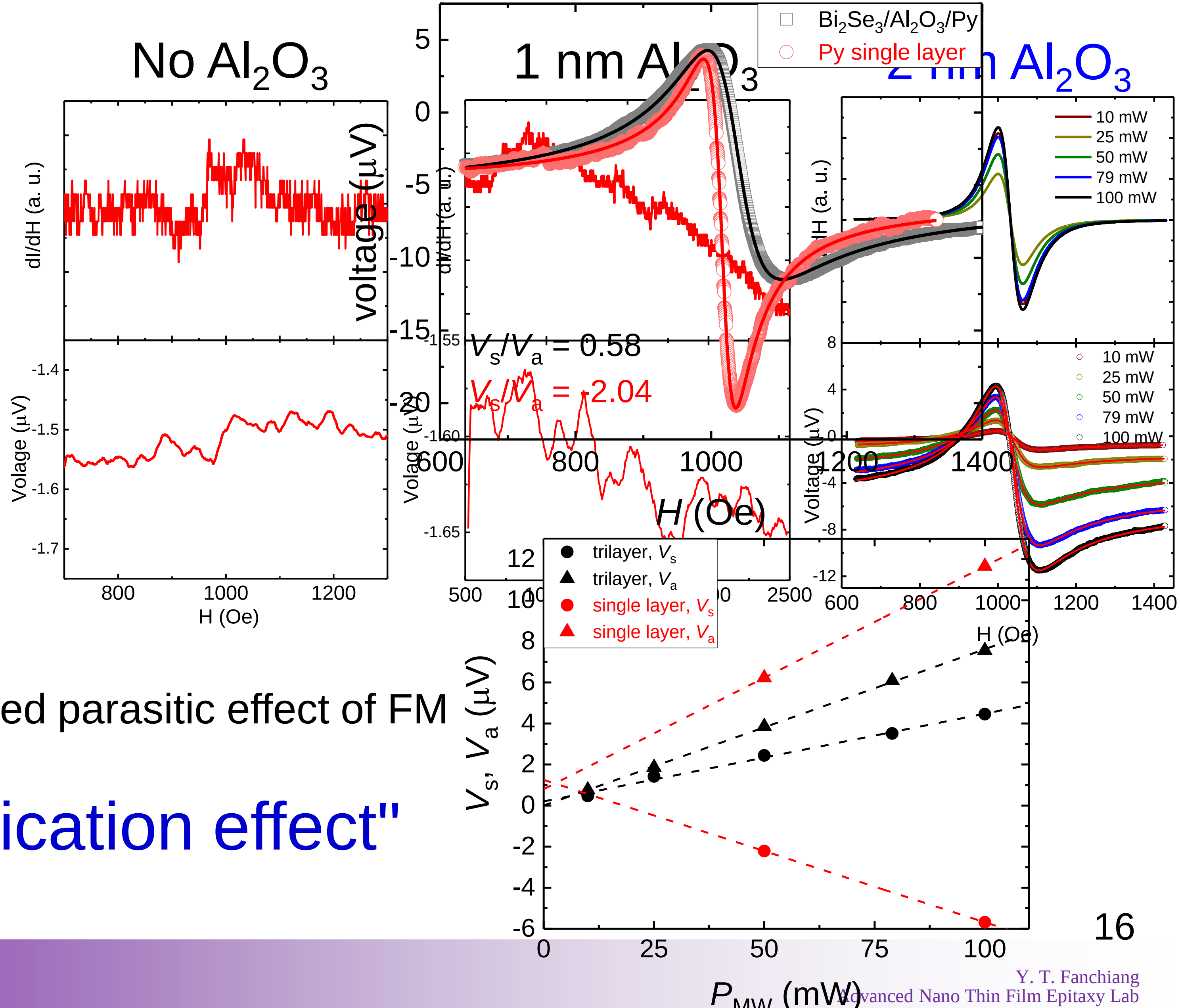

Microwave-induced parasitic effect of FM

"spin-rectification effect"

Y. T. Fanchiang
Advanced Nano Thin Film Epitaxy Lab

Benefits of the ferrimagnetic insulator YIG and TmIG

- **High T_C**: high-temperature MPE in TI/FI
- **High thermal stability with TIs**: Formation of sharp TI/FI interface
- **Insulating properties**: prevention of current shunting effect

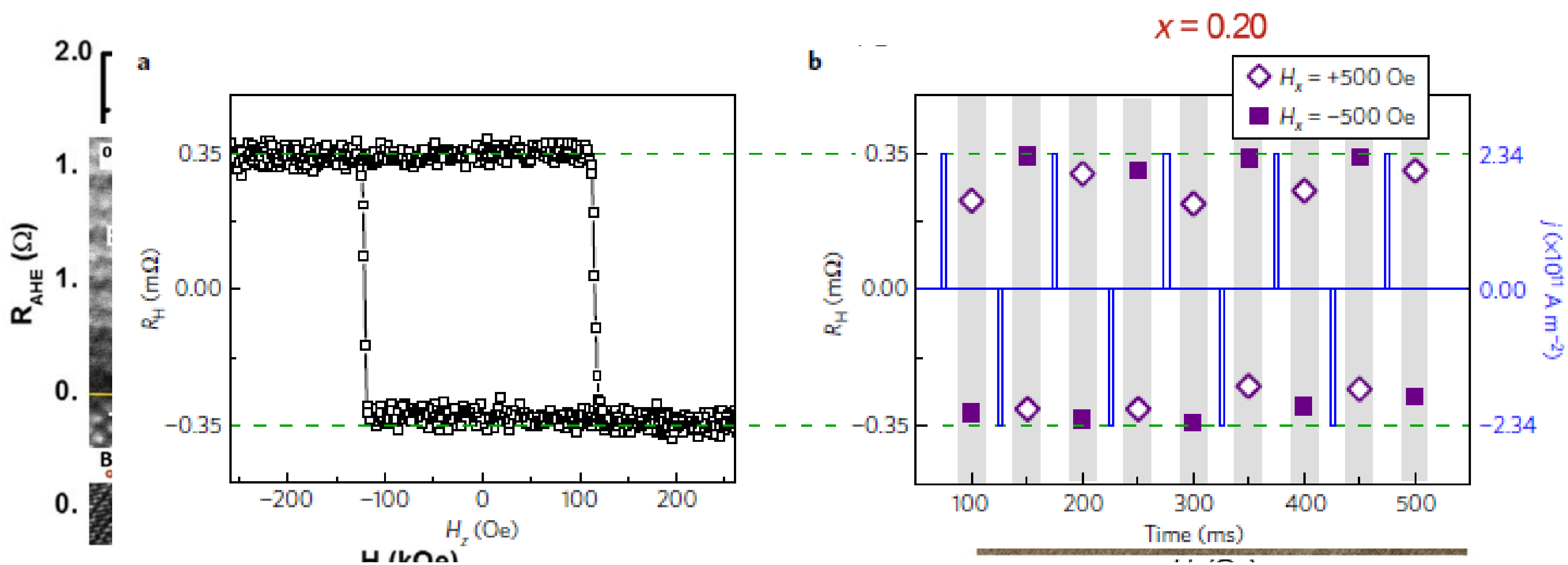

C. C. Chen et al., App   C. O. Avci et al., Nat. Mater. **16**, 309 (2016). **3**, e1700307 (2017).

M. Lang et al., Nano Lett. **14**, 3459 (2014).   C. Tang et al., Sci. Adv. **3**, e1700307 (2017).

High quality *off-axis* sputtered YIG and TmIG films

Low damping YIG films of excellent crystallinity

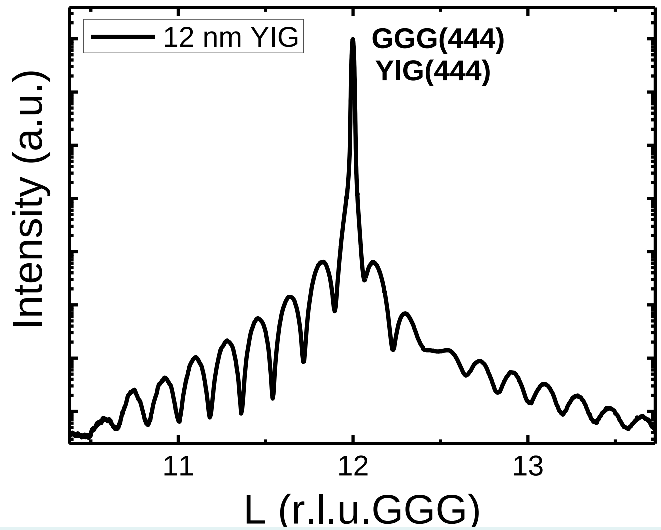

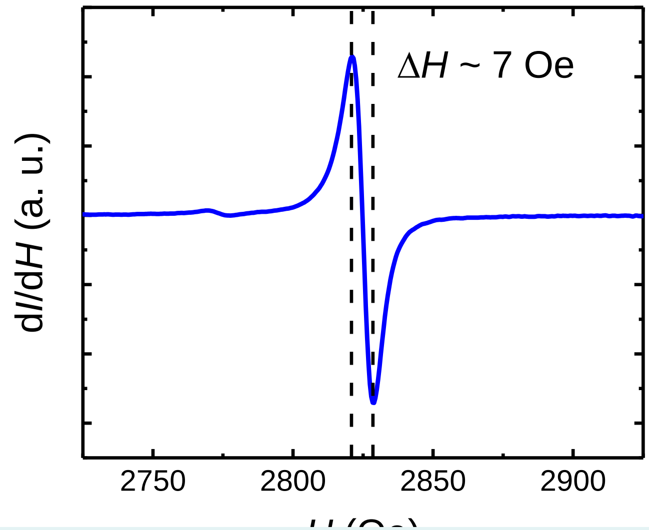

TmIG films with strain-tunable PMA

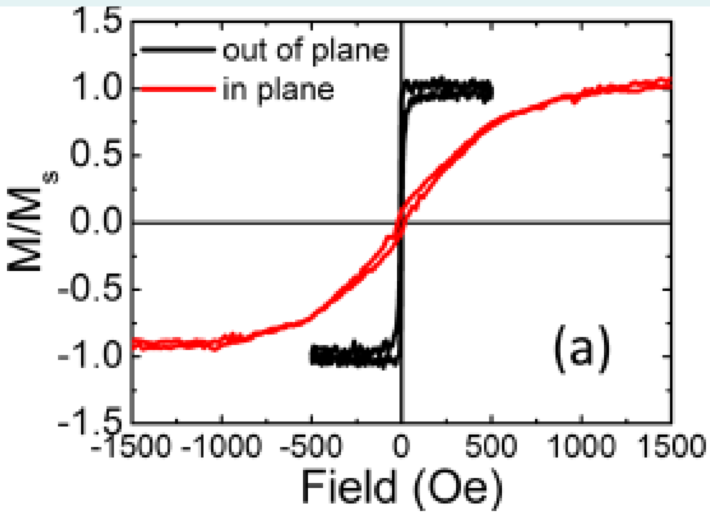

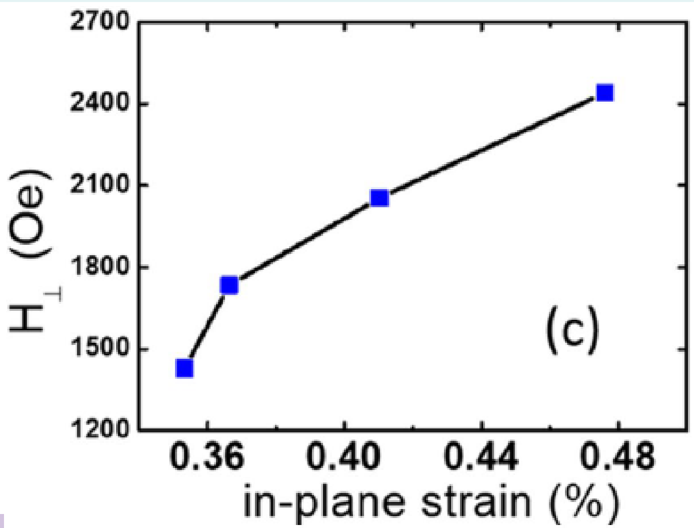

C. N. Wu et al., Sci. Rep. **8**, 11087 (2018).
C. N. Wu et al., AIP Adv. **8**, 055904 (2018).

Growth and structural characterization of Bi_2Se_3/YIG

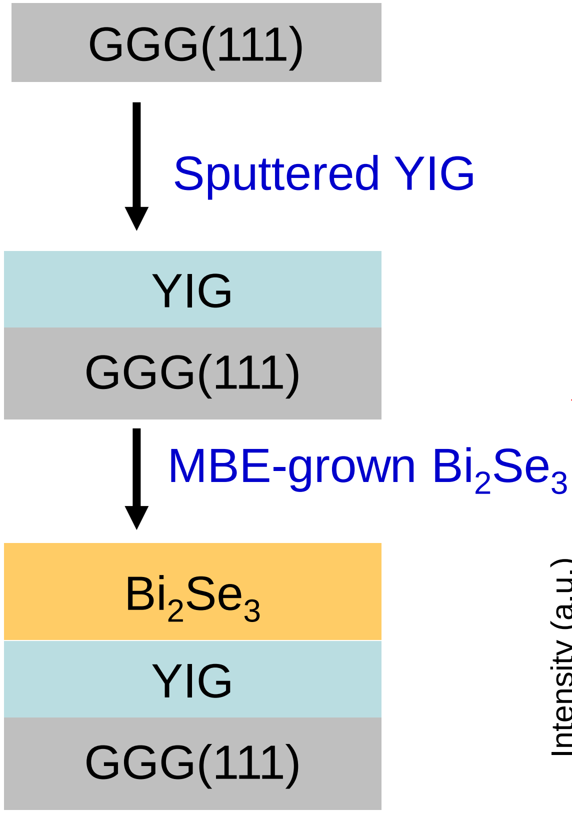

◆Streaky RHEED pattern

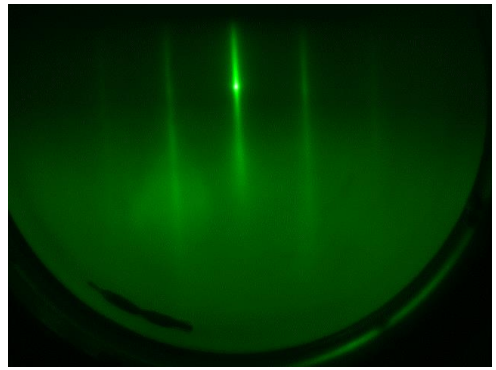

◆1 nm interlayer

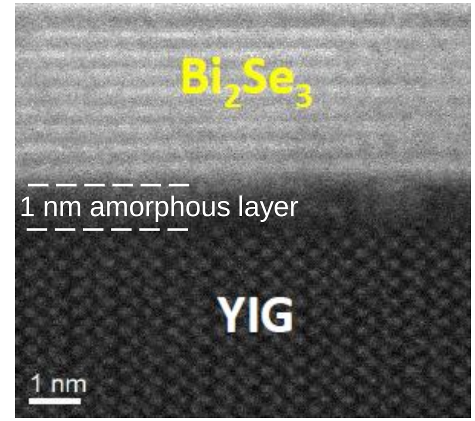

◆Excellent crystallinity

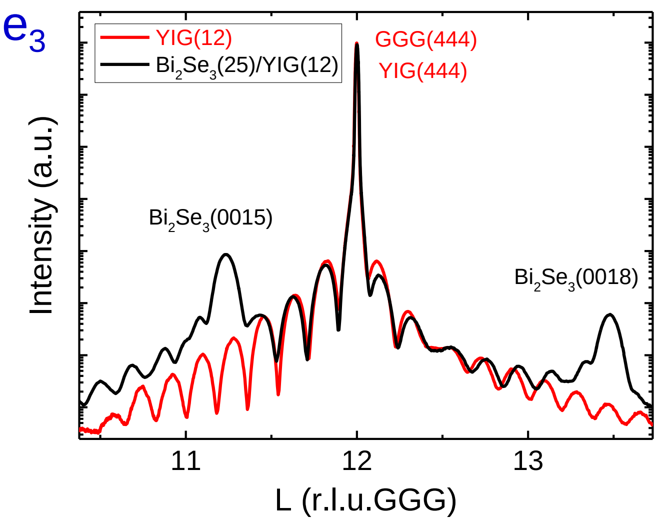

◆High quality layer-by-layer growth

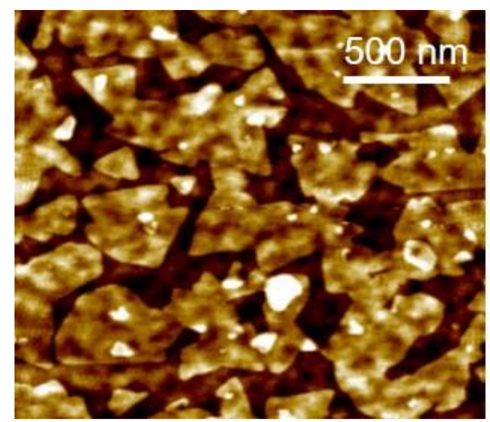

Magnetic anisotropy in Bi_2Se_3/YIG

25 nm Bi_2Se_3
13 nm YIG
GGG(111)

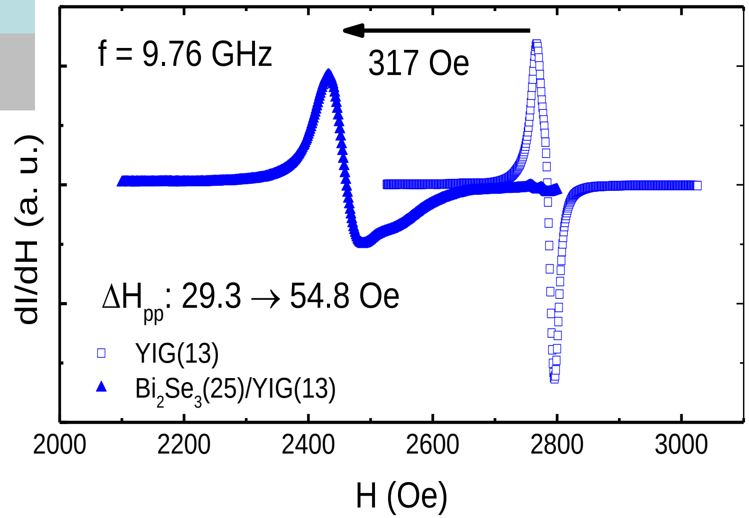

- Large H_{res} shift is observed after growing Bi_2Se_3 on YIG, due to change of magnetic anisotropy.
- Angle- and frequency-dependent FMR show an enhanced in-plane anisotropy introduced by Bi_2Se_3.

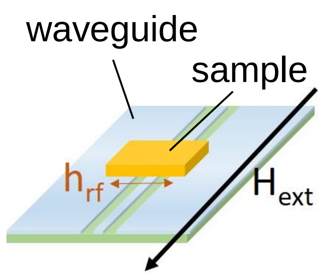

Frequency-dependent FMR

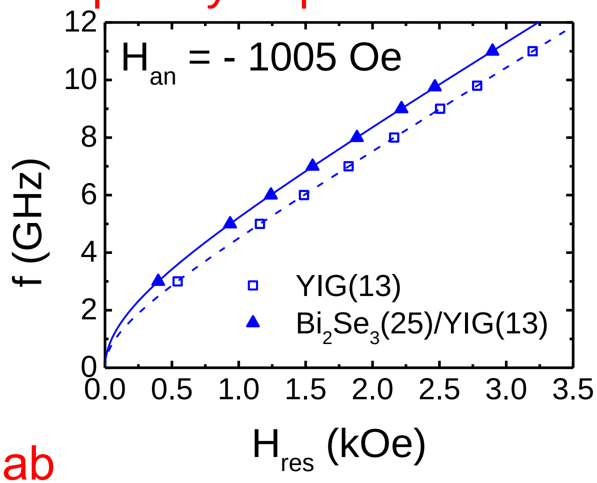

Angle-dependent FMR

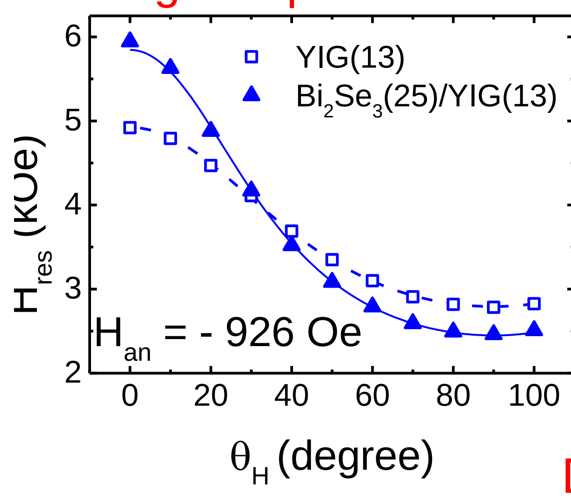

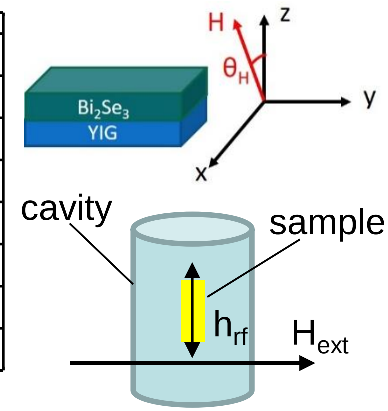

Dr. S. F. Lee's lab in Academia Sinica

Dr. J. G. Lin's lab In NTU/CCMS

Interfacial magnetic anisotropy favoring in-plane direaction

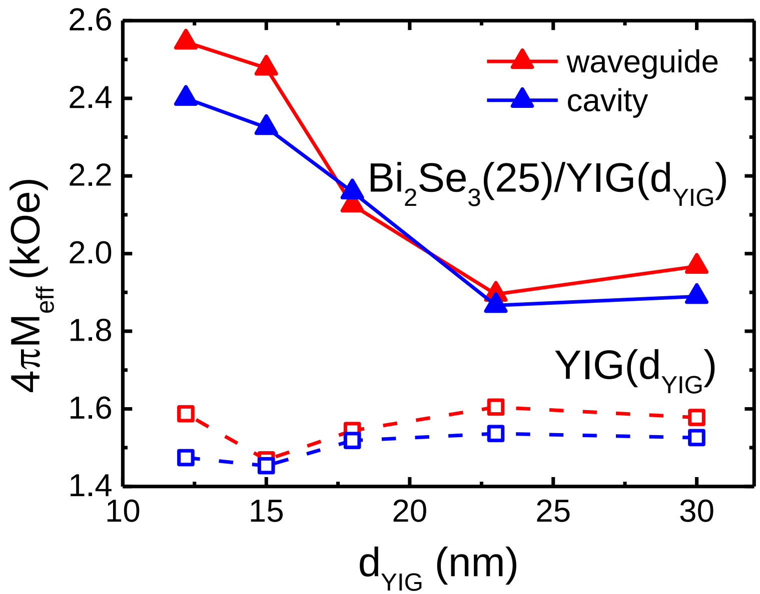

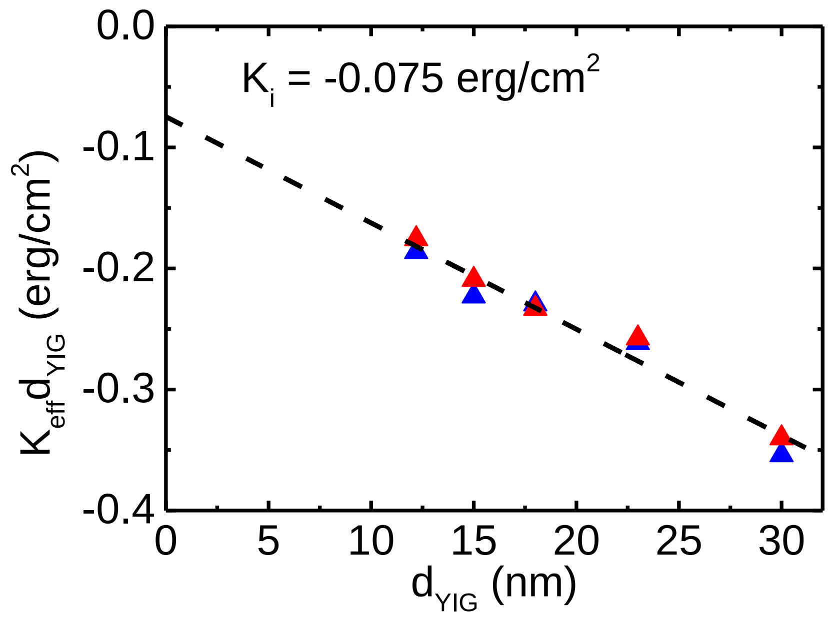

- The effective magnetization M_{eff} is larger in thinner YIG samples, which implies the change of anisotropy occurring at TI/YIG interfaces.

$$
\begin{aligned}
&4\pi\left(M_{eff}\left(\mathrm{Bi_2Se_3/YIG}\right)-M_{eff}\left(\mathrm{YIG}\right)\right)\\
&=-\frac{2}{M_S}\left(K_{eff}\left(\mathrm{Bi_2Se_3/YIG}\right)-K_{eff}\left(\mathrm{YIG}\right)\right)\\
&=-H_{an}\\
&\Rightarrow \frac{2K_i}{M_S}\left(\frac{1}{d_{YIG}}\right)=H_{an}
\end{aligned}
$$

Y. T. Fanchiang
Advanced Nano Thin Film Epitaxy Lab

Bi_2Se_3 thickness dependence of K_i and damping enhancement

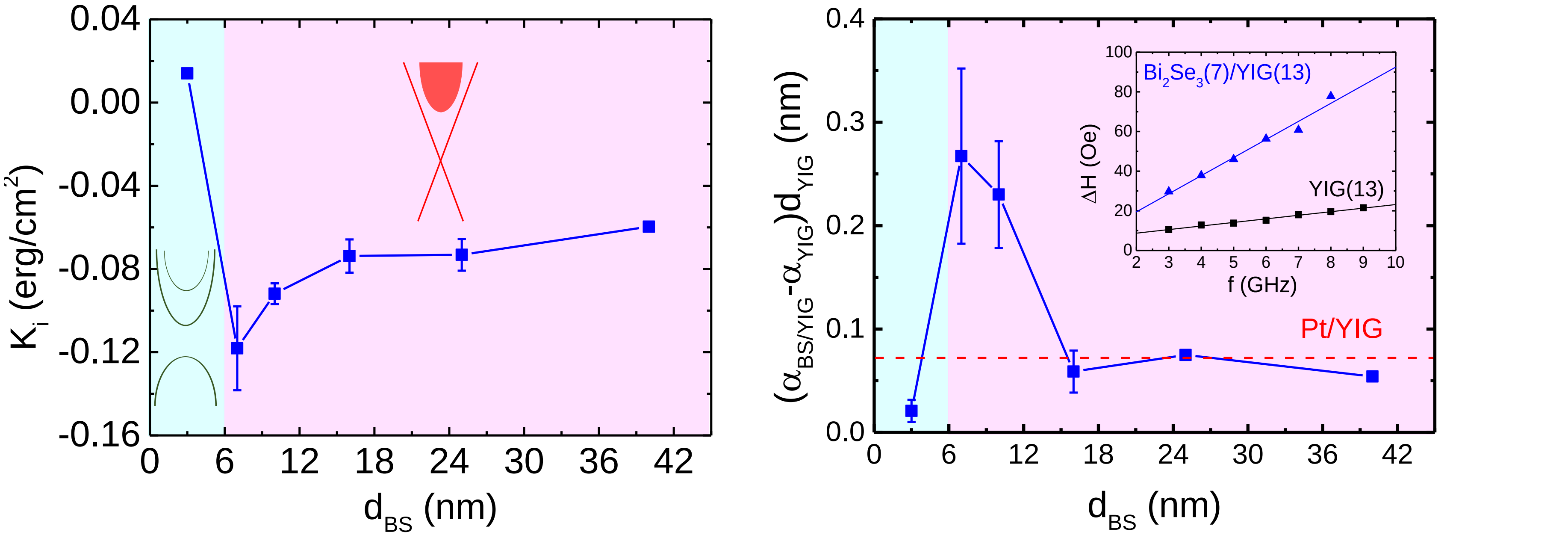

A. TSS can strongly enhance the magnetic anisotropy of the magnetic layer. (Kim *et al*., Phys. Rev. Lett. **119**, 027201 (2017))

B. Such unconventional thickness dependence might be related to the topological surface states of Bi_2Se_3.

C. The normalized damping enhancement peaks near the 2D limit (6 nm) of Bi_2Se_3, which is **3 times larger than that of Pt/YIG.**

Comparison with BiSbTe/YIG of Prof. Jing Shi (UC riverside)

25 QL Bi_2Se_3

13 nm YIG

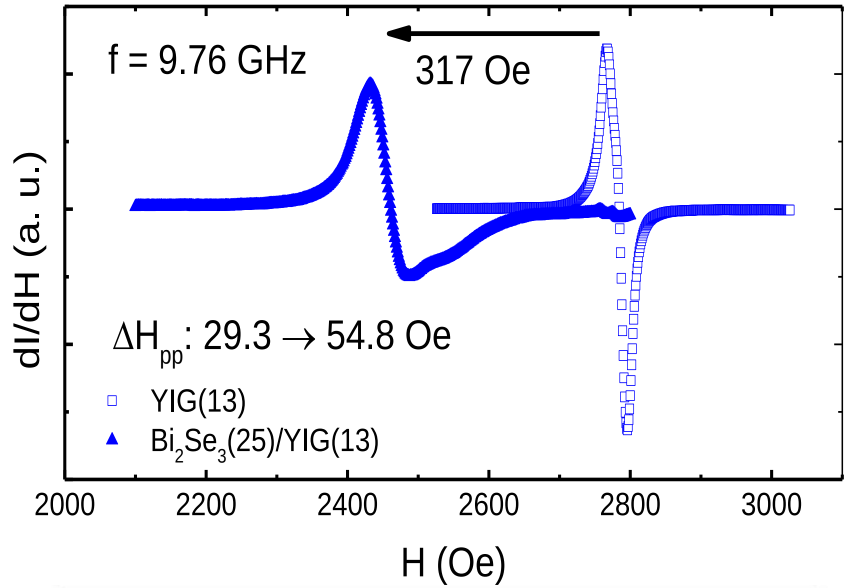

5 QL Sb_2Te_3

10 nm YIG

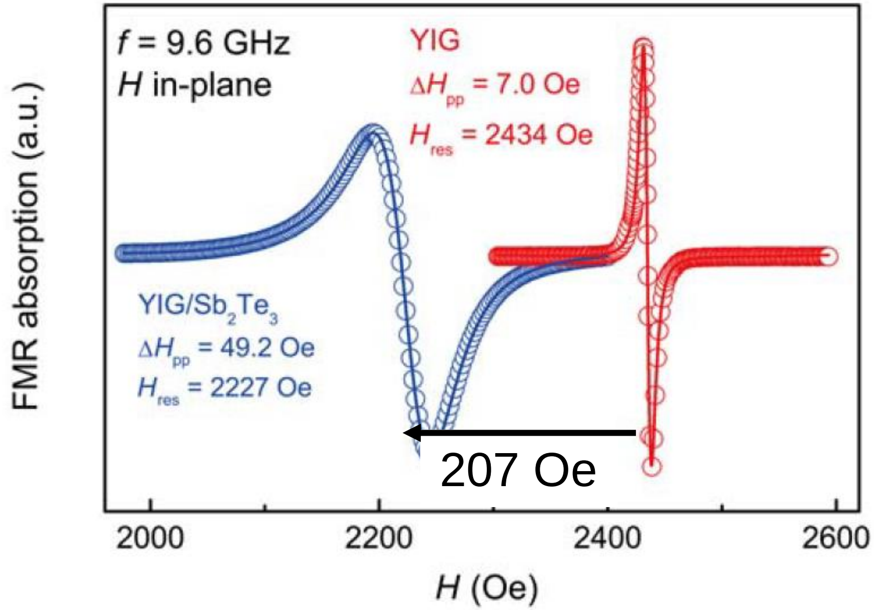

Fanchiang et al., Nat. Comm. **9**, 233 (2018)

Tang *et al.*, Sci. Adv. **4**, eaas8660 (2018)

Comparison with BiSbTe/YIG of Prof. Jing Shi (UC riverside)

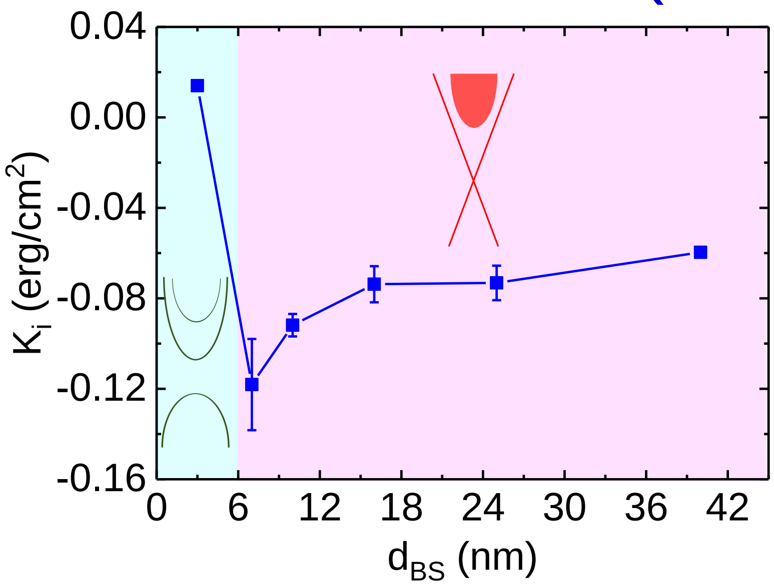

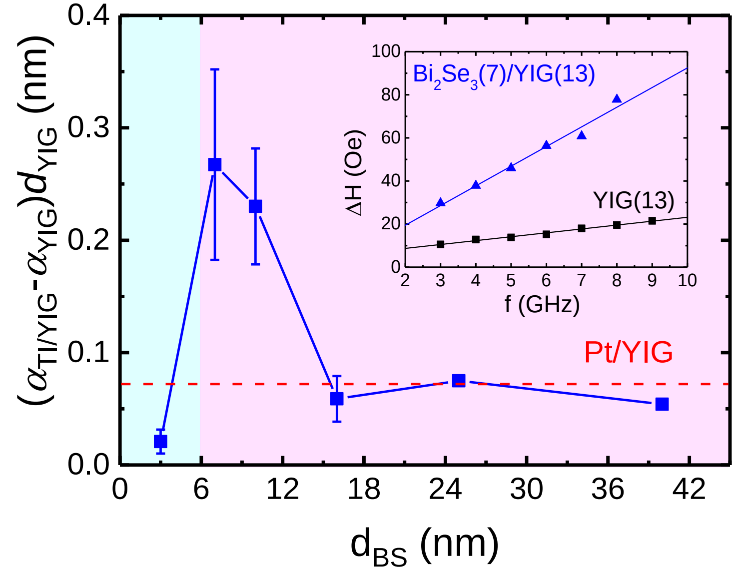

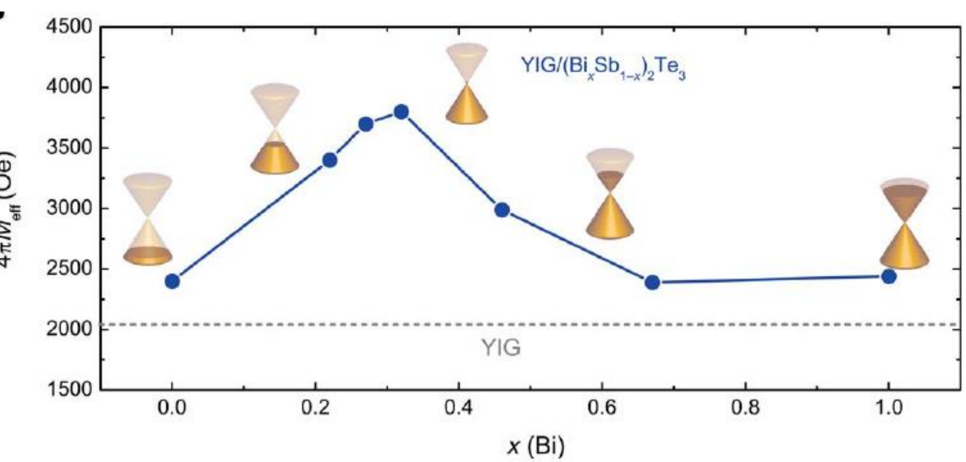

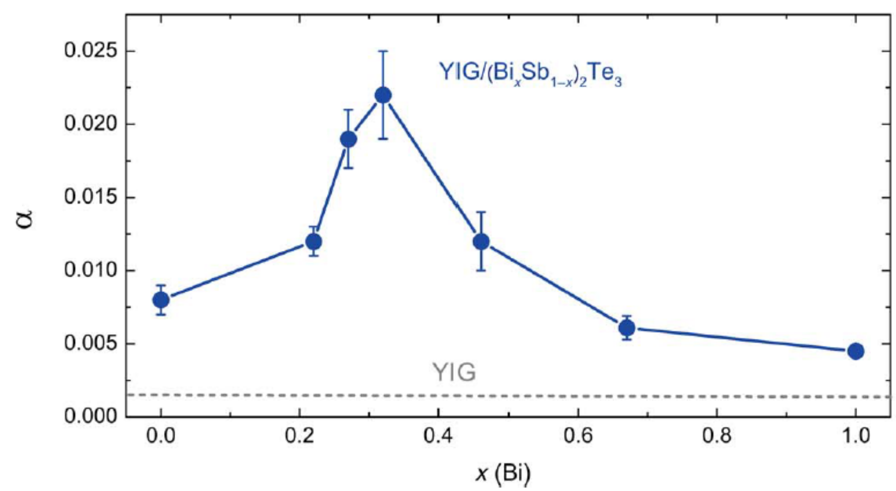

Fanchiang et al., Nat. Comm. **9**, 233 (2018)

Tang *et al.*, Sci. Adv. **4**, eaas8660 (2018)

Comparison with BiSbTe/YIG of Prof. Jing Shi (UC riverside)

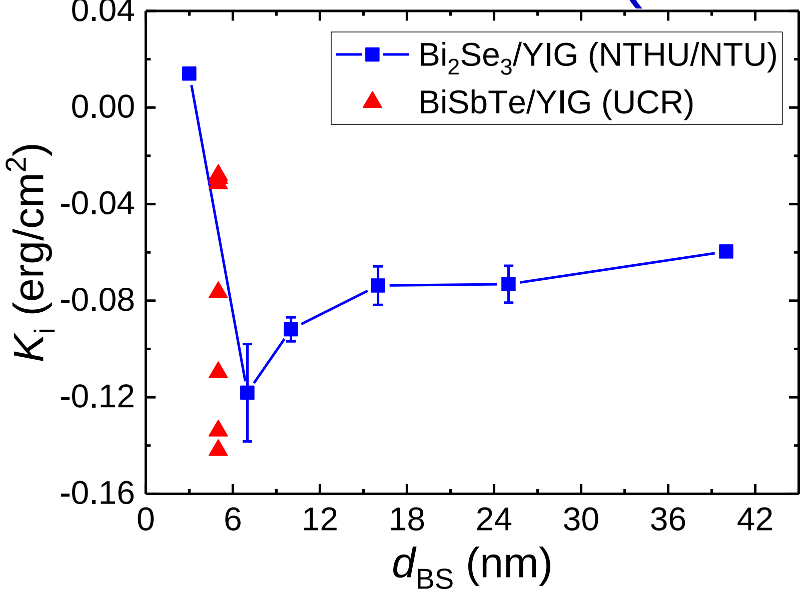

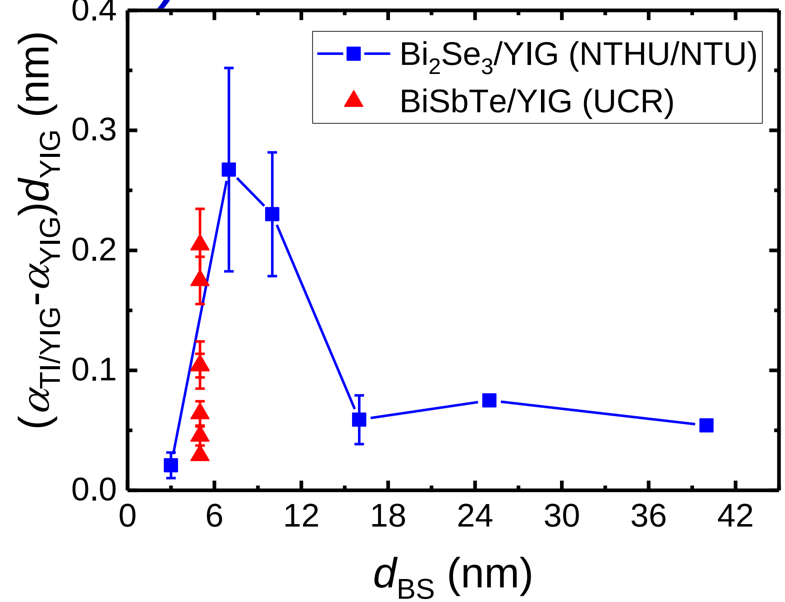

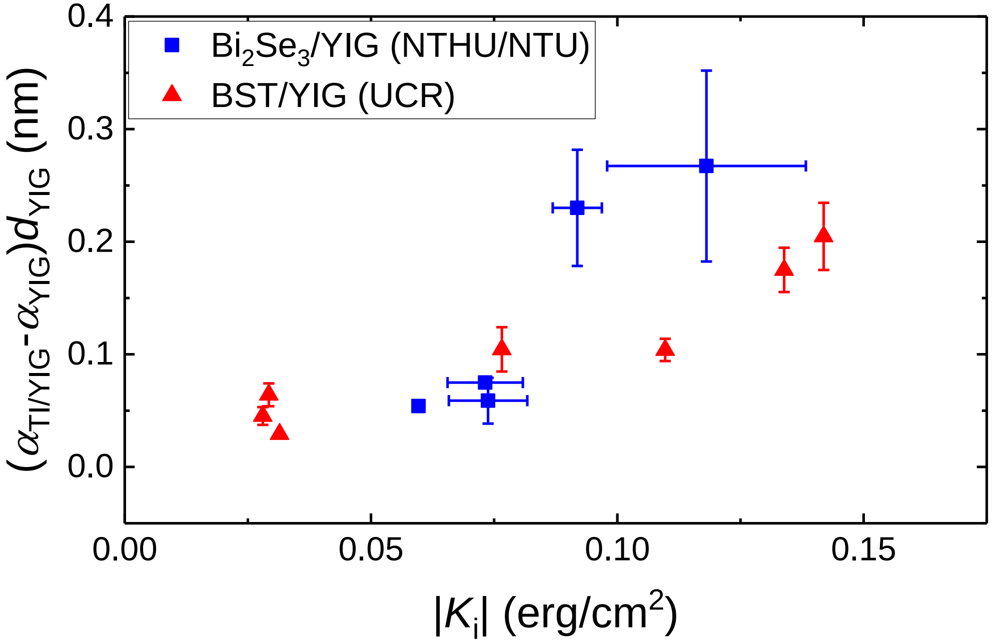

A. Comparable interfacial magnetic anisotropy and damping enhancement in Bi_2Se_3/YIG and BST/YIG

B. Close anisotropy vs damping relations of Bi_2Se_3/YIG and BST/YIG

Fanchiang et al., Nat. Comm. **9**, 233 (2018)

Tang *et al.*, Sci. Adv. **4**, eaas8660 (2018)

Surface-state-mediated exchange coupling: theoretical aspect

PRL 119, 027201 (2017) PHYSICAL REVIEW LETTERS week ending 14 JULY 2017

Understanding the Giant Enhancement of Exchange Interaction in Bi_2Se_3-EuS Heterostructures

Jeongwoo Kim,[1] Kyoung-Whan Kim,[2] Hui Wang,[1] Jairo Sinova,[2,3] and Ruqian Wu[1,*]
[1]*Department of Physics and Astronomy, University of California, Irvine, California 92697, USA*
[2]*Institut für Physik, Johannes Gutenberg Universität Mainz, Mainz, 55128, Germany*
[3]*Institute of Physics, Academy of Sciences of the Czech Republic, Cukrovarnická 10, 162 53 Praha 6, Czech Republic*
(Received 21 December 2016; revised manuscript received 22 March 2017; published 13 July 2017)

(a)

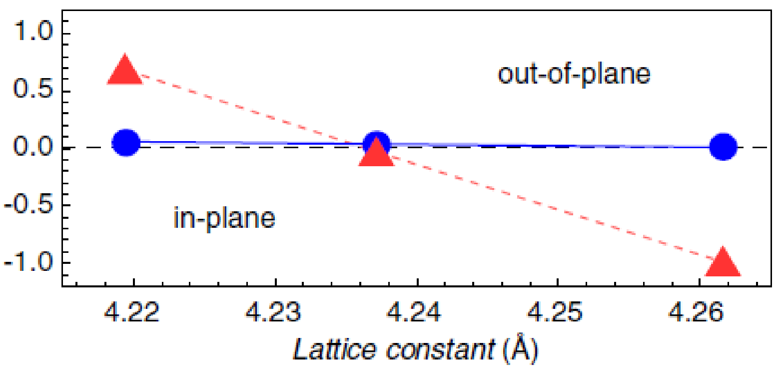

(a)

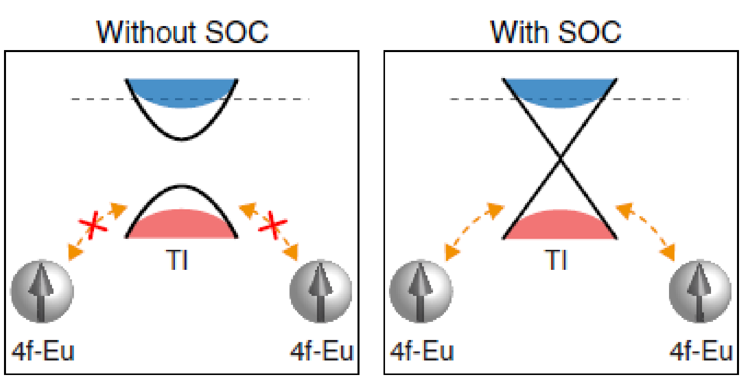

A. The strong SOC of TI can enhance the magnetic anisotropy of the magnetic insulator.
B. The sign of anisotropy may depend on atomic structure at the interface.
C. The TI surface state mediates the exchange coupling of the magnetic ion of the magnetic layer.

Temperature-dependent FMR of YIG and Bi_2Se_3/YIG

23 nm YIG

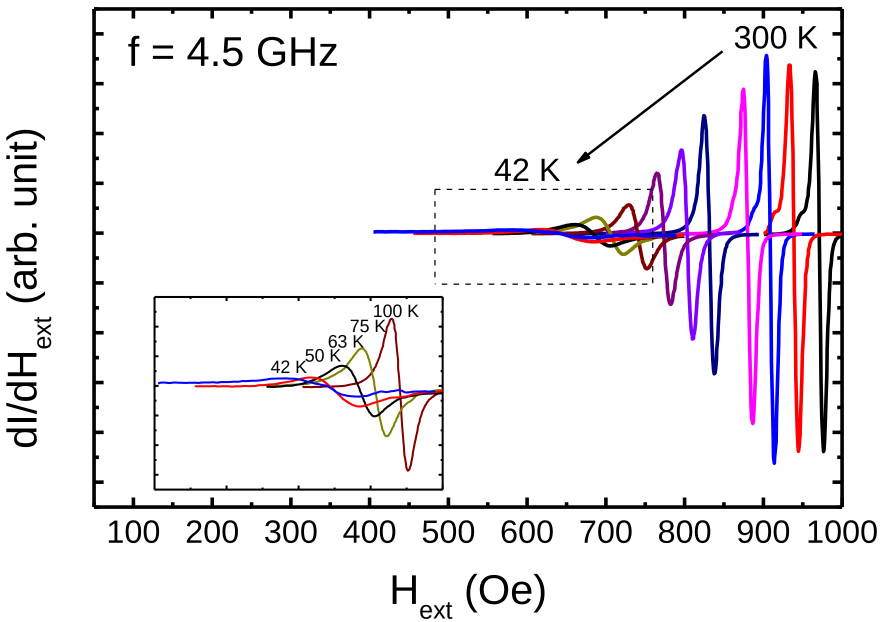

25 nm Bi_2Se_3

15 nm YIG

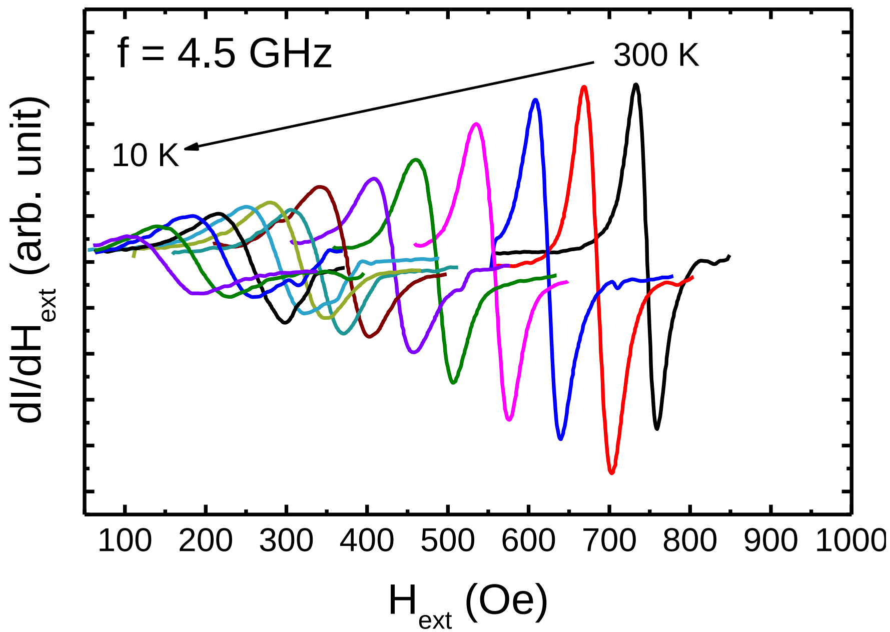

- Larger linewidth and damping → smaller microwave absorption
- Increasing H_{res} shift at low temperature
- Less damping in Bi_2Se_3/YIG below 50 K

Y. T. Fanchiang
Advanced Nano Thin Film Epitaxy Lab

Temperature-dependent FMR of YIG and Bi_2Se_3/YIG

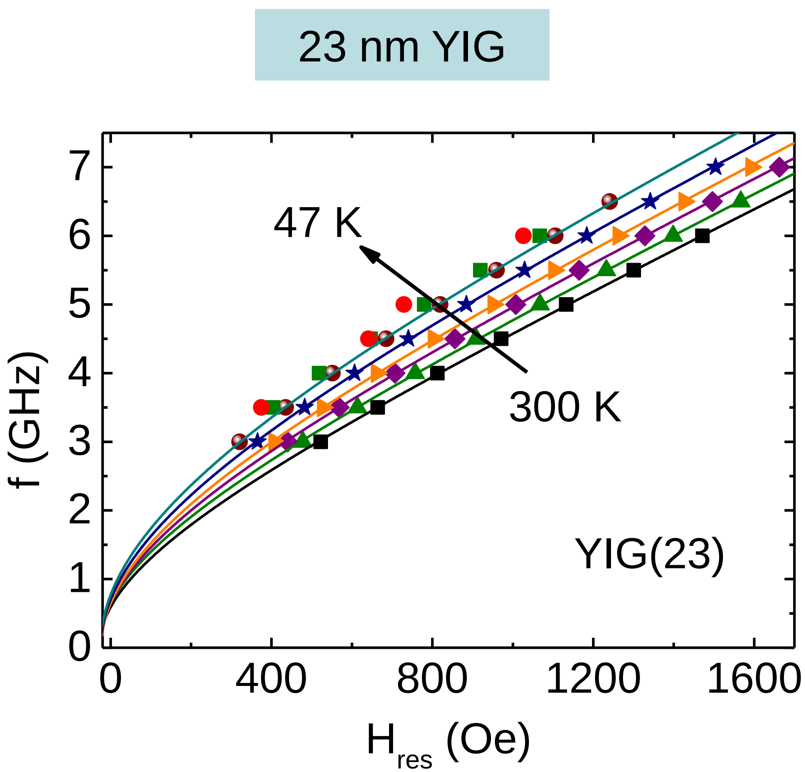

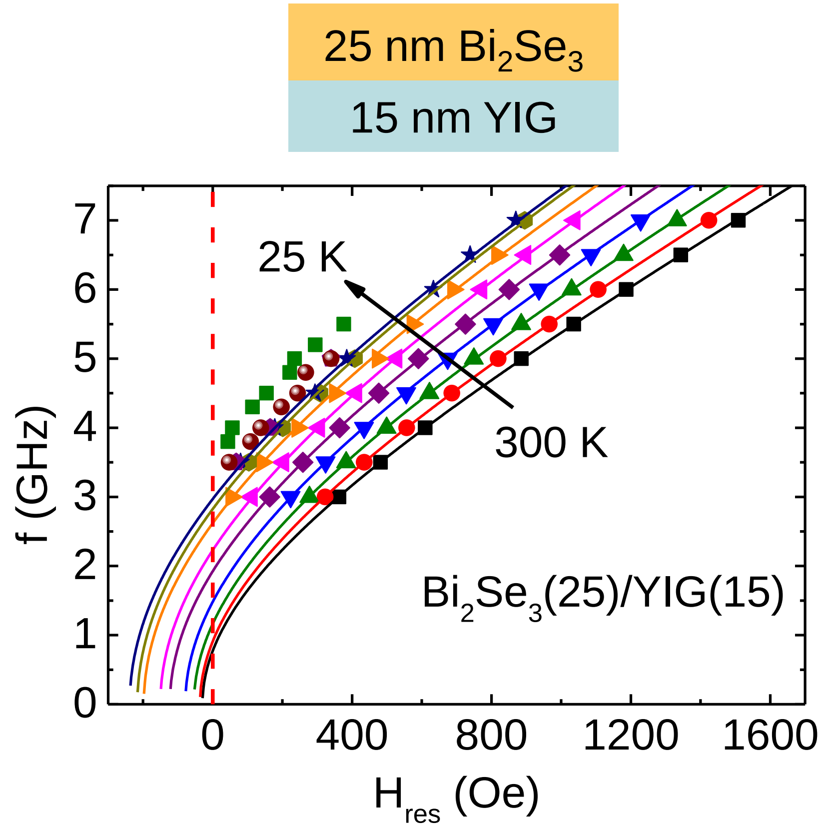

An effective field H_{eff} is necessary to fit the data.

$$f = \frac{\gamma}{2\pi}\sqrt{\left(H + H_{eff}\right)\left(H + H_{eff} + 4\pi M_{eff}\right)}$$

A possible indicator of MPE provided by spin pumping

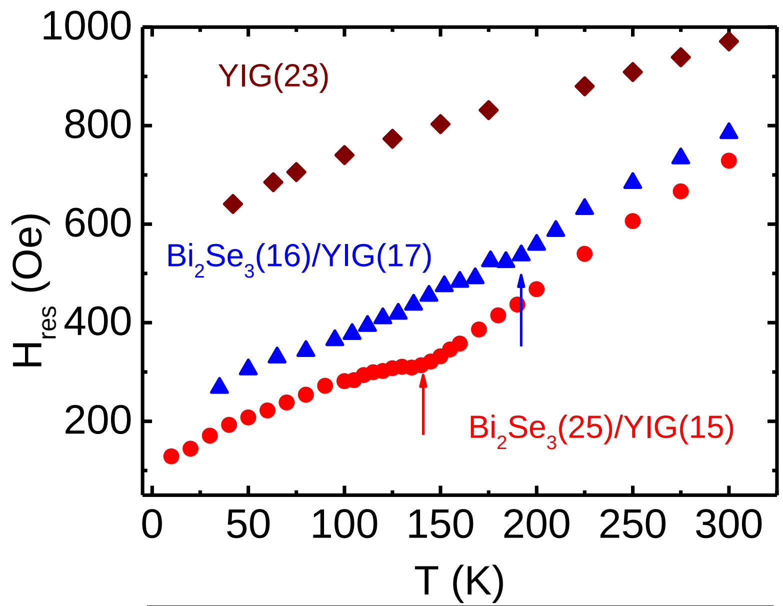

Pt/CoO/YIG

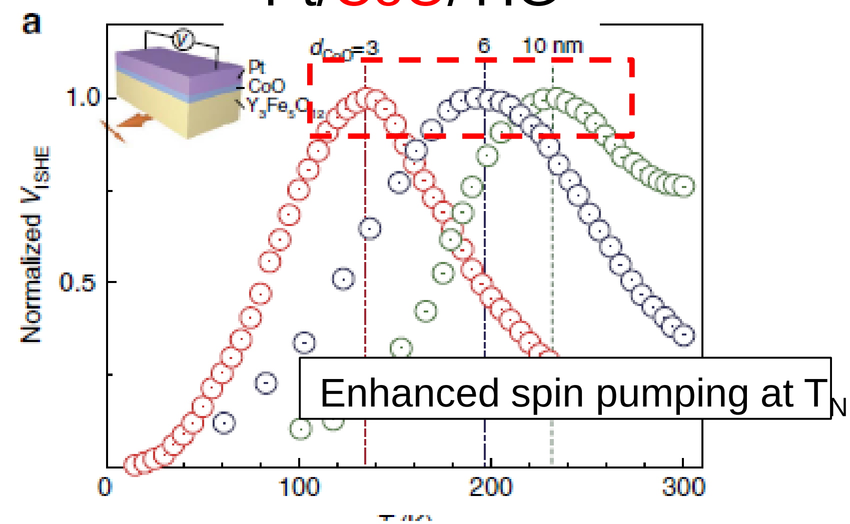

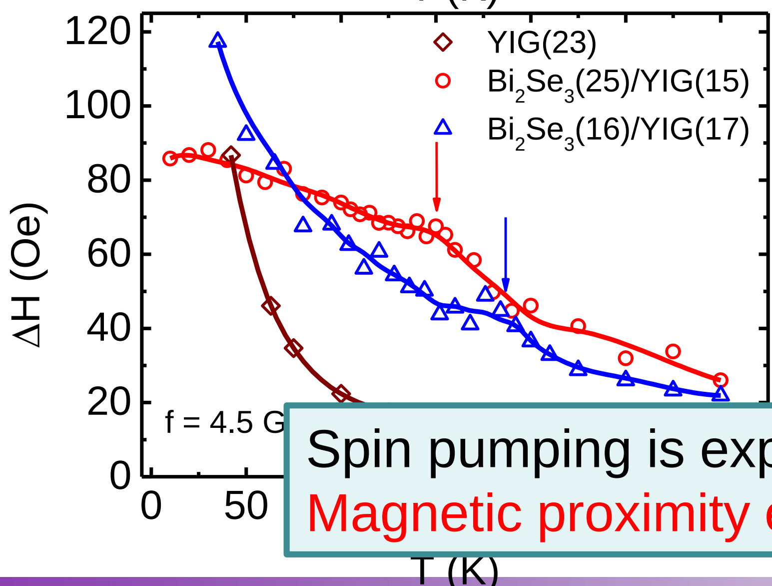

Al/IrMn/Cu/Py

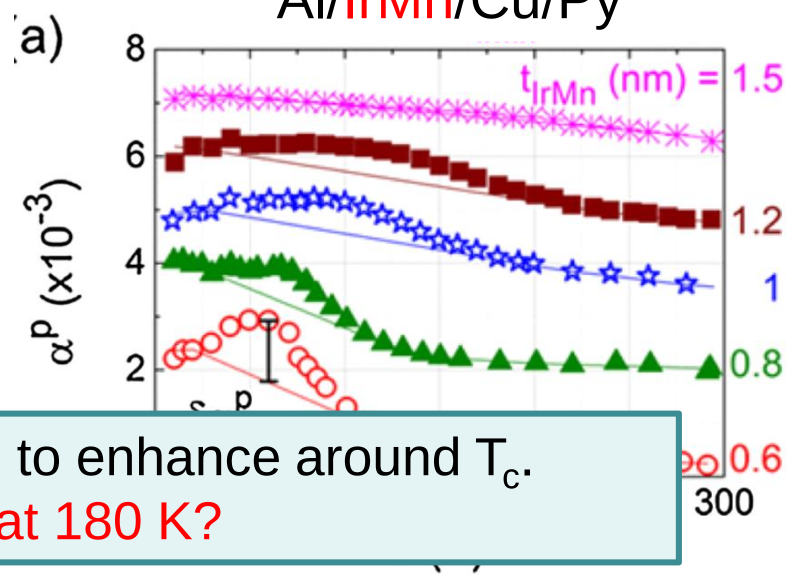

Spin pumping is expected to enhance around T_c.

Magnetic proximity effect at 180 K?

Ohnuma et al., PRB **89**, 174417 (2014).
Qiu et al., Nat. Comm. **7**, 12670 (2016).
Frangou et al., PRL **116**, 077203 (2016).

Emerging low *T* PMA and negative magnetoresistance

"hump" temperature

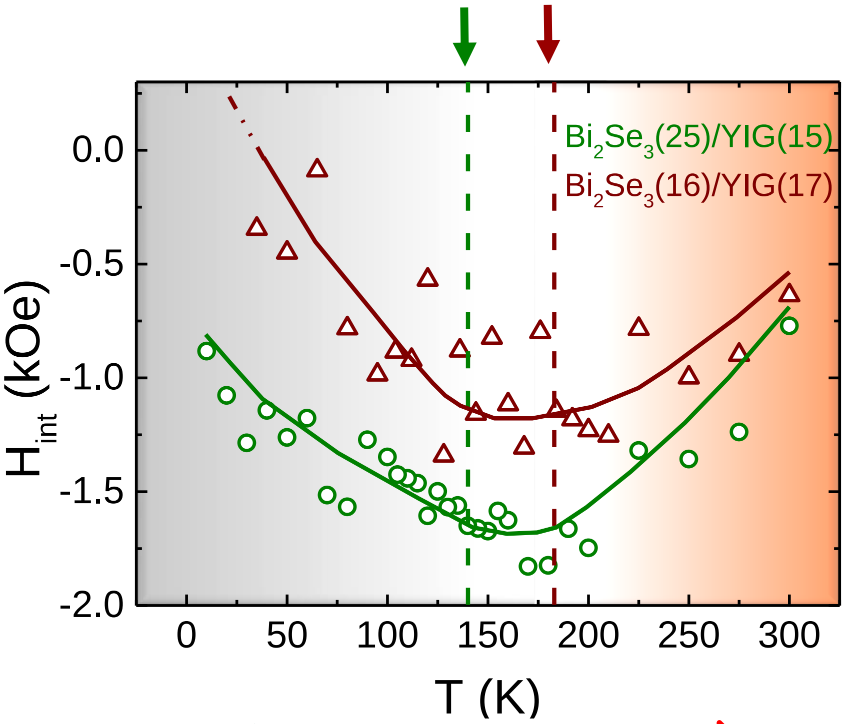

IMA
+ competing PMA

High *T* IMA

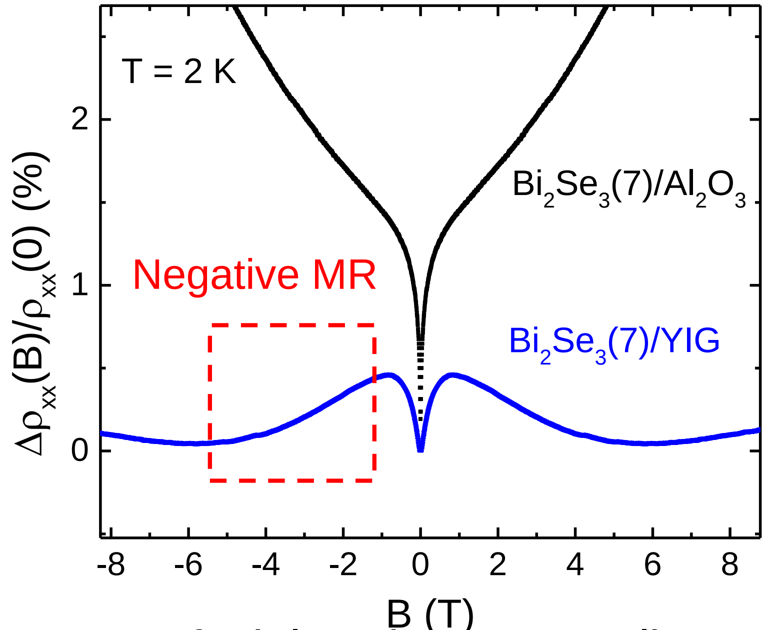

Interfacial exchange coupling

➡ Time-reversal-symmetry breaking

➡ Weak localization & Negative MR

Kim et al., PRL **119**, 027201 (2017).
Lu et al., PRL **107**, 076801 (2011).

Spin-pumping-induced exchange effective field H_{eff}

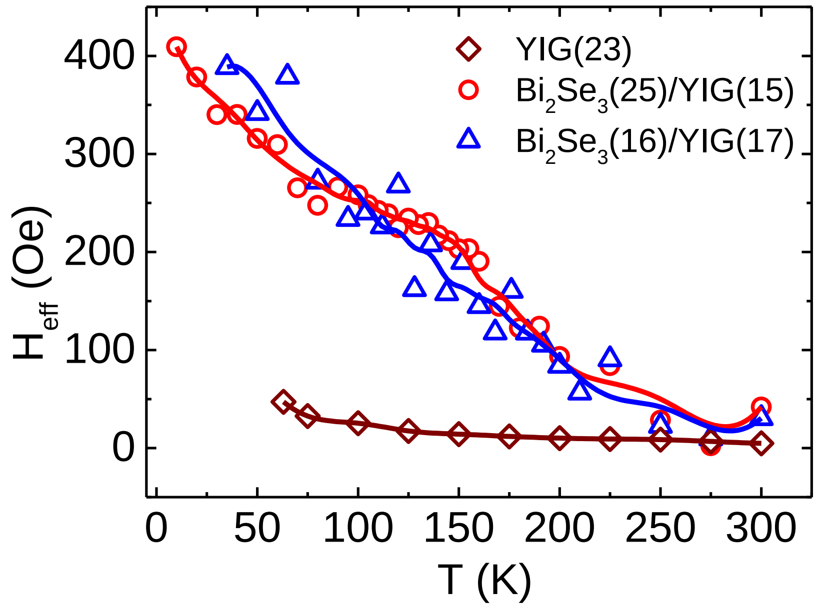

Reported ST-FMR in $CoFeB/Bi_2Se_3$

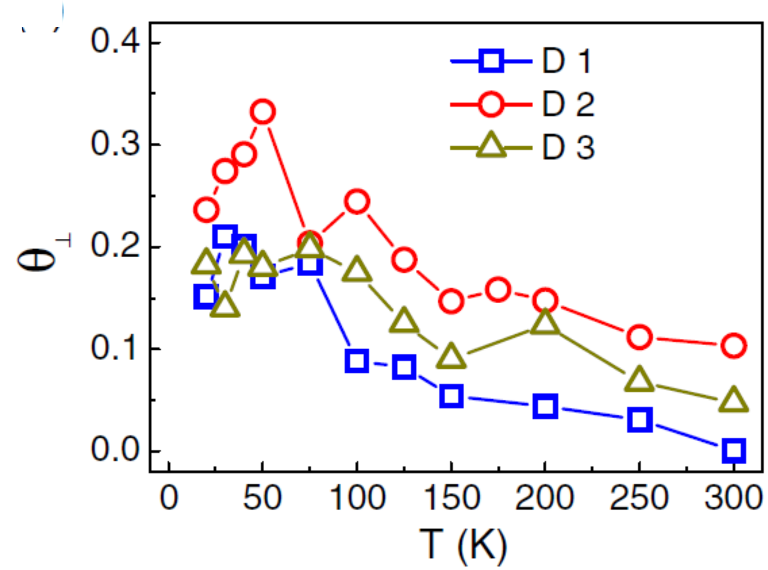

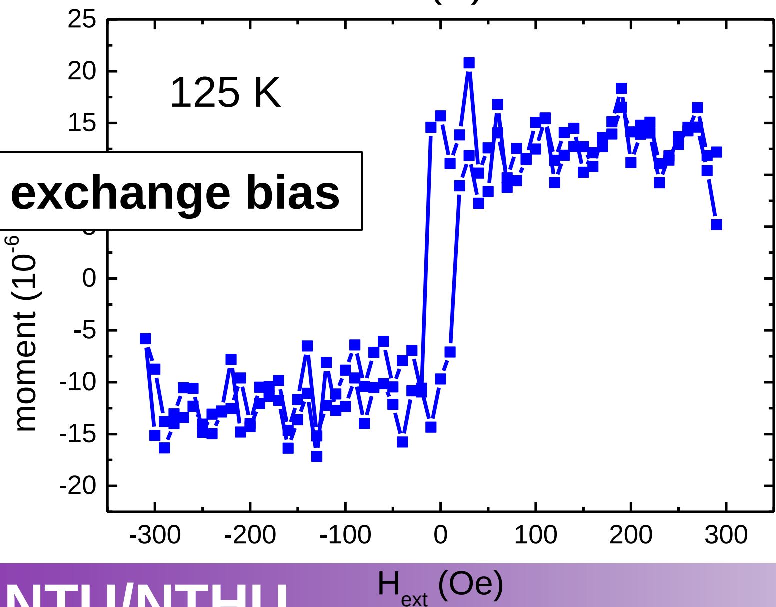

No exchange bias

Increasing field-like torque at low T

$$\mathbf{T}_{\mathrm{FL}} = \Delta_{ex}\mathbf{M} \times \langle \mathbf{S} \rangle_{\mathrm{neq}}$$

The $\mathbf{T}_{\mathrm{FL}}$ in ST-FMR corresponds to a $\mathbf{H}_{\mathbf{eff}}$ in spin pumping.

Wang *et al.*, PRL **114**, 257202 (2015).
Fischer *et al.*, PRB **93**, 125303 (2016).

Internal effective field induced FMR without an applied field

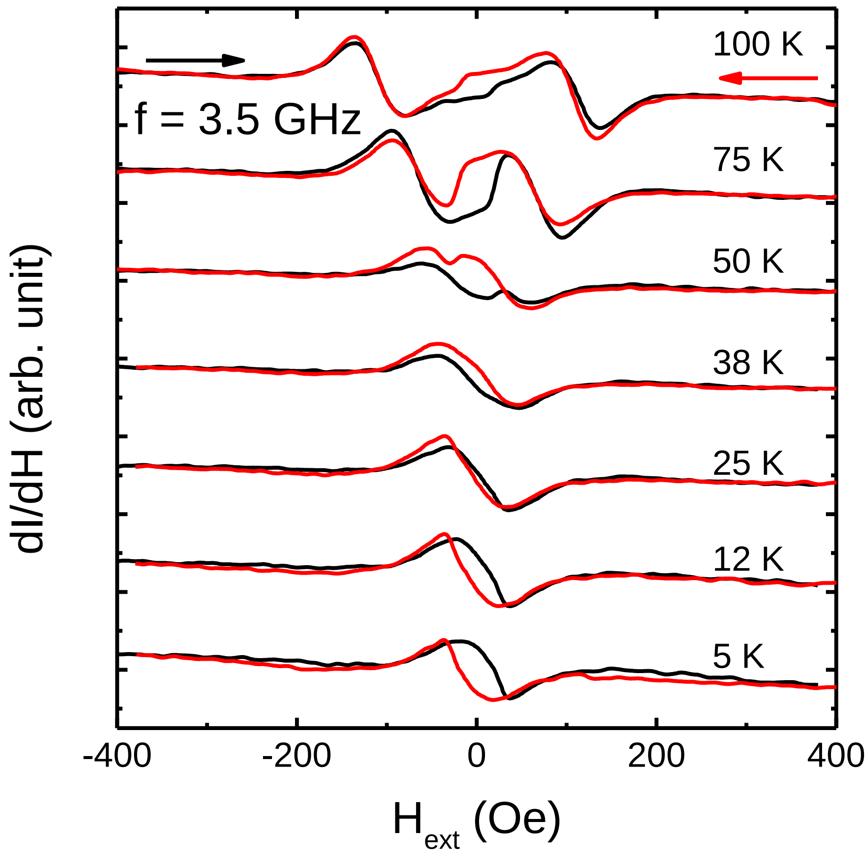

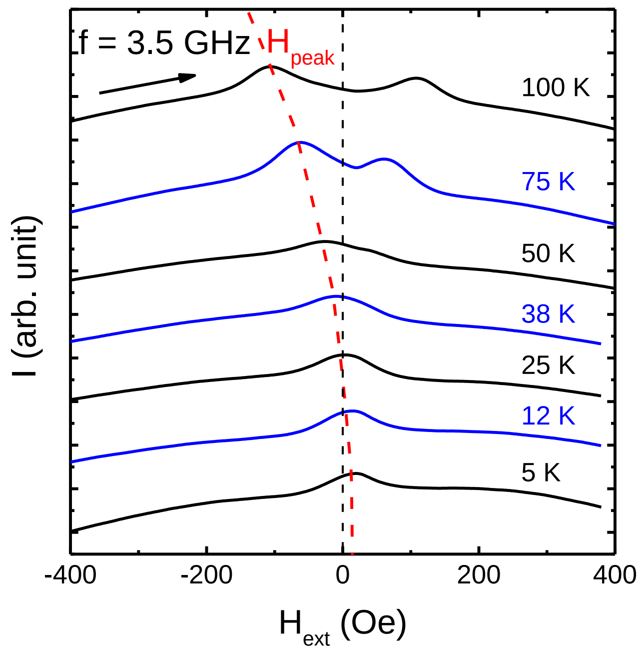

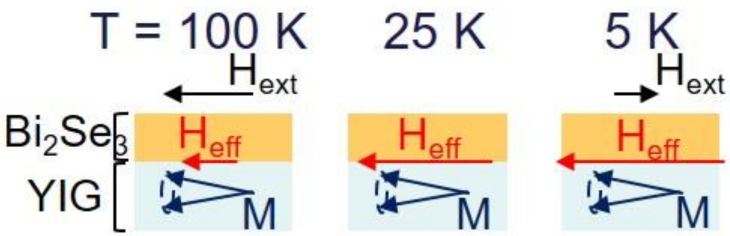

- Internal effective field = $4\pi M_s + H_{an} + H_{eff}$
- The exchange effective field H_{eff} becomes larger as T decreases.
- The strong H_{eff} has good potential for spintronic application.

Y. T. Fanchiang
Advanced Nano Thin Film Epitaxy Lab

Summary-1

- Ferrimagnetic insulator YIG provides thermally stable TI/YIG interface and avoides current shunting.
- Interfacial in-plane magnetic anisotropy in Bi_2Se_3/YIG is observed, and builds up as T decreases.
- A unprecedentedly large spin mixing conductance (2.2×10^{19} m^{-2}) for YIG systems was observed in Bi_2Se_3/YIG, implying an interface with very efficient spin injection.
- Temperature dependence of spin pumping in Bi_2Se_3/YIG resembles that of antiferromagnetic CoO/YIG, suggesting MPE with a T_c as high as 180 K.

Observation of spin-to-charge conversion in Bi_2Se_3/YIG

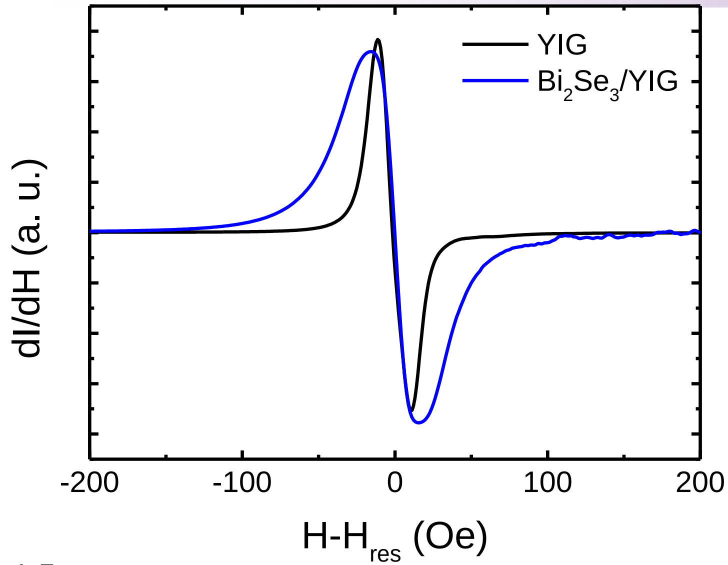

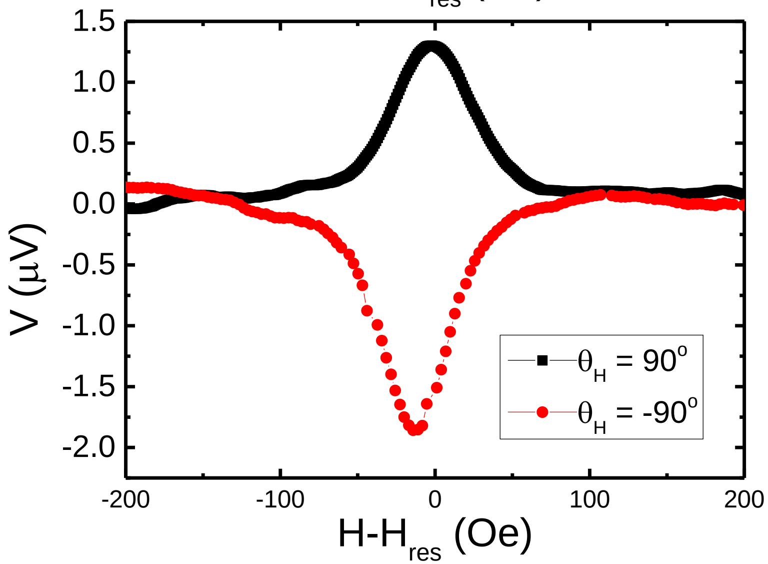

This work: $\theta_{SH} \sim 3 \times 10^{-4}$

Explanation of low θ_{SH} of our Bi_2Se_3/YIG:

1. Strong exchange coupling may modify the spin texture of Bi_2Se_3.
2. Spins are absorbed by the conducting bulk of Bi_2Se_3.

Prof. Samarth's work (PSU)

$\theta_{SH} \sim 0.02$

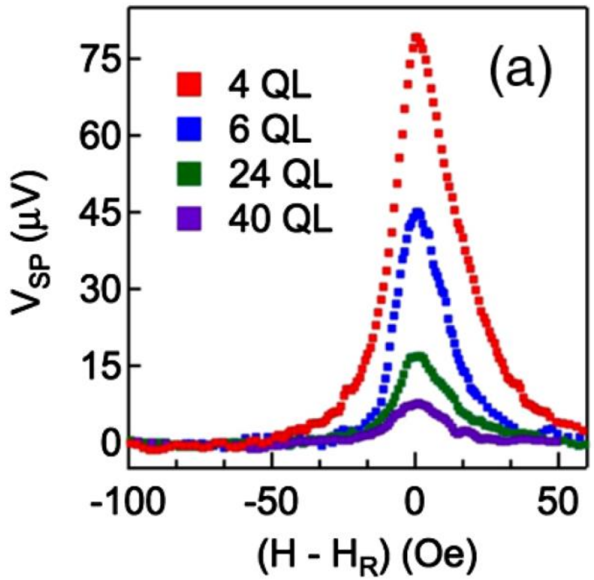

Wang et al., PRL **116**, 096602 (2016).

Negative magnetoresistance (MR) and exchange gap opening in Bi_2Se_3/ReIG

Challenges of studying the interfacial band structure and transport properties of TI/FI

- Independent check of (a) MPE and (b) Dirac surface gap

MPE, but no exchange gap

(Bi,Sb)$_2$Te$_3$/TmIG

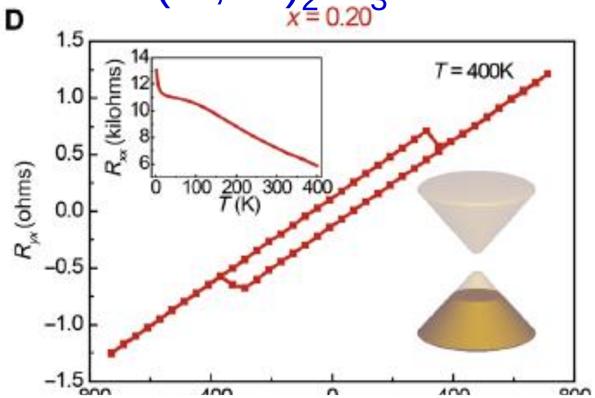

Tang et al., Sci. Adv. **3**, e1700307 (2017)

Signatures of surface bandgap, but no ferromagnetism

Bi$_2$Se$_3$/EuS

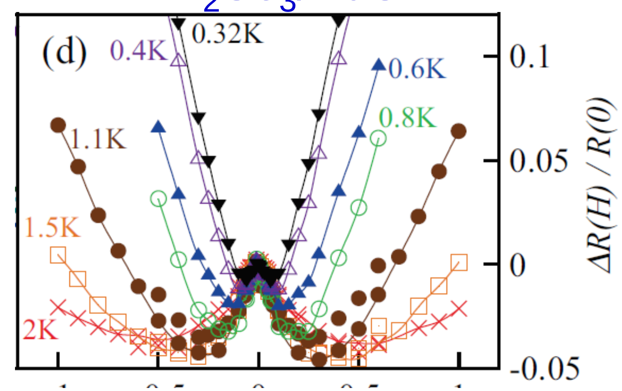

Yang et al., PRB **98**, 081407(R) (2013)

(Bi,Sb)$_2$Te$_3$/YIG

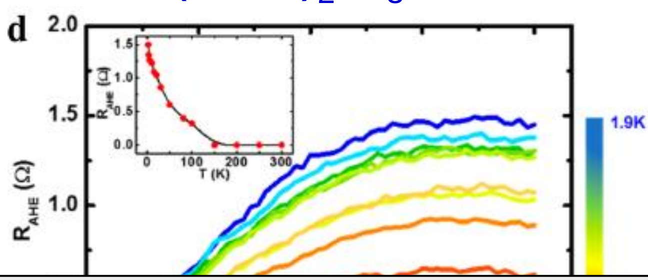

(Bi,Sb)$_2$Te$_3$/EuS

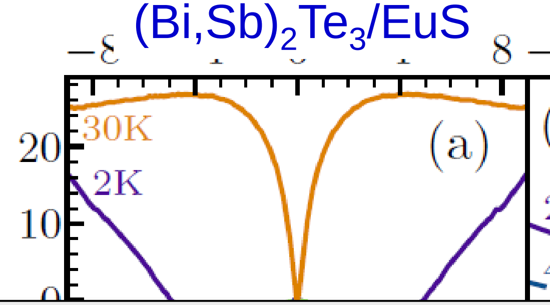

A coherent picture that shows transport signatures of the coexisting MPE and exchange Dirac gap is needed.

WL effect originated from TRS-breaking at the TI/FI interface: thickness dependent study

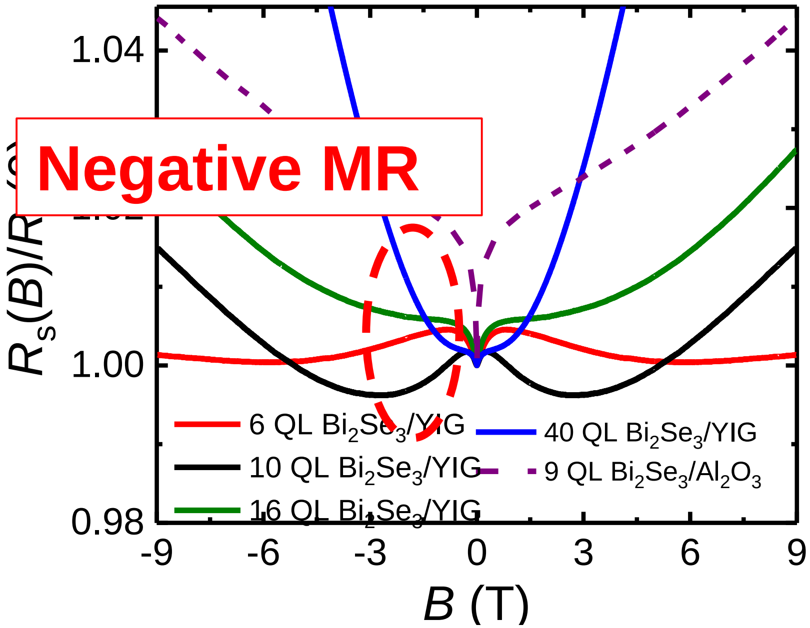

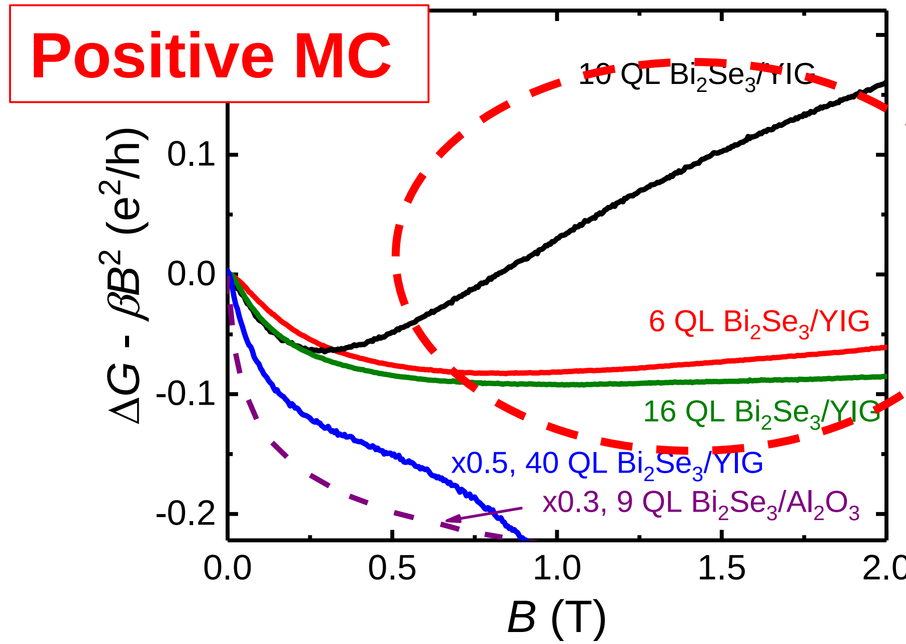

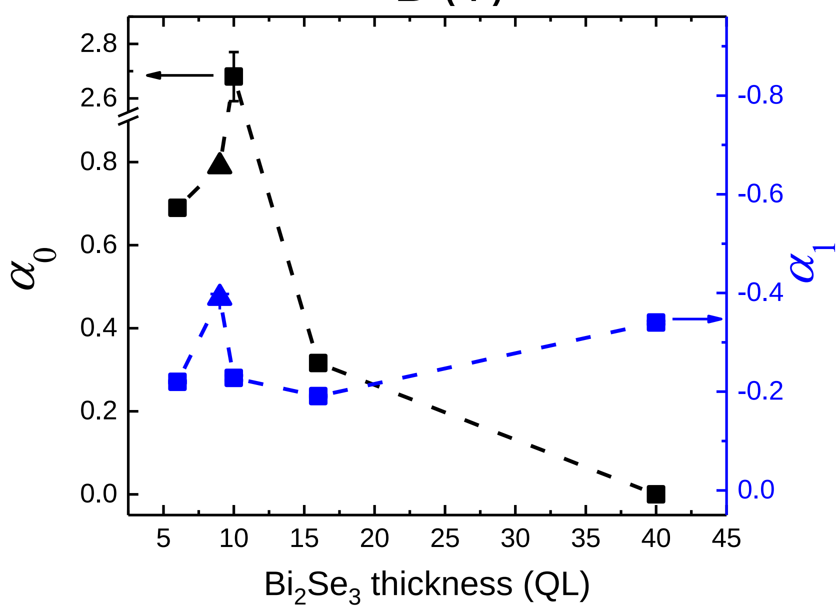

In thinner Bi_2Se_3

- stronger WL (α_0) and weaker WAL (α_1)
- **The WL is most likely due to the TRS broken by interfacial exchange interaction**

Y. T. Fanchiang
Advanced Nano Thin Film Epitaxy Lab

Strong interfacial exchange coupling

Transport signatures of exchange Dirac gap opening in Bi_2Se_3/TmIG

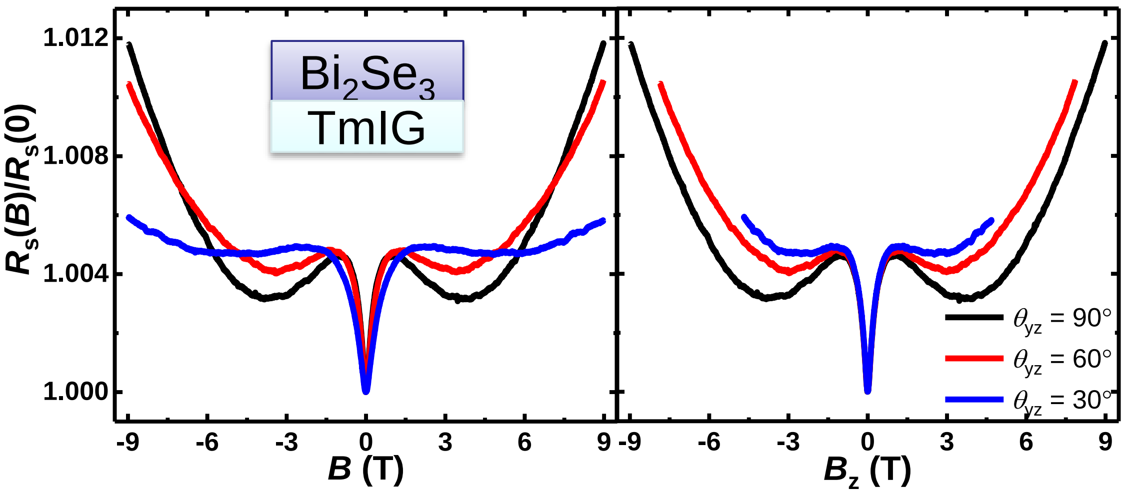

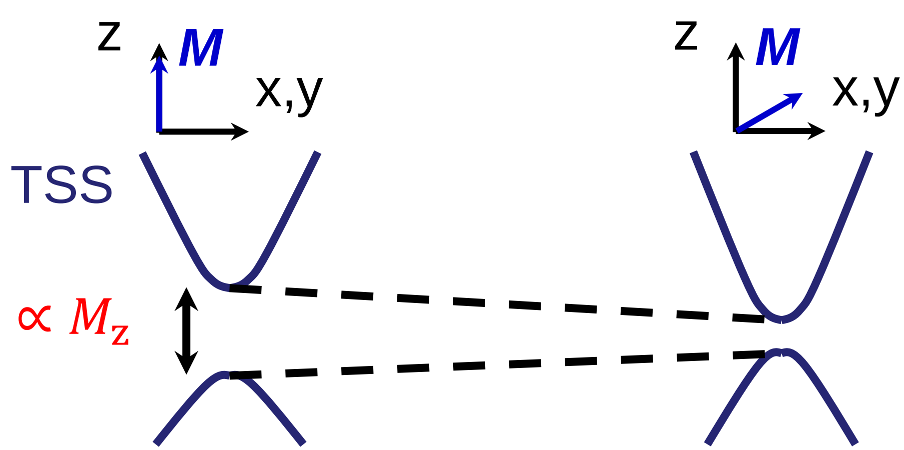

Interfacial magnetic anisotropy

Two-step growth

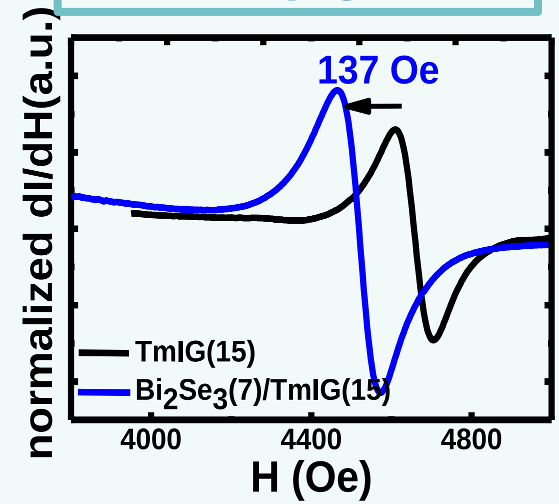

SBLT growth

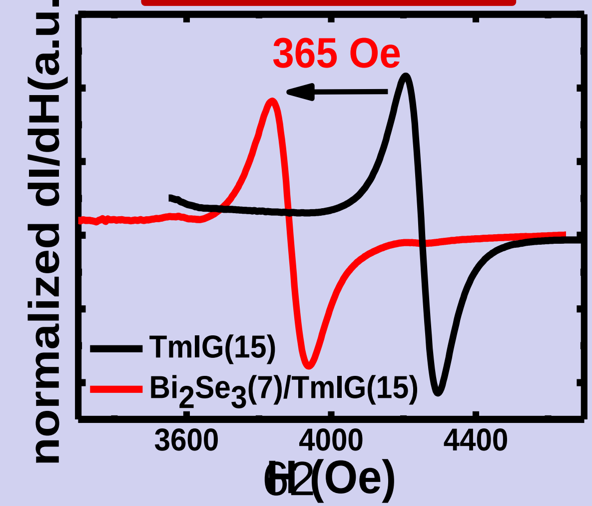

NTU/NTHU

Observation of AHE and AMR

Anomalous Hall effect (AHE) loops

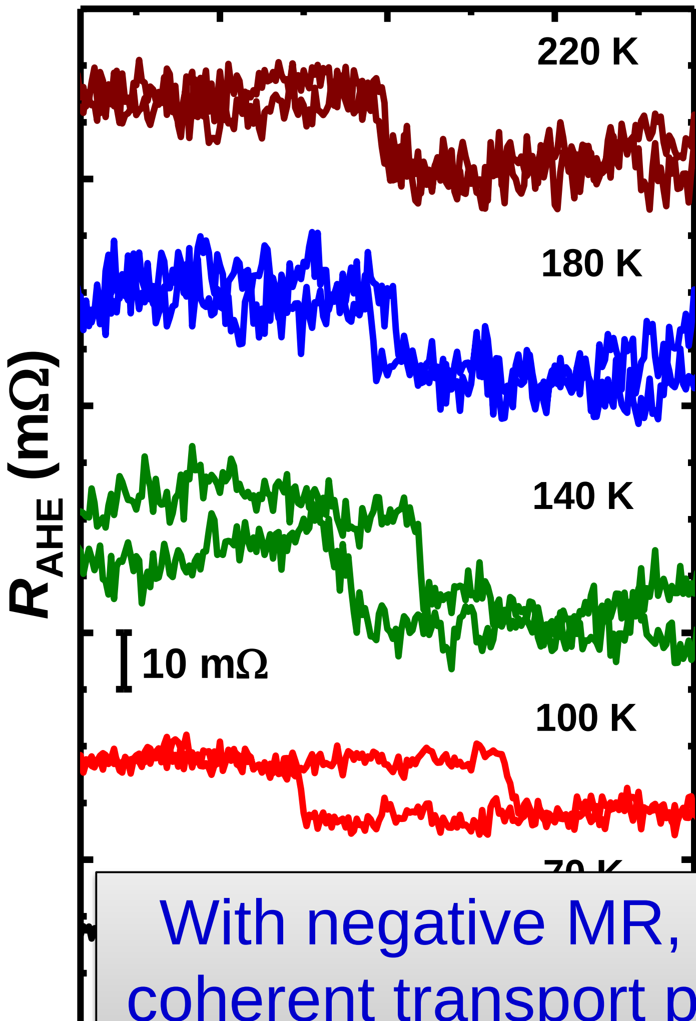

Anisotropic magnetoresistance (AMR) due to MPE

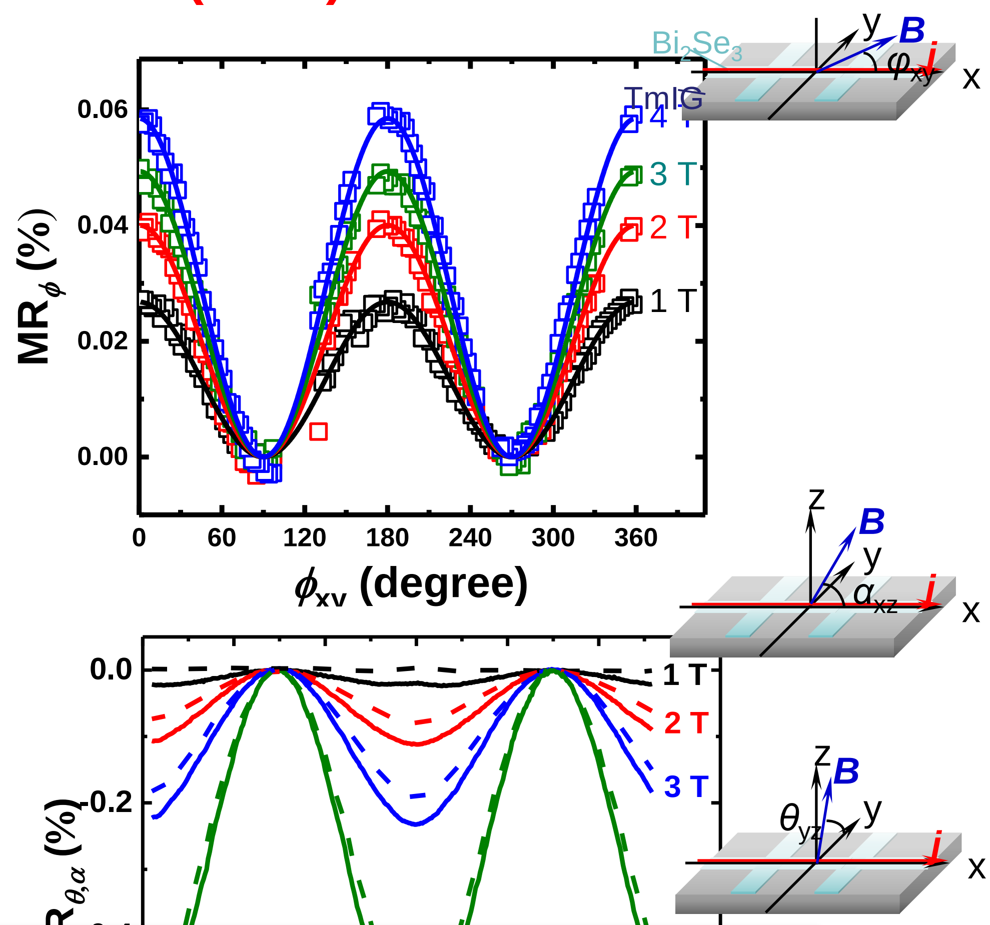

With negative MR, AHE and AMR, we obtained a coherent transport picture of the system that shows both gap opening and MPE.

Summary-2

– Observation of negative magnetoresistance (MR) of the weak localization (WL) effect in Bi_2Se_3/YIG and Bi_2Se_3/TmIG

– Correlation between the negative MR and exchange gap size

– Proximity-induced long-range ferromagnetic order in TI/FI evidenced by anomalous Hall effect (AHE) and anisotropic magnetoresistance (AMR)

Comparison

NTHU, NTU

Clear 1st harmonic signals
2nd harmonic signals?

UMN, PSU, CSU

No 1st harmonic signals
Strong 2nd harmonic signals: UMR

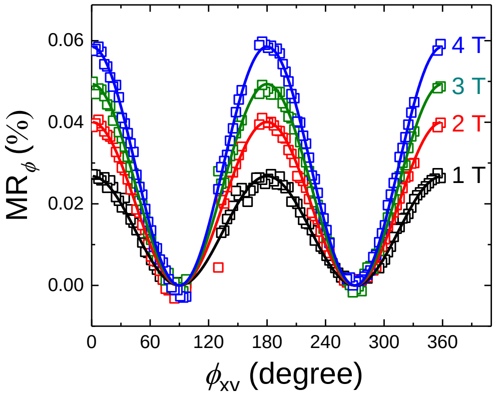

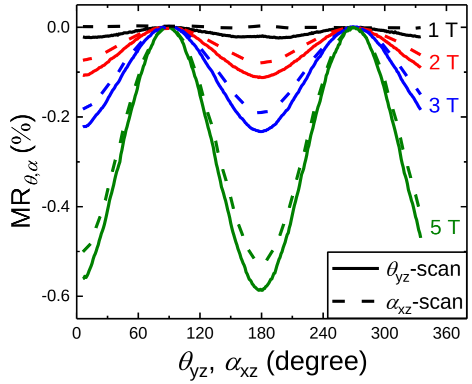

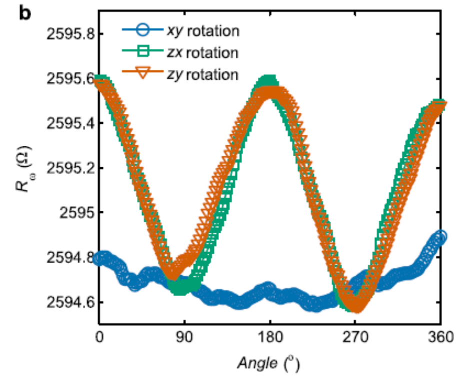

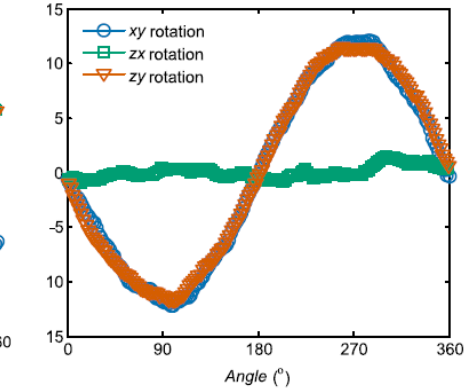

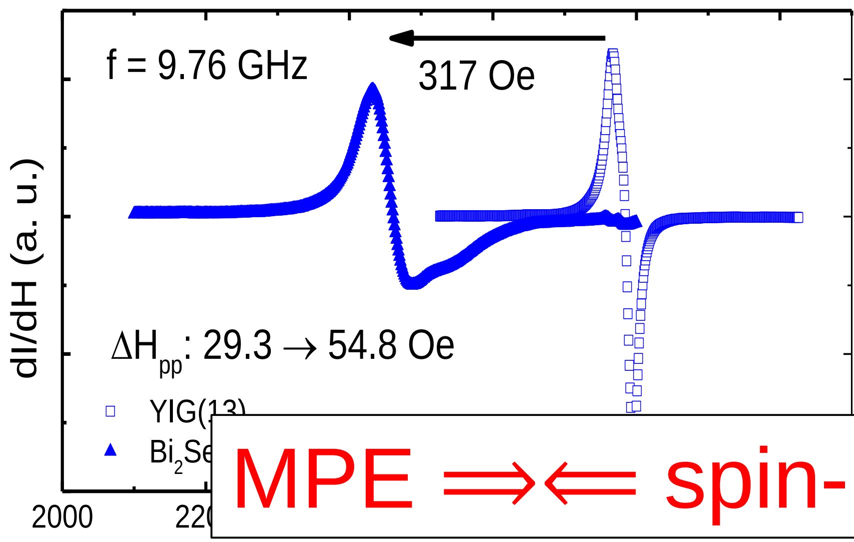

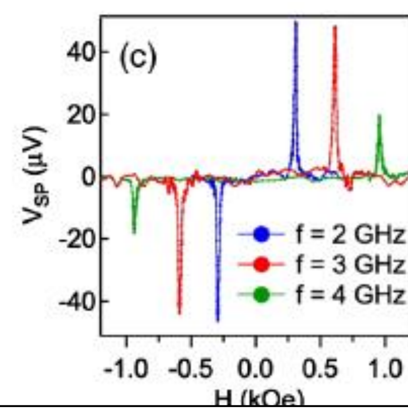

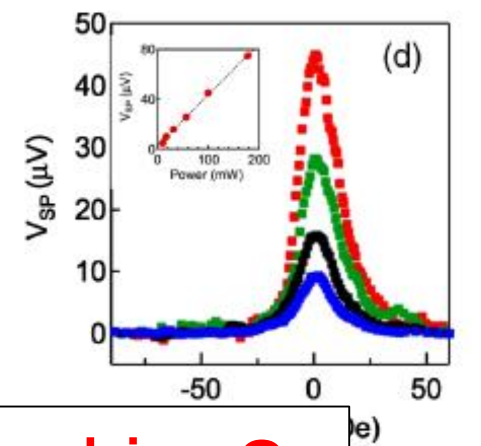

MPE ⇒⇐ spin-momentum locking?

o MPE

Strong MPE, little spin-charge conversion

Fanchiang *et al.*, Nat. Commun. **9**, 223 (2018)
Wang *et al.*, Phys. Rev. Lett. **117**, 076601 (2016)
arXiv:1806.09066 (2018)

Critical role of a normal metal spacer layer: Very efficient SCC in α-Sn at room temperature (A. Fert)

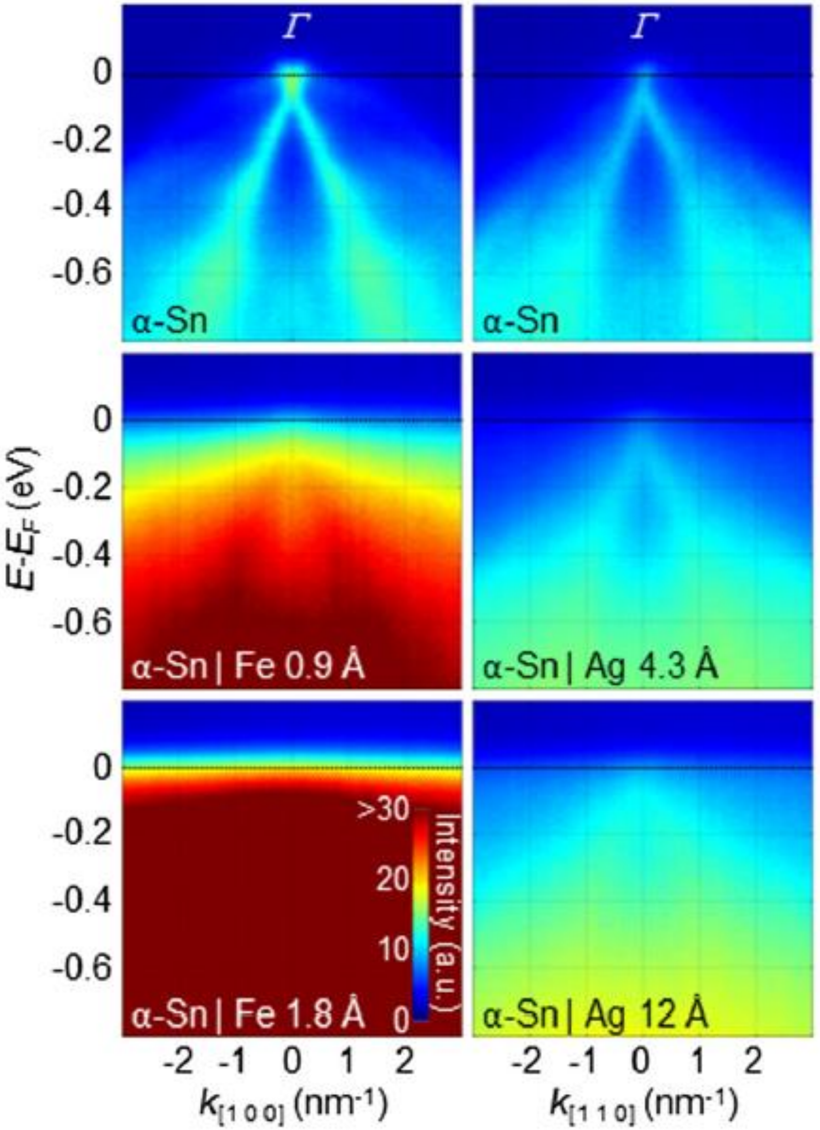

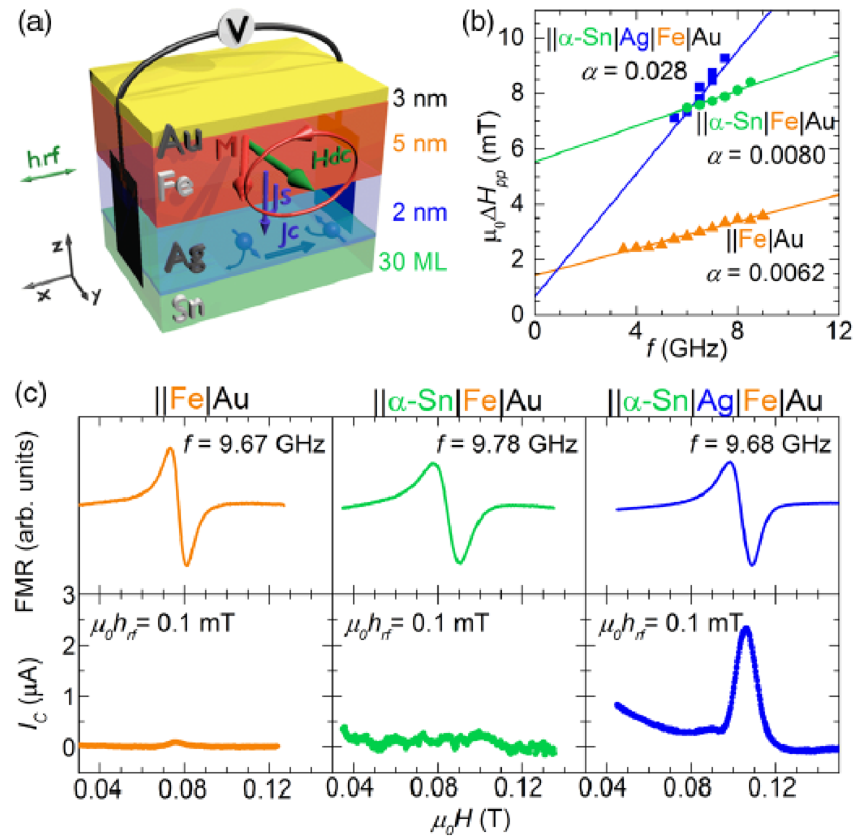

PRL **116**, 096602 (2016).

Electronic property and chemistry of metals in contact with Bi_2Se_3

C. D. Spataru *et al., Phys. Rev. B* **90**, 085115 (2014) L. A. Walsh *et al., J. Phys. Chem*. **121**, 23551−23563 (2017)

Calculated spectral function of Au/Bi_2Se_3

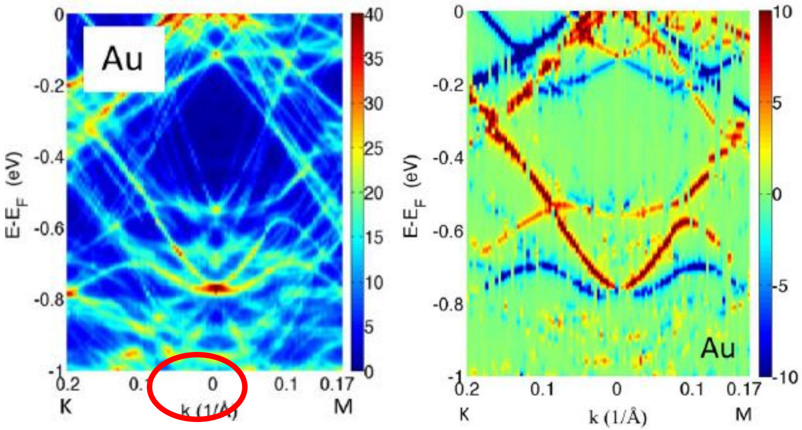

XPS result for Se 3*d* and Bi 5*d* **XPS result for Au 4*f***

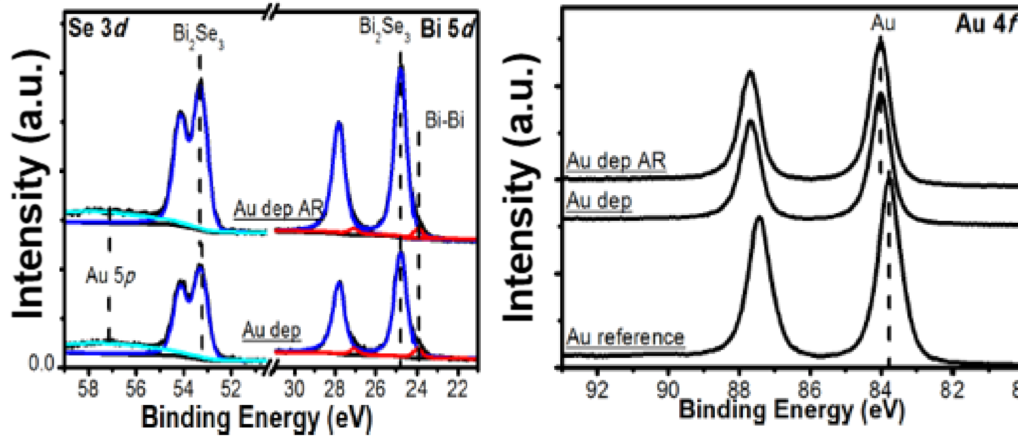

- **Preservation of Dirac cone and the spin texture in Bi_2Se_3 in contact with Au ➡ No chemical reaction detected**
- **No discernible change of the peak shape**

Au can serve as a promising interlayer, not only reducing the direct exchange coupling between YIG and Bi_2Se_3 film, but also preserving TI properties.

It is difficult to directly grow Bi_2Se_3 on Au/YIG because of the severe inter-diffusion.

Decreased interfacial coupling by Au layer

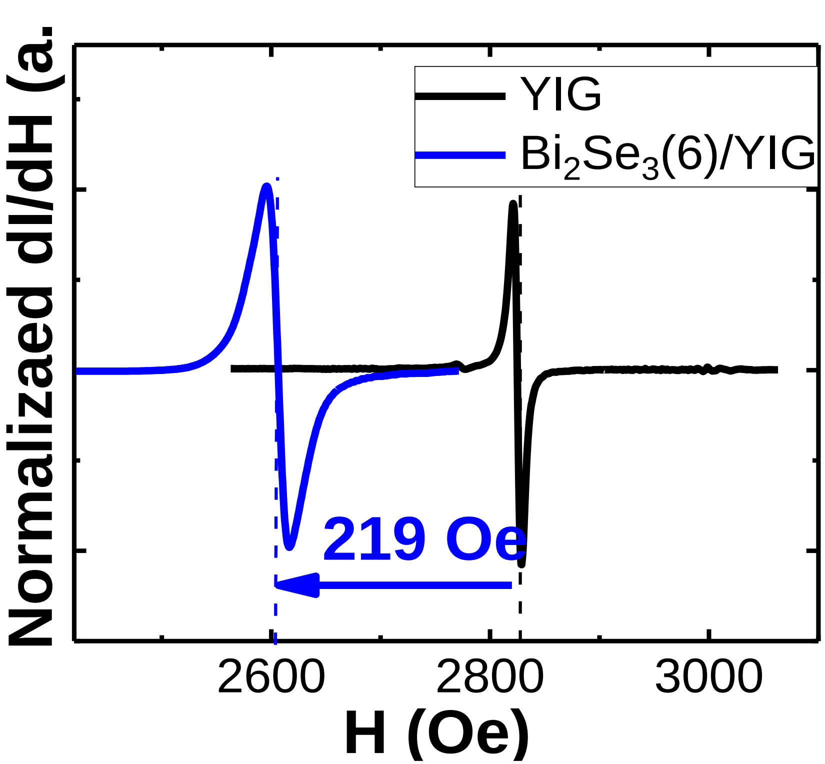

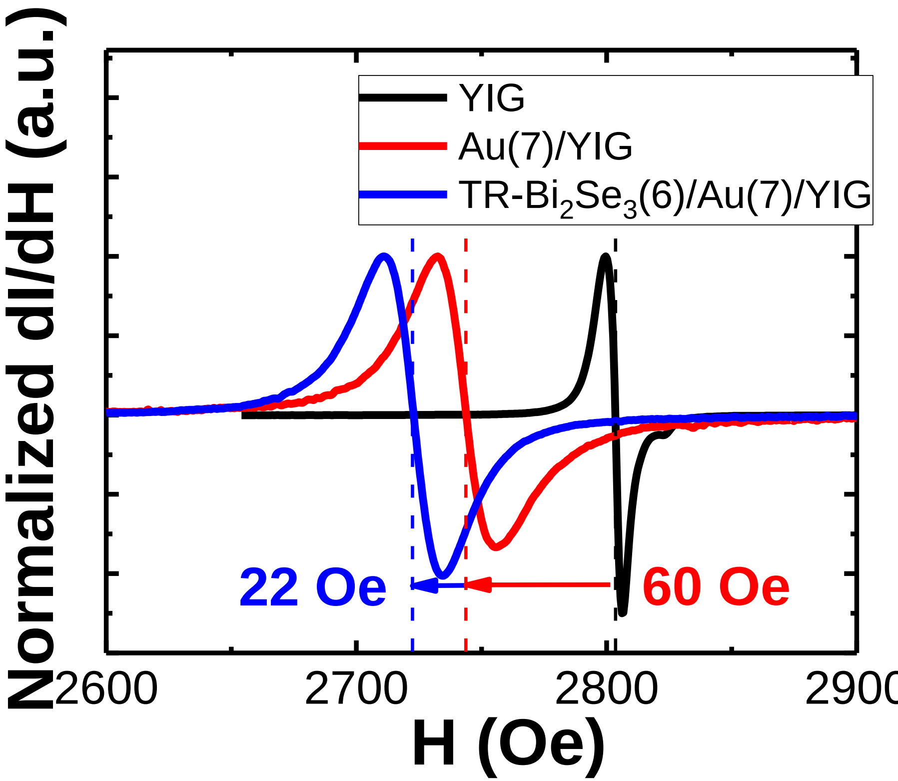

- Smaller H_{res} shift in Au/YIG compared to H_{res} shift of Bi_2Se_3/YIG
- H_{res} shift of ~22 Oe in TR-Bi_2Se_3/Au/YIG compared to H_{res} of Au/YIG

Slight enhancement of anisotropy in TR-Bi_2Se_3/Au/YIG implies that there is less direct exchange coupling between TR-Bi_2Se_3 and YIG.

Spin-to-charge conversion of Bi_2Se_3/Au

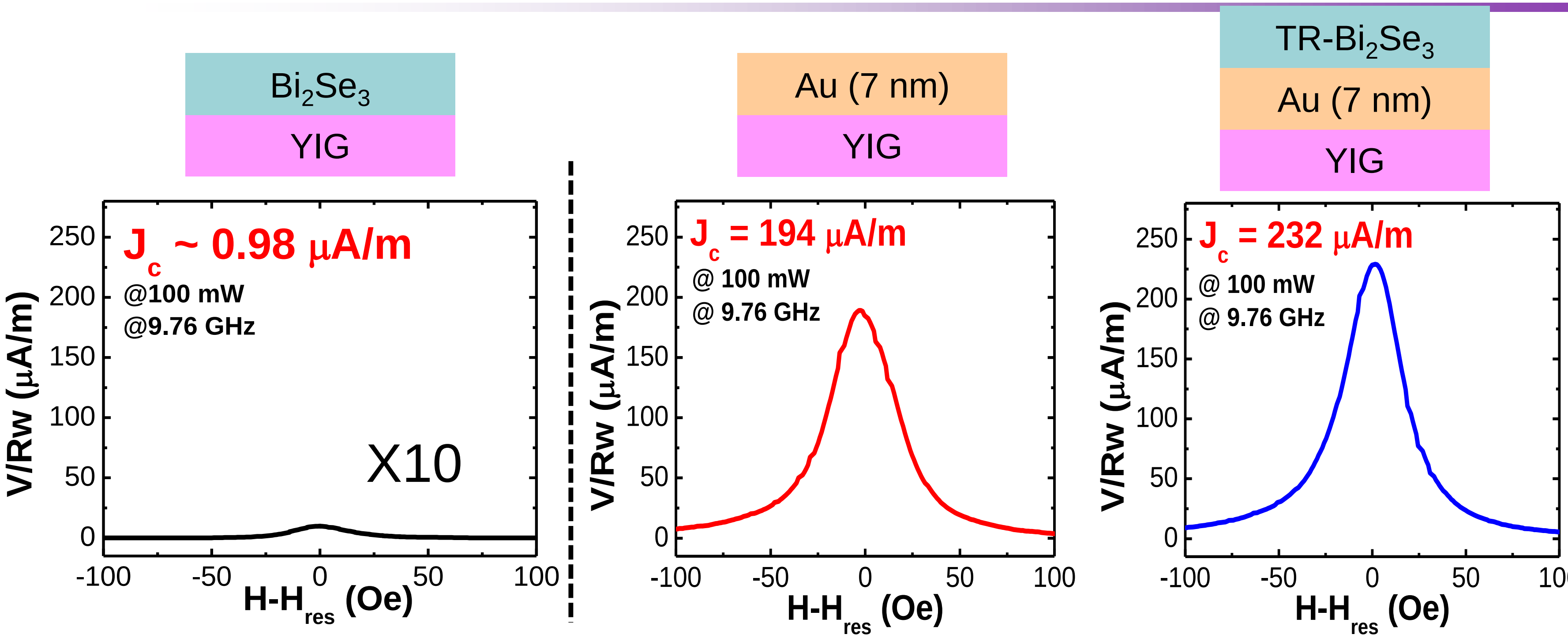

- **Small spin-pumping-induced current density in Bi_2Se_3/YIG**
- **Sizable enhancement of charge current in TR-Bi_2Se_3/Au/YIG**

- Enhanced charge current of TR-Bi_2Se_3/Au/YIG is significantly larger than the value of Bi_2Se_3/YIG, possibly resulted from the decoupling of TSS and YIG.
- First principle calculations show that there can exist large Rashba splitting at the interface.

C. H. Chang *et al*., *NPG Asia Mater.* **8**, e332 (2016)

Au thickness dependence of SCC in TR-Bi_2Se_3/Au

Assuming spin diffusion in normal metal: $\frac{J_C^{2D}}{J_S^{3D}} = \theta_{SH}\lambda_{SD}\tanh\left(\frac{t_N}{2\lambda_{SD}}\right)$

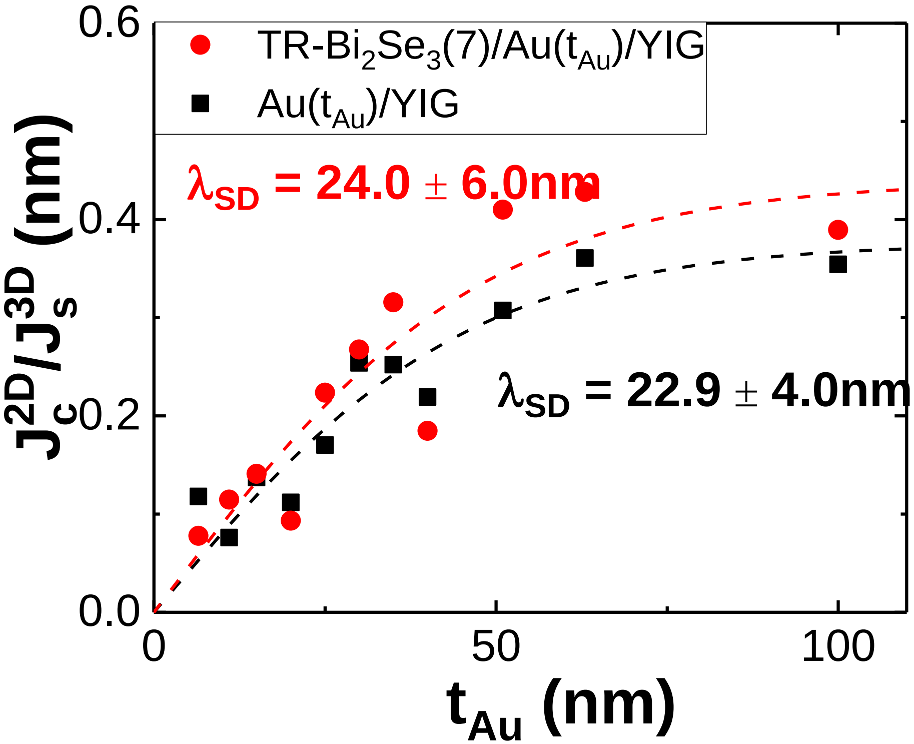

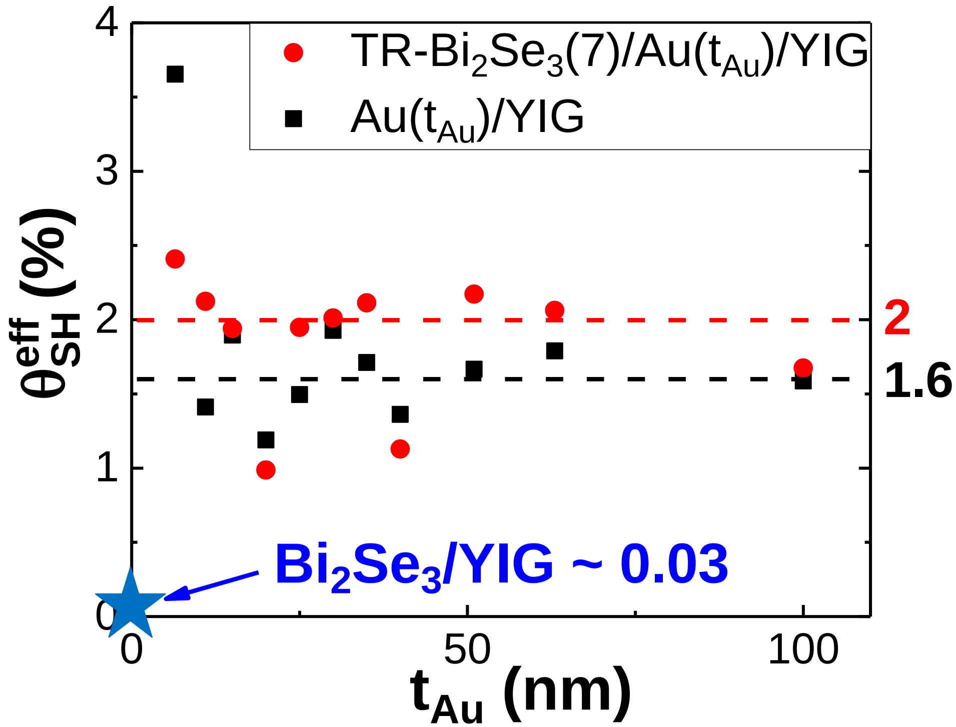

- **SCC shows overall enhancement in TR-Bi_2Se_3/Au/YIG**
- **TR-Bi_2Se_3/Au interface may play an important role in the SCC.**
- **Improving TR-Bi_2Se_3/Au interface could further enehance SCC.**

Y. T. Fanchiang
Advanced Nano Thin Film Epitaxy Lab

Summary-3

- Au served as an interlayer has effectively reduced the direct exchange coupling between TR-Bi_2Se_3 and YIG, so that little enhancement of IMA is observed.

- The SCC of TR-Bi_2Se_3/Au is larger than the value in Bi_2Se_3 on YIG, which may be caused by the decoupling of TSS and YIG, or Rashba splitting of the interface state.

Conclusions

- **Discovery of large interfacial magnetic anisotropy of TI/FI heterostructures**
- **First demonstration of spin pumping probe of magnetic proximity effect**
- **Realization of zero-field FMR in Bi_2Se_3/YIG**
- **Possible incompatibility of interfacial exchange coupling and spin-to-charge conversion (SCC) in TI/FMI**